Electrophoresis of DNA and other polyelectrolytes: Physical mechanisms

Jean-Louis Viovy*

Laboratoire Physico-Chimie Curie (UMR CNRS 168), Institut Curie Section de Recherche, 26 Rue d'Ulm, 75230 Paris cedex 05, France

The dramatic recent advances in molecular biology, which have opened a new era in medicine and biotechnology, rely on improved techniques to study large molecules. Electrophoresis is one of the most important of these. Separation of DNA by size, in particular, is at the heart of genome mapping and sequencing and is likely to play an increasing role in diagnosis. This article reviews, from the point of view of a physicist, the mechanisms responsible for electrophoretic separation of polyelectrolytes. This separation is mainly performed in gels, and a wide variety of migration mechanisms can come into play, depending on the polyelectrolyte's architecture, on the electric fields applied, and on the properties of the gel. After a brief review of the thermodynamic and electrohydrodynamic principles relating to polyelectrolyte solutions, the author treats the phenomenology of electrophoresis and describes the conceptual and theoretical tools in the field. The reptation mechanisms, by which large flexible polyelectrolytes thread their way through the pores of the gel matrix, play a prominent role. Biased reptation, the extension of this model to electrophoresis, provides a very intuitive framework within which numerous physical ideas can be introduced and discussed. It has been the most popular theory in this domain, and it remains an inspiring concept for current development. There have also been important advances in experimental techniques such as single-molecule viodeomicroscopy and the development of nongel separation media and mechanisms. These, in turn, form the basis for fast-developing and innovative technologies like capillary electrophoresis, electrophoresis on microchips, and molecular ratchets.

CONTENTS

*Electronic address: Jean-Louis.Viovy@curie.fr

LIST OF SYMBOLS

A	distance between charges
B	Brownian force
C	Numerical constant of order 1
D_b	blob diffusion coefficient
D_{tube}	tube diffusion coefficient
E	electric field
E_x	electric field along x
F_{drag}	friction force
F_{el}	electrophoretic force
F_{stall}	stall force
H	macroscopic orientational order parameter
I	ionic strength
J_i	local current of chain segments
K	longitudinal modulus
K_r	retardation coefficient
L	contour length of the tube
$\mathcal{L}$	Langevin function
L_0	contour length of the polyelectrolyte
M_w	Molecular weight (in mass)
N	number of blobs
N_A	Avogadro's number
N^*	crossover size between non-oriented and oriented reptation
N_b	number of Kuhn segments in one blob
N_k	number of Kuhn length
N_v	crossover size (in number of Kuhn segments) to excluded volume behavior
P	number of theoretical plates
Q	total charge
R	particle radius
R_{es}	resolution factor
R_g	radius of gyration
R_{gp}	radius of gyration of a polymer
R_N	end-to-end distance
R_p	resolving power
R_ν	crossover radius to excluded volume behavior
R_x	end-to-end distance, projected on direction x
S	entropy
T	Kelvin temperature
$T\%$	Acrylamide total concentration
V	electric potential
V_p	particle volume
V_s	surface potential
W	transition rate
a	lattice period
b	pore size of the gel and blob size
c	concentration
c^*	critical overlap concentration of polymer chains (dilute/semi-dilute transition)
c_k	concentration of species "k"
c_{kb}	concentration of species "k" in the bulk
c_s	salt concentration
d	chain diameter
d_c	dispersion coefficient
d_p	pore diameter
f	fractional free volume
f_k	force per Kuhn length
g	aggregation rate
h	local tube orientation
j	fiber length density
k	Boltzmann constant
l	Kuhn length of the polyelectrolyte ($=2l_p$)
l_0	persistence length in the absence of charges
l_B	Bjerrum length
l_p	persistence length
m	obstacle number density
p	probability
q	wave vector
q_{eff}	effective charge
q_k	charge per Kuhn length
r	fiber radius
s	obstacle surface density
t_{dis}	disengagement time
t_{or}	orientation time
t_p	pulse time
t_{rep}	reptation time
u	dimensionless curvilinear velocity
v	velocity
v_c	velocity in constant field
$v_{\text{sedimentation}}$	sedimentation velocity
υ_F	Flory excluded volume parameter
w	peak width
z_k	charge valence of ion "k"
Λ	particle largest dimension
Σ	particle surface area
μ	electrophoretic mobility
μ_0	electrophoretic mobility in free liquid
μ_{EEO}	electro-osmotic mobility
μ_{eff}	effective mobility
μ_s	electrophoretic mobility of background electrolyte ions

α	mobility reduction factor for gel electrophoresis in strong fields
β	reduced Brownian force
δ	Kronecker symbol
ε	reduced electric field
ε_b	dielectric constant
ε_0	permittivity of vacuum
ε_κ	reduced electric field per Kuhn length
ϕ	field-rotation angle in Crossed-Fields Gel Electrophoresis
γ	reduced electric bias
η	solvent viscosity
η_s	macroscopic solution viscosity
κ	inverse Debye length
ν	Flory exponent
θ	angle between tube axis and field
ρ	charge density
ρ_f	free charge density
ρ_v	velocity ratio (in pulsed-field electrophoresis)
σ	linear or surface charge density
τ	dimensionless time unit
τ_0	jump time
τ_b	Brownian time of a blob
τ_{opt}	optimal pulse time for separation
ξ	friction coefficient
ξ_b	blob friction
ξ_k	friction per Kuhn length
ξ_{tot}	total friction
ζ	Zeta potential

LIST OF ABBREVIATIONS

A	Adenine
bp	base pair
BRF	biased reptation with fluctuations
BRM	biased reptation model
C	Cytosine
DNA	Deoxyribonucleic acid
ELFSE	end-label free-solution electrophoresis
FIGE	field-inversion gel electrophoresis
G	Guanine
Mb	megabase pair
MRNA	messenger ribonucleic acid
T	Thymine
TBE $1X$	Tris 89mM, Borate 89mM, EDTA 2mM

I. INTRODUCTION

Application of physical methods and concepts to problems of biological interest is one of the major ''frontiers'' in the physical sciences at the beginning of the new millenium. The explosive development in this field, in particular in the communities of condensed matter and statistical physics, is quite recent, but some specific areas such as the chemical physics of DNA predated this recent trend and have been the object of a steady and long-standing interest among physicists. This is particularly true for the electrophoresis of polyelectrolytes (i.e., macromolecules bearing several charges), in which DNA has been the favorite paradigm. This is probably because, as we shall see, DNA combines ideal properties as a model molecule for physicists and a tremendous interest for biologists.

DNA is, first and foremost, the molecule of heredity. It is a linear flexible macromolecule made of four building blocks, the nucleotides constructed from the bases adenine, thymine, guanine, and cytosine (A,T,G,C).[1] In nature, it occurs mainly in a double-stranded form, the famous double helix discovered by Crick and Watson in 1954, in which the two complementary strands are kept together by specific attractions between the A and T and G and C nucleotides, respectively. The sequence of nucleotides contains the codes for the synthesis of all proteins (these codes are called the genes), plus other codes that specific enzymes can recognize (e.g., the ''start'' and ''stop'' codons indicating the beginning and the end of a given gene, and many others involved in the regulation of gene expression). Because these molecules go by pairs that are exact complements of each other, they are able to replicate (thanks to an enzyme, the polymerase, which is able to ''repolymerize'' along a single strand its complementary strand). This is the basis of life. It is now well known, but nevertheless a matter of endless amazement, that all of the information responsible for the biological identity of a species and for an individual in this species is contained in a few macromolecules weighting overall about 10^{-12} g.[2] Single-stranded DNA occurs in Nature only transiently and on a rather local scale, during replication or transcription into messenger ribonucleic acid (mRNA). This is synthesized using as templates the genes on the DNA, in order to be ''read'' by ribosomes, the ''molecular factories'' that synthesize proteins from the amino-acid building blocks.

Biologists realized very soon that deciphering the genes was the first key to the understanding of life: this was the beginning of molecular genetics. Among the broad array of tools used in molecular biology, separation of DNA molecules by size is one of the most essential, because major properties of the genes such as their organization or their alteration can be obtained through an analysis of DNA fragments by size. Also, the electrophoretic mobility of DNA is practically independent of the base content, so that strategies had to be developed (Sanger and Coulson, 1975, Sanger *et al.*, 1977, Maxam and Gilbert, 1975) for deciphering the genetic code (the

[1]The nucleotides should be called deoxyadenylic acid, etc. but by contraction, they are customarily called by the names of the ''bases'' they are derived from.

[2]This is a somewhat simplified view: actually, it is more and more clearly recognized that information essential for life is also contained in the internal organization of the cell, i.e., in the environment in which the genes are (or are not) expressed. This information is transmitted from one generation to the next ''somatically,'' i.e., independently of chromosomal DNA. Nevertheless, this somatic information is much less specific, in terms of species and of individuals, than is the genetic information, so that the common view of DNA as the carrier of biodiversity and biological identity remains largely true.

famous ''sequencing of the genome''). These strategies are also based on a sorting of fragments by size (Fig. 1). This task, as important and time-consuming as it may be, represents only a small portion of the future applications of DNA electrophoresis: following our improved understanding of the genetics of diseases and infectious organisms, diagnosis based on DNA analysis will assume increasing importance among the methods available to the clinician. Finally, the development of biotechnology is also creating an enormous demand for DNA analysis. Because of this biological importance, considerable efforts have been made in the last few years to improve DNA electrophoresis, and most of the theoretical developments in the field of polyelectrolyte electrophoresis have been guided by DNA separations.

In spite of this particular interest in DNA, it is important to stress that molecular biology is in need of separation methods for all the types of molecules existing in living organisms, and that the vast majority of these are polyelectrolytes. This is especially the case for proteins, another very important application of gel electrophoresis in biology. The natural continuation of genome analysis is *proteome analysis*, i.e., the study of the proteins produced in a given cell or ensemble of cells. The proteome is smaller than the genome (because only a small fraction of all the genes is expressed at a given time in a given cell), but much more variable (different proteins can be expressed in amounts that differ by several orders of magnitude, different cells with the same genome express different proteins due to their differentiation, and the same cell also expresses proteins differently at different moments of its life).

For DNA and protein analysis, as well as for the less developed but nevertheless important analysis of RNA or polysaccharides, gel electrophoresis is the method of choice, and it is probably the most common analytical tool overall for biomolecules. For a long time, however, this technique was considered rather simple and qualitative, and its molecular sieving mechanisms did not receive widespread attention from a fundamental point of view. After many years in obscurity, it is today regarded as a subject of current interest.

The idea of separating charged particles or ions in solution using electric fields is in itself rather old. Separations of proteins by zone-boundary electrophoresis were performed by Tiselius as early as 1937. The first difficulty encountered then was convection, which led to transport processes faster than electrophoresis itself unless rather drastic precautions were taken. Performing the separation in a gel (see, for example, Grabar *et al.*, 1953) provided an elegant solution to this convection problem and opened the way to decades of successful applications of electrophoresis. Had gel electrophoresis not been discovered, molecular biology would never have developed to the extent it has reached today. Gel electrophoresis is not only very simple, but also very versatile (see Andrews, 1986). For instance, the gel can be grafted with molecules presenting a specific affinity with the analytes, as in affinity electrophoresis. Macromolecules can also be separated according to their isoelectric point in isoelectric focusing, by grafting buffering functions onto the gel. Finally, the gel can also interact sterically with the moving particles, leading to size fractionation. In this review, we restrict our attention to the latter process. Essentially, all types of polyelectrolytes can be separated by size in gels, but the most common molecular mechanisms fall into two general categories, one for compact, more or less rigid objects, and one for linear flexible polyelectrolytes. Finally more exotic geometries or topologies exist and may lead to specific migration mechanisms. Describing how these different mechanisms can be studied and modeled is the aim of the present review. First, however, it is necessary to introduce a few general physical concepts about charged particles in viscous, obstacle-free ionic solutions and about their electrophoretic motion. This is done in Sec. II. A phenomenological description of the ''actors in the drama'' (i.e., the polyelectrolytes most commonly separated and the media most commonly used for this) is provided in Sec. III. Then we consider in Sec. IV the gel electrophoresis of globular particles. This corresponds to the first case considered in the literature and to particle-gel interactions that are easily amenable to a qualitative intuitive understanding. We then investigate in greater detail the case of flexible charged molecules. These molecules, which include DNA, RNA, denatured proteins, most polysaccharides, and synthetic polyelectrolytes, are of considerable applied importance and also of tremendous complexity. They have motivated intense theoretical and experimental work in the last twenty years. Therefore accounting for the current state of the art in the field will be the object of Secs. V–VII, describing, respectively, the most popular ''reptation'' model, the current experimental approaches to the problem, and the most recent theoretical and numerical work. We shall provide in Sec. VIII a look at some less common, but often thought-provoking separation mechanisms. Finally, Sec. IX is dedicated to the technique of capillary electrophoresis, which is gaining popularity at an amazing rate and is probably bound to overtake conventional gel electrophoresis in the vast majority of applications, in particular those requiring a high level of automation.

II. ELEMENTS OF THE THEORY OF POLYELECTROLYTES AND ELECTROPHORESIS

A. Introduction

Gel electrophoresis of polyelectrolytes is obviously rooted in the electrohydrodynamics of polyelectrolyte solutions. Therefore it is important to recall some aspects of electrophoresis in free solution before considering gel electrophoresis *per se*. At first sight, electrophoresis of polyelectrolytes may appear daunting to theorists, since it combines the difficulties of polyelectrolytes, one of the most challenging and controversial parts of polymer physics, electrodynamics of ionic solutions, also a rather difficult subject, and polymer dynamics. Fortunately, electrophoresis is generally performed

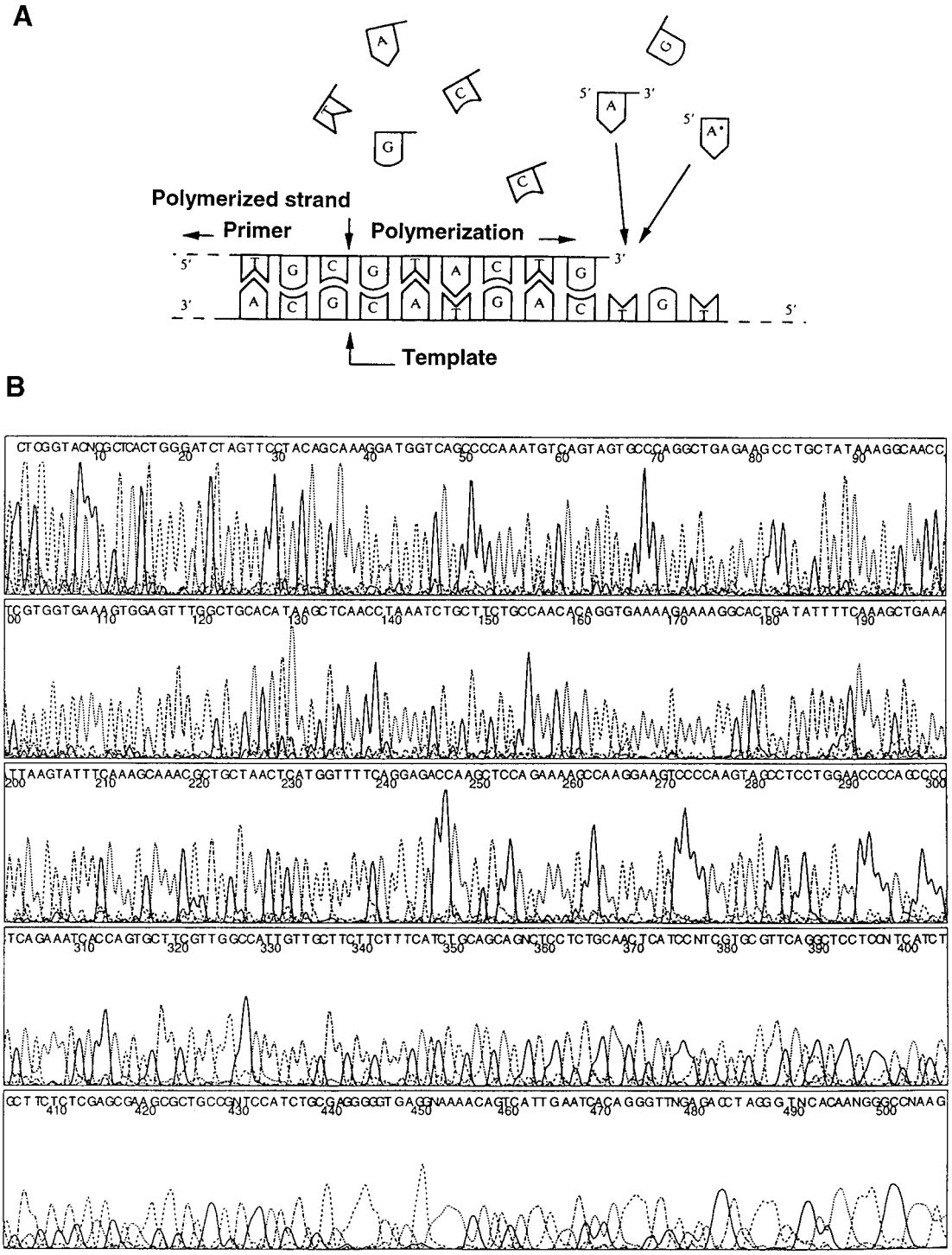

FIG. 1. Schematic representation of a sequencing process (“four-color Sanger”): starting from many copies of the single-stranded DNA to be sequenced, bearing a known “marker” at the beginning of the unknown sequence, a short oligonucleotide “primer” complementary to this marker is hybridized (i.e., paired) to the marker, in the presence of DNA polymerase and free nucleotides. This hybridization initiates reconstruction by the polymerase of a single strand complementary to the unknown sequence (A). Including in the nucleotide bath in which the polymerization takes place a small fraction of fluorescently labeled dideoxynucleotides (one different dye for each nucleotide type), which miss the OH group necessary for further extension of the strand, one is able to synthesize at random complementary strands with all possible arrest points (i.e., all possible lengths with an integer number of nucleotides). These newly synthesized single-stranded DNA’s are then separated by size electrophoretically [see electropherogram in (B)]: consecutive peaks correspond to DNA fragments differing by one base, and each line corresponds to one given nucleotide. Automated analysis of the data allows the determination of the sequence (symbols above the peaks). The symbol *N* indicates ambiguous determination. In the present case, the sequence determination was faultless up to 435 bases.

in relatively salty solutions, so that (as will be briefly recalled below) most of the "static" (i.e., conformational) specificities of polyelectrolytes are wiped out. The two other types of difficulties remain, however, and render the field very resistant to *ab initio* theoretical treatment. In the case of gel electrophoresis of polyelectrolytes, we shall fortunately discover that a number of the complications related to electrohydrodynamics of ionic solutions can be combined in a single phenomenological parameter, the free-liquid mobility. However, this point has only very recently been recognized, and the literature of gel electrophoresis most often refers to a rather ill-defined and misleading concept, the "effective charge" of the polyelectrolyte. The following introduction to electrophoresis theory is largely based on the superb textbook by Russel, Saville, and Schowalter (1989), and the reader is invited to refer to this book for a more detailed account.

B. A charged object in solution

Here we address the problem of describing the forces on a particle or a large molecule when it is immersed in a fluid which itself contains mobile ions. The molecule perturbs the distribution of ions in the surrounding solution, with the equilibrium determined by the balance between electrostatic and Brownian forces. It is common to make a distinction between the immediate layer of the fluid, in which the attracted ions may be considered permanently absorbed, and the farther layers in which the ions remain mobile. The region containing the immobile charges is called the *Stern layer*, the outer one the *diffuse layer*, and the combination of the two the *electric double layer*. However, the distinction between the Stern layer and the diffuse layer is somewhat arbitrary and depends on the time scale involved. The thickness of the Stern layer is roughly given by the *Bjerrum length*, defined as

$$l_B = e^2/(4\pi\varepsilon_b\varepsilon_0 kT), \tag{2.1}$$

where ε_b is the dielectric constant of the fluid. In water at room temperature, l_B is of the order of 0.7 nm.

In mean-field theory, the equilibrium distribution of mobile ions may be found using the Poisson-Boltzmann equation,

$$\varepsilon_b\varepsilon_0\nabla^2 V_p = -e\sum_k Z_k C_k \exp(-ez_k V_p/kT). \tag{2.2}$$

Here ez_κ and C_κ are the charge and bulk concentration of ions of species k, respectively. The linearized equation gives the Debye-Hückel theory, and is applicable to the diffuse layer. According to the Debye-Hückel theory, external fields are screened in the electrolyte with the potential $V_p(x)$ decreasing exponentially from its value on the boundary V_s,

$$V_p(x) = V_s e^{-\kappa X}. \tag{2.3}$$

The Debye screening length κ^{-1} is given by

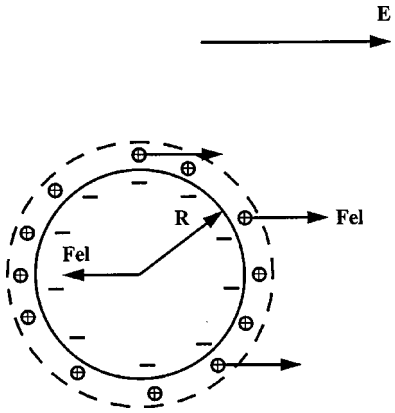

FIG. 2. Schematic view of a (negatively charged) spherical particle of radius $R > \kappa^{-1}$ during electrophoresis in an electrolyte.

$$\kappa^{-1} = \left(\frac{\varepsilon_b\varepsilon_0 kT}{e^2\Sigma_k z_i^2 C_i}\right)^{1/2}. \tag{2.4}$$

The general solution of the Poisson-Boltzman equation is called the Gouy-Chapman model. It has been compared with detailed numerical solutions as well as Monte Carlo simulations and found to be quite accurate (Russel *et al.*, 1989). However, for our purposes in this review, the simpler Debye-Hückel theory is adequate.

C. Electrophoresis and electro-osmosis

Consider now an external electric field (associated with a current in the solution embedding the probe ion. For simplicity, this current is considered uniform). This field exerts a force on the probe, but it also acts on the surrounding ions. In particular, the ion cloud, of typical thickness κ^{-1}, surrounding the polyelectrolyte contains an excess of counterions, which are dragged in the opposite direction and interact hydrodynamically with the probe ion (Fig. 2). The full calculation is rather complex (Russel *et al.*, 1989), but simple solutions can be found in two limiting cases: for a thick Debye layer (κ^{-1} larger than the particle size R), the electric force and the viscous drag force can be worked out independently, leading to a velocity scaling as QE, where Q is the total particle charge. For a sphere, for instance, one gets (Hückel, 1924)

$$\mu = v/E = Q/6\pi\eta R. \tag{2.5}$$

In the opposite case, of a Debye layer thin as compared with particle size, shear is essentially restricted to a layer of thickness κ^{-1} surrounding the particle, and one must solve the Navier-Stokes equation $\eta\Delta V_p = -\rho E$, where ρ is solution of the Gouy-Chapman (or Debye-Hückel) model inside the Debye layer and zero outside. The velocity becomes independent of the particle size and shape (Smoluchowski, 1903):

$$\mu = \frac{\varepsilon_b\varepsilon_0\zeta}{\eta}, \tag{2.6}$$

where we have introduced the zeta potential ζ, which represents the potential on the surface at which shear appears in the fluid surrounding the solution. Because of the possible presence of a Stern layer moving with the particle, this potential may be different from the surface potential. In the Debye-Hückel limit (i.e., ignoring, among other approximations, the Stern layer), the mobility can be expressed as a function of the surface charge density[3]:

$$\mu = \frac{\sigma}{4\pi\eta\kappa}. \tag{2.7}$$

Actually, due to a formal analogy between the hydrodynamic equations, describing the flow around a moving object, and the Laplace equations, describing the potential around an insulator, the electrophoretic velocity of a smooth object (as regards the Debye length) is independent of its size and shape. This has of course important consequences for electrophoretic separations.

Note also that the Smoluchowski theory, as presented here, describes the mobility of the particle, *because we made the assumption that the fluid is at rest at infinity*. Beyond the Debye layer, the fluid is neutral and undergoes no force. What the Smoluchowski equation actually does is to describe the relative motion of the charged surface and of the surrounding fluid. It equivalently applies to the motion of the electrolyte in the vicinity of an immobile charged surface, a phenomenon called electro-osmosis or electroendo-osmosis. To get a more practical insight, consider an infinitely long pipe filled with an electrolyte, with a nonzero zeta potential and a diameter much larger than the Debye length. The surface may be positively or negatively charged. Choosing for definiteness a negatively charged surface, e.g., glass in the presence of water at *p*H 7, we find that a positively charged Debye layer forms along the pipe surface. When an electric field is applied along the pipe, the portion of fluid contained in the Debye layer is dragged towards the cathode. Solving the Stokes equation with the boundary condition of zero velocity at the surface leads to a ''quasiplug'' flow profile, with shear localized within the Debye layer and a uniform velocity in the remainder of the pipe, given by Eq. (2.6). Electro-osmosis can have very dramatic consequences on the performance of practical electrophoretic separations, and it must be thoroughly controlled (for instance, by the use of neutral gels in the case of gel electrophoresis).

D. Review of polymer conformations

As a starting point, we consider a polyelectrolyte made of a sequence of monomers of typical size d. Most of the polyelectrolytes encountered in practice are persistent chains (their persistence length l_p is significantly larger than the monomer size).[4] For convenience, we represent them as a flexible cylinder of diameter d and contour length L. It is also convenient to introduce the *Kuhn length* $l = 2l_p$ (the chain behaves as a random walk of Kuhn segments). For L larger than l, the conformation of the polymer is a random walk of step l, with an average end-to-end distance R_N and a radius of gyration R_g related by

$$R_N = \sqrt{6}R_g = l\sqrt{N_k} = (lL)^{1/2}, \tag{2.8}$$

where we have introduced the number of Kuhn segments $N_k = L/l$. For very long chains, however, *excluded-volume interactions* (i.e., the fact that a position in space cannot be occupied by two monomers simultaneously) introduce an extra repulsion, which expands the chain. These interactions are characterized by the excluded-volume parameter v_F. The exact value of excluded volume depends on the details of molecular structure and solvation, but a rough scaling estimate in good solvent can be proposed:

$$v_F \approx l^2 d \tag{2.9}$$

(see, for example, Schaeffer *et al.*, 1980).[5] The crossover to this excluded-volume behavior occurs for a critical end-to-end distance,

$$R_\nu \approx l^2/d \tag{2.10}$$

i.e., for a chain size of order

$$N_\nu = (l/d)^2. \tag{2.11}$$

For larger chains the end-to-end distance scales as

$$\begin{aligned} R_F &= lN_k^{1/2}, && N_\kappa < N_\nu \\ R_F &= R_\nu (N_\kappa/N_\nu)^\nu, && N_\kappa > N_\nu, \end{aligned} \tag{2.12}$$

where the Flory exponent ν is approximately equal to $\frac{3}{5}$.[6] In practice, the two situations (Gaussian or excluded volume) can be encountered depending on the length and persistence length of the polymer. Duplex DNA, for instance, crosses over from Gaussian coil to excluded-volume conformation around 10 kilobases (depending on the salt environment; see Douthart and Bloomfield, 1968; Smith, Perkins, and Chu, 1996), a size very relevant for practical applications.

E. Polyelectrolytes at rest in solution

We now focus on a uniformly charged, linear polyelectrolyte. The conformation and Brownian dynamics

[3]Because of the complications raised by the Stern layer and by interfacial chemical equilibria, the absolute evaluation of the electrophoretic mobility is a rather difficult (and very specific) problem, especially for a biomolecule (see Stigter, 1978a, 1978b for the case of DNA). Therefore the zeta potential generally has the status of a phenomenological parameter, measured rather than calculated *ab initio*.

[4]Qualitatively, the persistence length is a measure of the chain's rigidity, or more exactly of the range of orientational correlations along a chain submitted to Brownian forces.

[5]Note that this is not just the occupied volume, since for conformational properties the important parameter is the probability that two segments *oriented at random* intersect.

[6]More precisely, Eqs. (2.16)–(2.19) correspond to an athermal solvent in the language of polymer physics, i.e., to a system in which all interactions are purely steric.

TABLE I. Kuhn length and excluded-volume parameters of a polyelectrolyte, for the different regimes.

Value of κ^{-1}	Kuhn length	Excluded volume	Conformation
$\ll l_0; < d$	l_0	$l^2 d$	coil
$\ll l_0; > d$	l_0	$l^2 \kappa^{-1}$	coil
$> l_0; < L$	κ^{-1}	κ^{-3}	coil
$> L$			rod

of polyelectrolytes in the absence of external forces obey very different laws, depending on the relative values of κ^{-1}, the local diameter d, the "intrinsic" (i.e., in the absence of electrostatic forces) Kuhn length l, the contour length L, and the charge density σ of the polyelectrolyte[7] (for a review, see Barrat and Joanny, 1996). In situations currently encountered in electrophoresis, i.e., relatively highly charged polyelectrolytes ($\sigma l_B \sim \varepsilon$) and high-salt solution (ionic strengths of order 10 ~100 mMol),[8] κ^{-1} is of order 1–3 nm. The conformation of the polyelectrolyte at rest obeys Eq. (2.12), with l given in Table I.[9]

It should also be noted that in electrophoresis conditions, κ^{-1} is smaller than the contour length of all polyelectrolytes except very short oligomers, but of the same order of magnitude as typical molecular diameters of biopolymers. This similarity (in addition to other problems mentioned above) makes direct *ab initio* calculations of electric properties difficult. κ^{-1} is also, in general, somewhat smaller than the intrinsic persistence length of these molecules, but not by much, so that the actual Kuhn length l is itself (moderately) dependent on the ionic strength of the solution. In the following, it will be convenient to consider the Kuhn length as the elementary chain unit, and to introduce the charge per Kuhn length $\sigma l = q_k$, and the friction per Kuhn length ξ_k (of order ηl, with η the viscosity of the surrounding solvent and ignoring numerical factors of order 1).

F. Polyelectrolytes in an external field

An external, nonelectric force, applied on each monomer (for example, in sedimentation), induces a motion at velocity v. For "low" velocities (which means, in practice, in all conditions reasonably achievable in aqueous buffers), the counterion cloud remains in quasistatic equilibrium around the polyelectrolyte (i.e., "retardation effects" are negligible; Russel *et al.*, 1989), and the behavior is the same as that of a neutral polymer: hydrodynamic interactions between monomers build up and the coil essentially behaves as a massive object of size R_g, impermeable to the flow (so-called Zimm behavior), with the well-known consequence that

$$v_{\text{sedimentation}} = F/\xi_{\text{tot}} = f_k N_k / \eta R_g \propto N^{1-\nu} \tag{2.13}$$

is size dependent (f_k is the force per Kuhn length).

Consider now the same polyelectrolyte in an external electric field. In electrophoresis buffers, κ^{-1} is small and we are in the Smoluchowski regime: counterions screen hydrodynamic interactions over distances larger than the Debye length.[10] Shear in the surrounding fluid is essentially restricted to a cylinder of diameter ($d + 2\kappa^{-1}$), and the mobility is often expressed in a formula of the type of Eq. (2.6). This explains the well-established (and unfortunate) fact that the electrophoretic mobility μ_0 of a long flexible polyelectrolyte in free solution is independent of its total length (the more general case of arbitrary fractal objects was considered by Brochard-Wyart and de Gennes, 1988).[11]

The independence of the electrophoretic mobility of uniformly charged polyelectrolytes prevents size fractionation in free liquid, so electrophoresis could be used for size fractionation only thanks to the use of gels. Before considering the models of gel electrophoresis *per se*, however, it is important to remark that in this case the polyelectrolyte is submitted to electric forces, to friction with the surrounding fluid (as in free electrophoresis), *and to steric forces exerted by the gel itself*. For a long time, this latter point was overlooked. The simplicity of Eq. (2.6) prompted the widespread use of a *local force picture*, in which each "monomer" (or Kuhn length, indifferently) of the polyelectrolyte is independently submitted to an electric force $E q_{\text{eff}}$, arising from an effective charge, and to its hydrodynamic friction,

$$v = \frac{F_{\text{el}}}{F_{\text{drag}}} = \frac{q_{\text{eff}} E}{\xi_k}. \tag{2.14}$$

This local force picture was applied to gel electrophoresis the same way as in free liquid. It has been recently pointed out by Long, Viovy, and Ajdari (1996a, 1996b, 1997) that the application of a local force picture to a flexible polyelectrolyte submitted to electric and nonelectric forces may lead to serious errors in the general case, e.g., in the evaluation of forces and chain conformations. The point is that the local force picture is cor-

[7]The conformation of polyelectrolytes in the semidilute regime, i.e., when polyelectrolytes overlap, is also a complex question, but is not useful for gel electrophoresis, so we do not consider it here.

[8]Indeed, because of counterion condensation (Manning, 1969), σl_B cannot exceed e, so this expression represents a good order of magnitude for a relatively large range of densely charged linear polyelectrolytes.

[9]The theory of polyelectrolytes yields a further characteristic length (see Odijk, 1977 and Skolnick and Fixman, 1977). In the situations encountered in electrophoresis, though, this length is smaller than κ^{-1} and irrelevant for the dynamics.

[10]More exactly, the long-distance hydrodynamic coupling of the polyelectrolyte motion with the surrounding fluid decays as $(1/\kappa r)^3$, instead of $1/r$ as in the Zimm case (Ajdari, 1992), which is sufficient to render hydrodynamic coupling negligible.

[11]Actually, experiments suggest that a weak orientation of polyelectrolytes, which could lead to a size dependence of the mobility, may occur in free liquid at very high fields (Jonsson *et al.*, 1993). This effect, however, is probably too weak to be practically useful.

rect only if the surrounding fluid is at rest (at distances larger than the Debye length). Consider, for instance, the extreme case of a polyelectrolyte completely arrested by strong interactions with an immobile obstacle. Without going into the details of the interaction and conformation changes, it is clear that the polyelectrolyte will reach a steady state in which its center of mass has no net motion in the direction of the field.[12] It will then act as an immobile microgel, i.e., it will pump fluid by electro-osmosis in a direction opposite to its spontaneous direction of electrophoresis. It is obvious in this case that hydrodynamic interactions on scales larger than κ^{-1} cannot be ignored. We proposed a general scheme for treating the case of polyelectrolytes submitted to a combination of electrical and non-electrical forces, taking advantage of the fact that, in the low-velocity/low-Reynolds-number situation relevant to electrophoresis, the electrohydrodynamic equations can be linearized. Then, the motion of the polyelectrolyte (and of its surroundings) submitted to an electric field E and to an external force F_{ext} is solved by superposing the flows obtained in the pure electrophoretic ($F_{\text{ext}}=0$) and pure nonelectrophoretic ($E=0$) cases. The mobility of an object in the general case is given by the balance of forces:

$$F_{\text{ext}}-\xi(v-\mu_0 E)=0, \tag{2.15}$$

where ξ is the friction of the polyelectrolyte in the conformation it reaches in the steady state. Generally, the evaluation of this conformation has to be done self-consistently, and this is the difficult part of this formalism. However, simple solutions can be found in several cases, e.g., in the limit of small fields (weak deformation) or strong fields (fully stretched chain). As a particular case of Eq. (2.15), the stall force (force at which $v=0$) for a polyelectrolyte in a low electric field is

$$F_{\text{stall}}=\xi\mu_0 E\cong\eta R_g\mu_0 E, \tag{2.16}$$

a result very different from the one obtained from a local force picture,

$$F_{\text{stall}}=Eq_{\text{eff}}. \tag{2.17}$$

Note in particular that, if Eq. (2.16) does not explicitly take into account the polyelectrolyte charge, it is dimensionally equivalent to Eq. (2.17) and actually represents the combination of the direct electric force exerted on the polyelectrolyte and of the indirect action of the electric field on the counterions, via hydrodynamic coupling. Equations (2.16) and (2.17) become equivalent at scaling level in the limit of strong fields, when the polyelectrolyte is fully stretched.

III. A FEW NUMBERS AND EXPERIMENTAL FACTS

The theoretical elements presented above and most models that will be discussed in the course of this review are quite general and can be applied to various types of molecules, by providing the values of a few molecular parameters such as the free-flow mobility, the persistence length, or the friction of the polyelectrolyte. Therefore it is useful to have in mind such values for the major families of polyelectrolytes (and separation media) used in electrophoresis.

A. Polyelectrolytes most often separated by electrophoresis

1. Duplex DNA: "The" model polyelectrolyte

For a polymer physicist, DNA is a dream model macromolecule. It occurs naturally in totally monodisperse size distributions and in a huge range of sizes, from one base to several hundreds of Megabase pairs (Mb; the largest human chromosomes actually have a contour length of several cm!). Due to its polyelectrolyte character, the persistence length of duplex DNA varies somewhat with the ionic strength of the buffer. In electrolytes currently used in biology, it is of the order of 30–60 nm (we shall use a typical value of 50 nm in the following). The aromatic parts specific from each nucleotide are buried in the interior of the double helix, which, at neutral to alkaline pH, exposes negatively charged phosphate groups (about two charges per base pair).[13] The persistence length is also relatively independent of base-pair content, although specific repetitive sequences are known to induce local "kinks" or increased flexibility, which may be important recognition sites for DNA-binding proteins (Lebrun *et al.*, 1997) and may also affect electrophoretic properties (Levene and Zimm, 1989). Also note that, depending on the organism, DNA may exist in linear or circular form. Since duplex DNA has a finite torsional elasticity, its local conformation requires three variables to be fully characterized, the bend, the twist, and the writhe. A detailed account of the exciting problems raised by DNA topology is beyond the scope of this article (see, for a review, Dubochet *et al.*, 1992 or Katrich *et al.*, 1997), but it is worth noting that biologically pertinent circular DNA with nonzero twist and writhe (supercoiled) can be separated by electrophoresis (see Sec. VIII.B.1).

2. Single-stranded nucleic acids

In Nature (and in the usual *in vitro* buffers), DNA occurs mainly as a double helix, but RNA exists only in single-stranded form. Because the aromatic parts of the nucleotides are rather hydrophobic, however, they tend to self-hybridize and form secondary structures (local

[12]This situation is of direct relevance to gel electrophoresis: for instance, we shall see that analytes can get hooked around gel fibers for times long enough to reach a quasiequilibrium conformation similar to that of a tethered chain.

[13]The purine nucleotides are chemically instable at low pH, so in most practical instances DNA is used at pH above 6. It is worth noting, though, that Perego *et al.* (1997) recently were able to separate by fast capillary electrophoresis at low pH, oligonucleotides with the same size but different base compositions, using the difference between the pK's of the nucleotides.

intramolecular double helices) with a semicompact and complex topology. These structures generally lead to poor resolution and difficult to interpret size information in electrophoresis. The same is true of single-stranded DNA. Therefore RNA analysis—and most importantly DNA sequencing, which is performed on single-stranded DNA—use a combination of elevated temperature and *denaturating buffers* (hydro-organic solvents which solvate single-stranded DNA more efficiently than water and destroy secondary structures: the most common is 7 M urea aqueous solution, but others such as formamide-water mixtures can be used). In such conditions, the DNA or RNA behave as flexible linear polyelectrolytes with about one charge per base and a persistence length of order 5 nm (Tinland *et al.*, 1996).[14]

3. Proteins

Protein electrophoresis is about as important as DNA electrophoresis applicationwise, but it has not attracted as much attention from physicists, probably because it depends on much more specific and ''chemical'' parameters. In contrast with DNA, proteins occur in Nature as globular objects with a number of different acidic or alkaline sites, related to their amino acids *and* to their tertiary structure (the famous protein folding problem). This tertiary structure can be destroyed by performing electrophoresis in the presence of a strong surfactant like sodium dodecyl sulfate (SDS), which transforms the protein into a linear uniformly charged polyelectrolyte (Andrews, 1986). To my knowledge, the persistence length of protein-SDS complexes has not been accurately determined, but one can expect a value of the same order as for DNA in denaturating conditions, of a few nm. However, no equivalent of DNA sequencing, in which mobility information can be transposed into sequence information, exists for proteins, so that size fractionation is only a relatively minor part of the story. The major tool of proteome analysis is 2D electrophoresis. In this technique, proteins are separated in a first dimension in the native state by isoelectric focusing, a technique in which species are focused in a *p*H gradient according to their isoelectric point, and in a second dimension by size fractionation in the denaturated state (for a review, see for example, Dunn, 1997).[15]

4. Other polyelectrolytes

In principle, all charged objects can be separated by electrophoresis, and many examples of applications exist, although these are far fewer for other polyelectrolytes than for DNA and proteins. The use of gel electrophoresis in the analysis of synthetic polymers is still not as common among chemists as, say, chromatography, but it is developing rapidly for two main reasons. The first is the increasing range of technical applications of polyelectrolytes, and the second is the development of capillary electrophoresis, which offers more versatile detection methods than do gels (see Sec. IX). Carbohydrates, particularly biological polysaccharides, are also attracting increasing interest, and these are relevant to the mechanisms discussed here (for a review, see El Rassi, 1997). Finally, applications of electrophoretic size fractionation of mesoscopic particles such as latex or cells also appear here and there in the literature and often give rise to specific mechanisms (see Secs. VIII.A.4 and IX.D).

B. Gels used in electrophoresis

Several criteria enter in the choice of a gel for electrophoresis, such as compatibility with the molecules to be separated (attractive interactions between the analytes and the gel generally lead to considerable dispersion), compatibility with the detection method (for instance, turbidity or interactions with staining dyes may be detrimental), ease of preparation and of manipulation, cost, reproducibility, and pore size. A large number of hydrophilic gels have been employed for gel electrophoresis (see Righetti, 1989, for a review), but the most popular by far remain polyacrylamide and agarose. Polyacrylamide is a flexible neutral polymer. For gel electrophoresis, it is prepared in the presence of a few percent of bifunctional cross-linker (e.g., Bis-acrylamide). Cross-linked acrylamide has a low modulus, so it is generally cast vertically between glass plates or in tubes. Agarose is a rather rigid polysaccharide. It is soluble in water only at high temperature and forms upon cooling a gel by lateral association of the chains into rigid helical bundles. It is actually a physical, reversible gel, but one with such a large hysteresis that it behaves as a permanent one on any reasonable time scale at room temperature. Its particular structure is responsible for its large pore size. In contrast to polyacrylamide, agarose gels are brittle when thin, so they are generally used in the ''submarine'' mode, as a thick slab resting on the bottom of a shallow cuvette filled with buffer. In both methods, several samples are introduced simultaneously in small slots (loading wells) reserved in the gel during casting, and the field is then applied along the larger dimension of the gel. Detection of samples after migration can be performed by various means—coloration, autoradiography, fluorescence, etc. The basic electrophoresis apparatus is very simple and can fulfill many needs. Sophisticated automated apparatuses also exit for applications in which high output and reproducibility are necessary, such as sequencing.

Probably the most important parameter for choosing one type of gel over another for size fractionation is the average pore size. In principle, there are numerous ways

[14]Note that electrophoresis in a gradient of denaturant conditions (buffer or temperature) can be used to gain information such as the global stability of secondary structures in single-stranded DNA or RNA, or local base-pairing mismatches in duplex DNA. See, for example, Gelfi *et al.*, 1997, and references therein.

[15]The mechanism of separation in isoelectric focusing depends on chemical equilibria, and is not discussed in the present review. The ''second dimension'' of 2D protein, though, is relevant to the mechanisms described here.

to measure the pore size of a gel, but unfortunately they yield rather different results. For agarose, for instance, the mobility of latex spheres yields about 150 nm in a 1% gel (Griess, Moreno, *et al.*, 1989), whereas atomic form microscopy studies yield a value larger than 350 nm (Pernodet, Maaloum, and Tinland, 1997). More indirect methods, involving, for example, the fitting of DNA mobility with a model, yield values in the same range, but with discrepancies between different groups (see Slater, Rousseau, *et al.*, 1988; Mayer, Sturm, and Weill, 1991; Mayer, Sturm *et al.*, 1993; Viovy, 1996; Tinland, Pernodet, *et al.*, 1998). A probable reason for these discrepancies is that different methods probe different moments of a relatively large pore-size distribution. In addition, agarose gel is a natural product and an out-of-equilibrium structure so that, as shown for example, by Griess, Guiseley, and Serwer (1933), its pore size depends significantly on the gelation history, chemical derivatization, and average molecular weight of a given batch. Moreover, it was shown by Stellwagen and Stellwagen (1989) that gels are not inert and deform in the course of electrophoresis. To summarize, it is probably not reasonable to claim a very accurate and definite measurement of a gel pore size for electrophoresis, but agreement can be obtained on orders of magnitude, typically 200–500 nm for agarose. For a very flexible polymer like acrylamide, chains dynamically sample the whole volume, so that the concept of a ''pore'' is even more disputable. Experimental evaluations of the pore size of acrylamide ranged from 5 to 100 nm depending on the model used. Generally, ''Ogston-type'' models (see Sec. IV below and Holmes and Stellwagen, 1991a, 1991b; Stellwagen, 1998), yield values around 100 nm, much larger than those based on the reptation model, around 10 nm (Sec. V, Pluen *et al.*, 1998). These latter values seem more consistent with electron microscopy (Hsu *et al.*, 1989) and also with theoretical approaches identifying the pore size with the screening length for hydrodynamic interactions (Grossman and Soane, 1991; Viovy and Duke, 1993; Viovy and Heller, 1996). The concentration dependence of the pore size also suffers from some uncertainty, but it generally lies in the range $c^{-0.5}$–$c^{-0.8}$, i.e., between the theoretical predictions for a random suspension of rodlike fibers (exponent -0.5) and that for a semidilute solution of flexible polymers in good solvent (exponent -0.75, de Gennes, 1979).

Finally, we should point out that capillary electrophoresis has promoted the use of non-gelled polymer solutions as a support for polyelectrolyte size fractionation. This procedure will be discussed in Sec. IX.

C. Elementary phenomenology of gel electrophoresis

Early applications of gel electrophoresis generally involved relatively small polyelectrolytes, notably proteins in their native state. In such cases, it was found empirically that the ratio of the gel electrophoresis mobility μ to the free-solution mobility μ_0 was reasonably described by the expression (Ferguson, 1964)

$$\ln(\mu/\mu_0) = -K_r c, \tag{3.1}$$

where c is the gel concentration and K_r, the *retardation coefficient*, is proportional to the particle radius squared. This approach was tentatively applied to flexible macromolecules, assuming that the particle radius in this case was the macromolecule radius of gyration R_g, but it encountered uneven success (Stellwagen, 1987, presents an extensive review; see also Holmes and Stellwagen, 1991a, 1991b). Most strikingly, large DNA, for which an extrapolation of the Ferguson plot would predict a mobility decaying very fast with the radius of gyration, exhibited the opposite behavior (Flint and Harrington, 1975; McDonnel *et al.*, 1977; Fangman, 1978; Hervet and Bean, 1989; see also Stellwagen, 1987; Calladine *et al.*, 1991): The mobility of large DNA saturates at a finite value independent of molecular size. Moreover, it becomes dependent on the field, in contrast with the behavior of smaller molecules. It was readily anticipated that this behavior was due to the flexibility of the DNA molecules, as very clearly stated by McDonnel as early as 1977: ''High voltage gradients can presumably drive large molecules through gel channels too small for them to penetrate in their unperturbed conformations, and the larger the DNA the more readily it is deformed.'' These observations were the starting point for the development of theoretical models which in turn motivated a number of new experimental ways of investigating migration mechanisms in gel electrophoresis.

D. Band broadening and resolution

Electrophoretic mobility has been the first parameter of interest for theorists, but experimentalists are actually more interested in the resolution between peaks than in the mobility. The resolution between two bands or peaks corresponding to monodisperse samples of close sizes $N-n$ and $N+n$ (with $n \ll N$) is conveniently measured by the ratio $R_{\rm es}$, given by

$$R_{\rm es}^2 = [\langle x(N_k - n)\rangle - \langle x(N_k + n)\rangle]^2 / w^2(N_k). \tag{3.2}$$

For the case of conventional gel electrophoresis, in which the bands are analyzed after a common migration time, $\langle x(N_k)\rangle$ and $w^2(N_k)$ represent, the electrophoretic drift of a species of size N_k after time t, $\mu(N_k)Et$, and the squared band width, respectively. For an analysis after a constant migrated distance as in automated sequencers or capillary electrophoresis, $\langle x(N_k)\rangle$ and $w^2(N_k)$ represent the average time taken by the analyte to travel the distance Z from the injection point to the detector $(Z/\mu(N_k)E)$ and the squared time-based peak width, respectively.

In the analytical sciences, one defines the ''efficiency'' of a separation method as (Grossman and Colburn, 1992)

$$P = 16x^2(N_k)/w^2(N_k). \tag{3.3}$$

A more useful quantity for electrophoresis is the resolving power, defined as

$$R_p(t)=\frac{N_k}{w(N_k,t)}\left(\frac{\partial x(N_k,t)}{\partial N_k}\right)=\frac{tEN_k}{w(N_k,t)}\left(\frac{\partial \mu(N_k)}{\partial N_k}\right). \tag{3.4}$$

This dimensionless resolving power depends on electrophoretic mobility and on bandwidth. It shows that resolution can be lost in spite of a high separation length, due to saturation of the mobility at a finite value independent of size.[16] There are many factors that can affect the experimental bandwidth, such as the size of the initial band, inhomogeneities in the gel composition and/or topology, inhomogeneities in the temperature or in the electric field, or interactions between the polyelectrolytes to be separated due to "overloading." We leave aside these effects here, to concentrate on the intrinsic band broadening related to the mechanism of molecular migration. We also ignore dispersion related to the frozen disorder of the gel (some effects of gel inhomogeneities will be discussed in Sec. VIII.A.1). Intrinsic band broadening gives the highest resolution achievable due to the physical mechanisms of the separation process and is therefore of paramount importance. It can be expressed as

$$w^2(N_k,t)=\langle[x(N_k,t)-\langle x(N_k,t)\rangle]^2\rangle=2d_c(N_k)t, \tag{3.5}$$

where the brackets denote an average over an ensemble of chains. This is the definition of the dispersion coefficient d_c. Until recently, band dispersion had not received as much attention as mobility, either from theoreticians or from experimentalists, probably because it is more difficult to measure accurately. This situation, however, is changing rapidly.

IV. GEL ELECTROPHORESIS OF GLOBULAR PARTICLES

A. The free-volume model

In this rather straightforward approach to gel electrophoresis, the gel is assumed to act as a sieve with a distribution of pore sizes, and the separation is viewed as a kind of electric-field-driven filtration. The modeling of the mobility is based on the rather drastic assumption that the ratio of the electrophoretic mobility in the gel μ relative to the mobility in free solvent μ_0 is f, the fractional volume available to the particle in the gel,

$$\frac{\mu}{\mu_0}=f. \tag{4.1}$$

Using geometrical models in which the gel and the moving particle are represented by simple objects, this fractional free volume can be calculated exactly by the statistics of the intersections between the particle and gel components distributed randomly. This was done first by Ogston (1958) for spheres in a suspension of long fibers. A similar model, in which the obstacles are approximated as two-dimensional objects (like thin sheets) was treated by Giddings *et al.* (1968). Finally, these results were generalized to a combination of different geometries by Chrambach and co-workers (Rodbard and Chrambach, 1970, 1971; Lunney *et al.*, 1971; Chrambach and Rodbard, 1971). This model is known as the *free-volume model*. The fractional free volume is expressed as

$$f=\exp(-sL) \tag{4.2}$$

for a particle of largest dimension L in a suspension of planar obstacles with surface area s per unit volume,

$$f=\exp(-jS) \tag{4.3}$$

for a particle with excluded area S in a suspension of long fibers with total length j per unit volume, and

$$f=\exp(-nV_p) \tag{4.4}$$

for a particle with excluded volume V_p in a suspension of point objects with number density n. For a spherical particle,

$$\begin{aligned} L&=2(R+r),\\ S&=4\pi(R+r)^2,\\ V_p&=(4\pi/3)(R+r)^3, \end{aligned} \tag{4.5}$$

where R is the effective particle radius, and r is the smaller dimension of the obstacles (half thickness of a sheet, fiber radius, or radius of a spherical obstacle, respectively). These expressions, combined with Eq. (4.1) lead to an expression for the mobility identical to the empirical one proposed by Ferguson [1964; Eq. (3.1)], provided the retardation coefficient is identified with

$$K_r=c_1(R+r) \tag{4.6}$$

for sheetlike obstacles,

$$K_r=c_2(R+r)^2 \tag{4.7}$$

for fiber obstacles, and

$$K_r=c_3(R+r)^3 \tag{4.8}$$

for spherical obstacles (ignoring coupling terms, i.e., assuming that fractional free volumes arising from different types of obstacles are simply multiplicative. The model can even be generalized to particles in a more complicated suspension as $f=\exp[-(sL+jS+nV_p)]$).

In this model, optimal separation is expected when the particle size is comparable with the average pore size of the gel. This pore size can be adapted to the particles to be separated, by changing the gel concentration (in a limited range imposed by the chemistry and by the mechanical properties of the gel) or the nature of the gel. In spite of a few attempts to take into account effects ignored in the free-volume model, such as hydrodynamic interactions (Lumpkin, 1984), gel flexibility (Bode, 1979), or random potential barriers (de Gennes,

[16]Biologists also find it convenient to specify the quality of separation by the "separation factor" $S=N_k/R_p$ (Lerman and Sinha, 1990). This factor indicates the smallest difference in size that can be resolved. Note that this factor is not dimensionless, i.e., it depends on the "elementary unit" chosen to measure the polyelectrolyte's size.

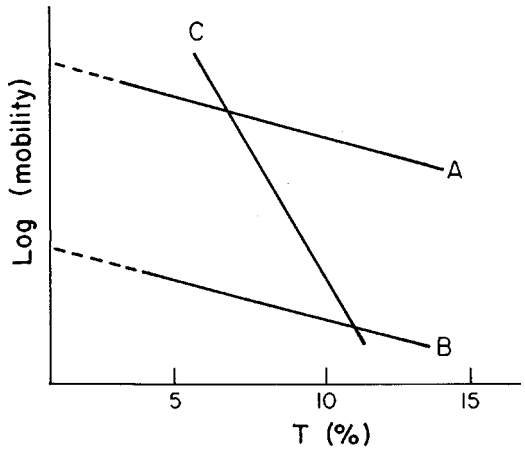

FIG. 3. "Ferguson plot" of mobility vs gel concentration. According to the free-volume model, Log(mobility) should decay linearly with gel concentration $T\%$. The intercept at $T\%=0$ is the free mobility (proportional to charge ratio), whereas absolute value of the slope increases with particle size, i.e., with decreasing fractional free volume. For instance, A corresponds to particles with a high charge ratio (high free-flow mobility) and a small size (weak slope), B to a particle with low charge ratio and small size, C to a particle with a high charge ratio and a large size (steep slope).

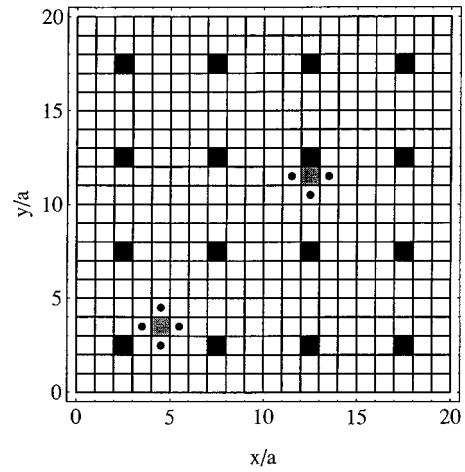

FIG. 4. Example of a lattice system used in the Slater-Guo lattice model. Black squares represent obstacles (here of size 1×1) and gray ones moving particles. Particles can move to sites marked by the black dots. From Slater and Guo, 1996a, reprinted with permission.

1982), this model has remained until now the dominant approach for interpreting the gel electrophoresis mobility of small and relatively globular objects, such as native proteins. An in-depth review of the free-volume model and of its implications and limitations was published by Tietz (1988). Equation (3.1) has been widely verified in starch, polyacrylamide, and agarose, and it is still being used for molecular weight determination by means of the Ferguson plot (1964); see Fig. 3. Once the linear plot of K_r versus R has been determined using standards of known radius and charge, the measure of the retardation coefficient for an unknown particle gives access to its effective radius and to its effective charge.[17] Equation (4.7) seems to prevail for both agarose and acrylamide, suggesting that these gels are valuably modeled by a random suspension of rods. This square dependence is not always observed, however, and other gel geometries, in which the gel is better represented by pointlike or sheetlike obstacles have been invoked to explain these differences. Those geometries involving planar or pointlike objects, however, do not seem very plausible from a molecular point of view and appear more as curve-fitting commodities than as real mechanistic evidences. For instance, one can hardly imagine how a solution containing a few percent of globular objects could form a gel with mechanical rigidity. On the other hand, it is also difficult to understand how a random suspension of extended sheetlike objects could be permeable to particles. More generally, this raises questions about the topology of the gel, a topic that is not addressed at all in the free-volume model. Experimental occurrences of nonlinear Ferguson plots are not uncommon either and cast further doubts on the generality of this model. A very interesting analysis of the conceptual difficulties raised by the generalization of the free-volume model to nonspherical particles is that of Arvanitidou, Hoagland, and Smizek (1991).

B. Slater-Guo model

A rather radical reconsideration of the free-volume model has recently been undertaken by the Slater group (Slater and Guo, 1995, 1996a, 1996b). These authors have pointed out numerous drastic assumptions and problems implicit in the model (including the few already mentioned here) and proposed a simple lattice model in which key parameters such as the gel concentration, the available free volume, the pore size, etc. are trivial, and dynamic parameters such as the diffusion coefficient or the electrophoretic mobility can be calculated exactly. The model is based on a square lattice with periodic boundary conditions (Fig. 4). Obstacles can be distributed periodically or randomly and can occupy one (as in Fig. 4) or more lattice sites. The moving particles are also inscribed on single or multiple sites on the lattice, and a hard-core excluded-volume interaction is applied between particles and obstacles. In an electric field, the mean trial time (duration of one simulation step) of a particle is given by

$$\tau_0=\frac{\tanh(\varepsilon)}{\varepsilon}\approx1-\frac{\varepsilon^2}{3}+O(\varepsilon)^3, \tag{4.9}$$

where

[17]In real systems, the presence of extra viscous friction and residual electro-osmosis may affect this simplified view and lead to mobilities extrapolated at zero concentration, different from the actual free-solvent mobility. We ignore this complication here.

$$\varepsilon = \frac{QEa}{2kT} \tag{4.10}$$

is a reduced electric field, Q is the particle charge, and a is the lattice period.[18] In most of the cases considered to date by Slater and Guo, calculations are done to first order in ε, i.e., Eq. (4.9) is linearized and the $E \to 0$ limit is taken. The jump probabilities (in the absence of obstacles) are

$$P \pm y = \tfrac{1}{4},$$

$$P \pm x = \frac{\frac{1}{2}}{1+\exp(\mp 2\varepsilon)} \approx \frac{1 \pm \varepsilon}{4} + O(\varepsilon^2) \tag{4.11}$$

for the directions perpendicular and parallel to the field, respectively. Jumps to sites occupied by obstacles are forbidden. Then, a master equation for the evolution of the probability of occupancy of each site can be written as a system of $P_L^2 - r^2$ rate equations (P_L is the lattice period and r the size of an obstacle, assuming one obstacle per lattice unit cell). This system can be solved exactly, formally up to arbitrary cell sizes, and in practice up to sufficiently large sizes to be close to the asymptotic limit. For random lattices, several independent realizations of the system must be averaged. The first conclusion of the model is that the fractional free volume is not the only parameter influencing the mobility. Expansion of the mobility in the concentration of obstacles leads to solutions of the form

$$\mu/\mu_0 = 1 - (\pi - 1)c + a_2 c^2 + \ldots, \tag{4.12}$$

where the a_2 term (and higher-order ones) are nonuniversal, and depend on the crystallographic arrangement of obstacles (for a periodic lattice), or on the degree of randomness (for lattices with various degrees of randomness; see Fig. 5). Equation (4.12) is equal at first order to an earlier prediction for particle diffusion on a square array of randomly distributed obstacles (Ernst *et al.*, 1987), which has been empirically verified (Griess *et al.*, 1989), but this equation is not the lattice equivalent of the free-volume prediction,

$$\mu/\mu_0 = 1 - c = f. \tag{4.13}$$

The free-volume prediction always overestimates the mobility (see Fig. 5). Actually, it corresponds to an "annealed" gel (i.e., a gel in which obstacles would be moving rapidly as compared with the particles). The reduction of mobility, in the case of fixed obstacles, is due to an increase in the residence time of particles on sites where they are less mobile (upstream obstacles). It is also worthwhile to point out that more disordered gels tend to decrease the mobility, at equal f. In spite of these disagreements, the lattice model of Slater and Guo has demonstrated that the free-volume model can be viewed as a reasonable approximation for compact particles at low fields and low gel concentrations. In particular, Slater and Guo could define a "generalized Ferguson-plot" approach, adapted to their 2D lattice model, which correctly predicts "molecular" parameters such as particle size, obstacle size, or pore size. This model is still under development and has recently been extended to 3D lattices (Mercier and Slater, 1998). It opens the way to an in-depth renewal of this field, which will certainly prove useful.

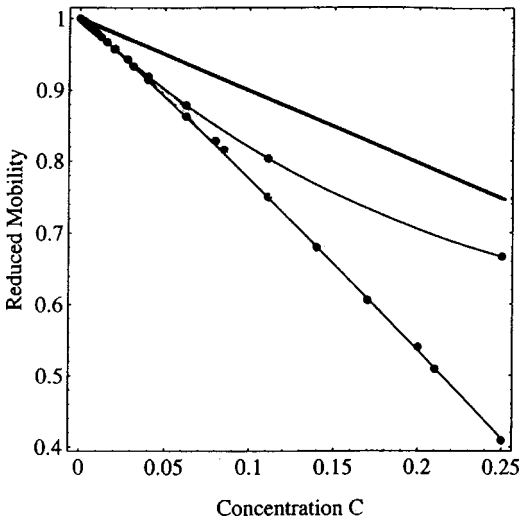

FIG. 5. Reduced mobility vs obstacle concentration, as predicted in the Slater-Guo lattice model. Curves represent, from top to bottom, the free-volume model, the periodic gel, and the random gel. Adapted from Slater and Guo, 1996b, reprinted with permission.

V. REPTATION MODELS

Neither the free-volume, nor the Slater-Guo model are able to account for the saturation of the mobility at a finite value for increasing size, observed in flexible polyelectrolytes such as DNA. The route to a theoretical understanding of the migration of linear polyelectrolytes and to modern gel electrophoresis theory was really opened up in 1982 by two seminal articles, one by Lumpkin and Zimm and the other by Lerman and Frisch. These authors independently remarked that thin flexible chains can thread their way in the gel like a snake in thick grass by a "reptation in a tube" process similar to that proposed by de Gennes in 1971 for entangled synthetic polymers. Following these ideas, a whole corpus of theoretical developments and of experiments directly inspired by theoretical predictions was developed.

A. Reptation concept

Consider a flexible, linear, uniformly charged polyelectrolyte, made of N_k Kuhn segments of length l, each bearing a charge q_k. This chain is embedded in a gel.

[18]This expression for the jump rate is derived by assuming an electric force QF and neglecting hydrodynamic interactions. Therefore the charge Q should be considered as an effective charge. For a real particle in an array of obstacles, neglecting hydrodynamics might be a problem, but the authors do not pretend at this stage to this level of realism.

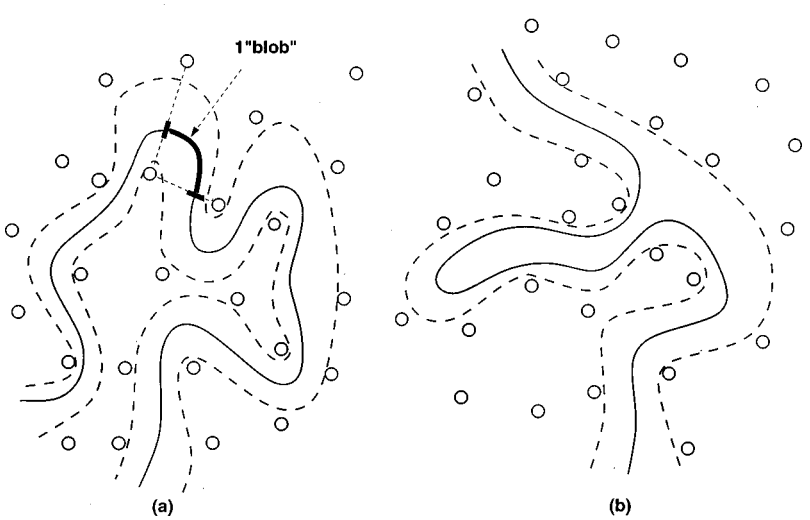

FIG. 6. Schematic representation of the chain (solid line) and its "tube" (dotted lines) in the gel (bold circles). Note that this particular figure corresponds to a rather stiff chain ($l \sim b$): (a) chain without a loop or hernia; (b) chain with a loop or hernia.

Solving the raw equation of motion of all monomers subject to the repulsive interactions of all individual obstacles in the gel can be done only by computer simulation, and analytical modeling of the dynamics of the chain requires a mean-field approach. We assume that the gel is rigid and presents a uniform pore size b, smaller than the radius of gyration of the polyelectrolyte, R_g. Note that, in the absence of electric field, driving the polyelectrolyte into the gel from an outer solution has an entropic cost. This cost is minimal if the chain follows a random-walk sequence of pores, called the *tube* after an original idea of Edwards (1967). The section of chain contained in one pore is called a "*blob*." We first consider the large-pores case in which the chain is flexible on the scale of one pore. Then, the tube can be approximated as a random sequence of N connected segments of size b. In practical situations, excluded-volume interactions are generally negligible on scale b (R_ν is larger than b), so that blobs can be considered as Gaussian.[19] Then, the chain is Gaussian at all scales larger than l, so that

$$N = N_k \left(\frac{l}{b} \right)^2 . \tag{5.1}$$

This value of the number of occupied pores corresponds to a minimum of the free energy. The fluctuations of the chain length around N were studied by Doi (Doi and Edwards, 1986). It is of order $N^{1/2}$, i.e., small for large chains, with a square averaged end-to-end distance of $R_N = N^{1/2} b$. This large-pores case reasonably describes single-stranded DNA or flexible synthetic polyelectrolytes such as polystyrene sulfonate in acrylamide or agarose, or duplex DNA in agarose (the persistence length of duplex DNA is around 50 nm, while the average pore size in agarose is of order 200–500 nm) but not, for instance, duplex DNA in acrylamide. The opposite case of *tight gels* (with $l > b$ and $R_N = l N_k^{1/2}$) will be discussed in Sec. V. F. Brownian diffusion, i.e., escape from the tube, can occur by either of two mechanisms: (i) a sliding motion along the chain contour associated with the creation of new tube sections at the chain ends [Fig. 6(a)], a mechanism called *reptation* by de Gennes, (1971; see also de Gennes, 1979); or (ii) the creation of loops or "hernias" [Fig. 6(b)], in which each pore of the gel is crossed by the chain twice instead of once. It was predicted by de Gennes in 1979 that, in the absence of electric field, such events would be exponentially improbable due to the entropy loss associated with hernias [the existence of such entropy barriers was recently supported experimentally by studies of the kinetics of field-driven loop formation (Akerman, 1996b)]. In the absence of field, then, reptation is the dominant mode of Brownian motion, and it can be described as a curvilinear 1D diffusion along the tube axis (de Gennes, 1971; Doi and Edwards, 1986). The curvilinear diffusion constant is then given by the average time for 1D diffusion over a distance Nb:

$$D_{\text{tube}} \approx kT/N\xi_b \approx kT/N\eta b, \tag{5.2}$$

where k is the Boltzmann constant, T the absolute temperature, and ξ_b the blob friction coefficient. Here and in the following sections, we ignore numerical prefactors of order one, except when specified. Theoretically "exact" numerical prefactors for the reptation theory and polymer dynamics in general can be found in Doi and Edwards (1986), but they have little practical meaning considering the crudeness of the initial assumption of uniform pore size and tube diameter involved in the model, and the nonuniversal prefactors involved in excluded-volume interactions. The thermal disengagement time is

[19] If necessary, extending the model to blobs with excluded volume using Eq. (2.12) would be straightforward and would not change the physics of the problem. It is also worth noting that for large DNA at equilibrium in a gel, excluded-volume interactions may play a significant role in the total radius of gyration, which has been neglected in biased reptation models. This has no practical consequences in the predictions of the model, however, because as we shall see, for any practically useful electric field, the effect of electric forces on the chain dimensions is generally much larger than that of excluded volume.

$$t_{\rm rep} \approx \frac{N^2 b^2}{D_{\rm tube}} \approx N^3 \tau_b , \tag{5.3}$$

where we have made use of the fluctuation-dissipation theorem and introduced the *microscopic Brownian time* of a blob,

$$\tau_b \approx \xi_b b^2/kT \approx \eta b^3/kT. \tag{5.4}$$

B. Reptation in a field: The biased reptation model

The application of an external field is able to deeply affect the reptation picture and to induce a rich and nontrivial phenomenology. Theoretical investigation of this subject was initiated independently by Lumpkin, Déjardin, and Zimm (1985) and Slater and Noolandi (1985). These two pioneering articles were followed by many others (e.g., Slater and Noolandi, 1986a, 1986b; Slater, Rousseau, and Noolandi, 1987; Slater *et al.*, 1988; and reviews in Slater and Noolandi, 1989, 1990; Zimm and Levene, 1992; Zimm, 1993). The theoretical corpus was popularized under the acronym BRM (for biased reptation model), a term introduced by Slater and Noolandi (1985). There are subtle differences between the models developed by these two groups, but they mainly correspond to the same physics, so in the following, I shall use the acronym BRM for both models.

When an electric field is applied along, say, the x direction, all blobs are subject to electric forces. For a tube not fully aligned in the field direction, the field tends to push the polyelectrolyte against the gel fibers and to ''pull'' hernias out of the tube, against the entropic barriers discussed above. Qualitatively, one expects that this tube leakage will remain improbable as long as the external force is smaller than the entropic (thermal) force. Assuming that the polyelectrolyte velocity in the gel is small compared to the free-flow velocity (this point will be checked for self-consistency later on), one can use the stall force in Eq. (2.16) as a good approximation for evaluating electrohydrodynamic forces on the blob. (hydrodynamic interactions over distances larger than b are screened by the gel, so b is the relevant scale for the application of Eq. (2.16). Therefore the condition of weak external force (on the blob scale) can be expressed as

$$\varepsilon = \eta b^2 \mu_0 E/kT \ll 1, \tag{5.5}$$

where ε is the ratio to the thermal energy, of the electrostatic potential energy associated with the displacement of one blob by a distance equal to its size. Note that this definition is different from the one previously used in the biased reptation model,

$$\varepsilon_{\rm BRM} = \frac{Eqb}{kT}, \tag{5.6}$$

which uses a local force picture (and defines q as the effective charge per blob). Also note that, assuming from free draining behavior that $\mu_0 \approx q_k/\eta l$, one expects $\varepsilon/\varepsilon_{\rm BRM} \approx l/b$: for large pores, ε is significantly smaller than predicted by the biased reptation model.

The dimensionless parameter ε, which plays the role of a reduced electric field, reflects the balance between electrohydrodynamic and thermal energy on the scale of a blob. Putting into Eq. (5.5) reasonable numbers issued from experiments, $\mu_0 \sim 3.5\times10^{-8}$ m^2/V/s, and $b \sim 200$–500 nm (see Sec. V.C.2 and discussions in Pluen, 1996; Viovy, 1996; Pernodet and Tinland, 1997; and Stellwagen *et al.*, 1997), one finds that $\varepsilon = 1$ occurs around 10 V/cm in 1% agarose. This suggests that the weak-field condition [Eq. (5.5)] is actually fulfilled only for rather low fields, consistent with direct observations by Akerman (1996b), suggesting a threshold for hernia nucleations of order 1 V/cm. The parameter ε is crucial in the theory of DNA electrophoresis and will be encountered often in the following. It can be related to another dimensionless parameter ε_k, depending on the polyelectrolyte and field only (ε also depends on the pore size):

$$\varepsilon_k = \frac{n l^2 \mu_0 E}{kT} = \varepsilon \left(\frac{l}{b}\right)^2 . \tag{5.7}$$

The second main assumption in the original reptation model is that, when Eq. (5.5) is satisfied, the chain length remains of order b [$N + O(N^{1/2})$]. These two assumptions,

(1) no hernias or tube leakage

(2) weakly fluctuating tube length,

are at the basis of an ensemble of analytical and numerical developments, loosely classified here under the generic name of ''biased reptation theories.''

The early versions of the model (Lumpkin *et al.* (1985); Slater and Noolandi, 1985; Slater, Rousseau, and Noolandi, 1987) completely ignored length fluctuations. The problem of curvilinear motion is then equivalent to the motion of a single particle submitted to electrohydrodynamic and Brownian forces, and can be mapped to the diffusion of a particle in a potential between two absorbing barriers (Feller, 1968). The nonrandom force (derivative of the potential) is the sum of electrohydrodynamic[20] forces on all blobs, projected onto the tube axis,

$$F_{\rm eff} = \mu_0 \eta R_x , \tag{5.8}$$

where R_x is the projection of the end-to-end vector onto the field direction (if the chain is arbitrarily labeled such that the ''head'' is in the most probable direction of motion, i.e., the average curvilinear mobility is positive, then R_x is also positive). The instantaneous mobility (on a time scale smaller than the tube renewal time) is then given by a projection of the curvilinear motion of the whole chain onto the field direction,

$$v = \mu_0 E \left(\frac{R_x}{Nb}\right)^2 . \tag{5.9}$$

[20]For the sake of consistency, the BRM results are recast in terms of an electrohydrodynamic rather than a local force image. This simply amounts to replacing $\varepsilon_{\rm BRM}$ [Eq. (5.6)] by ε [Eq. (5.5)].

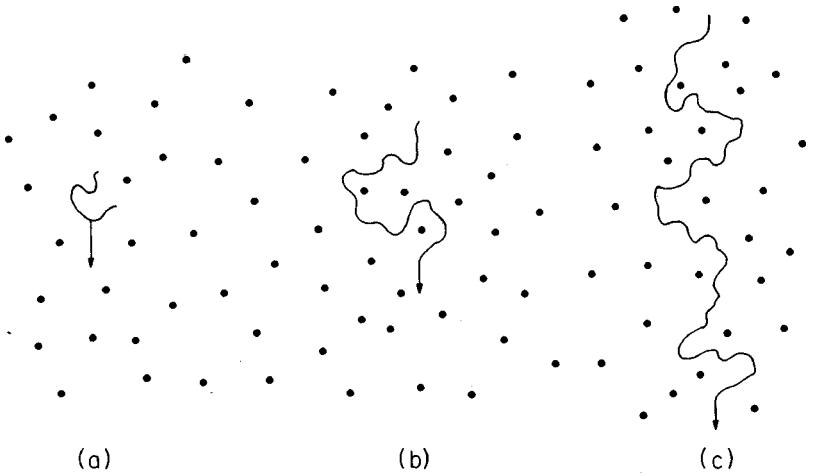

FIG. 7. Different regimes of migration in constant-field electrophoresis: (a) Ogston sieving; (b) reptation without orientation; (c) reptation with orientation.

This equation shows that the key parameter of the model is the dimensionless variable R_x/Nb. Note that, since a tube section is abandoned and another is created at each reptation step, this parameter is defined by the sequence of choices of new pores in the gel, made by the head blob in the course of reptation. It is a dynamic quantity, with a typical correlation time equal to the reptation time. Most importantly, in the general case, it is coupled with the field (Slater and Noolandi, 1985; Lumpkin *et al.*, 1985). Since the head blob is charged and submitted to the field, its choice for a new "gate" (and as a consequence the average orientation of the newly created tube segment) is also biased by the field. The early versions of the biased reptation model assumed that the average orientation was given by the balance of electric and Brownian forces on the scale of one blob and finally led to a mobility scaling as

$$(\mu/\mu_0)_{\mathrm{BRM}} \approx \frac{1}{3}\left(\frac{1}{N}+\frac{\varepsilon^2}{3}\right). \tag{5.10}$$

For small N, the first (size-dependent) term dominates, accounting for the experimental dependence of the mobility with N^{-1}. For large N, the second term ($\propto \varepsilon^2/9$) overcomes the N^{-1} Brownian one, qualitatively accounting from the fact that the mobility of large polyelectrolytes becomes independent of size and dependent on field. So reptation ideas qualitatively account for the sigmoidal shape of mobility versus size curves and identify three different regimes of migration, summarized in Fig. 7: (a) free volume model, in which R_g is of the order of the pore size or smaller, (b) unoriented reptation, in which the polyelectrolyte has to thread its way among obstacles but is not significantly oriented, and finally (c) oriented reptation. These regimes have been very useful guidelines for experiments, but BRM predictions were not quantitatively correct for flexible chains at scaling level, as we now demonstrate.

C. Taking internal modes into account: Biased reptation with fluctuations

1. Model

It was recognized later, thanks to progress in computer simulations and experiments (see Secs. VI and VII below), that the simple view of the orientation process presented above had to be amended. As shown by Duke, Semenov, and Viovy (1992), Duke *et al.* (1994), and Semenov *et al.* (1995), for flexible chains the "direct" orientation term used in the biased reptation model is indeed dominated by another term, arising from the coupling between local chain orientation and fast fluctuations in the (curvilinear) position of the end of the chain. In other words, internal modes can never be ignored.[21] These modes are more easily accounted for in the continuous approach used by Semenov *et al.* (1995). The motion of the chain inside its tube is described by the following Langevin equation:

$$\xi_b \frac{\partial s(n,t)}{\partial t} = K\frac{\partial^2 s}{\partial n^2} + \mu_0 \eta b E \cos\theta(n,t) + B(n,t), \tag{5.11}$$

where n is the blob number ($0<n<N$), s is the curvilinear position of blob n at time t, K is the longitudinal modulus of the chain (of order kT/b^2 for a Gaussian blob), and $\theta(n,t)$ is the orientation of the local axis of the tube segment occupied by blob n at time t. The first term on the right-hand side corresponds to the longitudinal elasticity of the chain, the second term is the electrohydrodynamic driving force, projected on the direction of the tube. Note that the term appearing in Eq. (5.11) is different from the one introduced in Semenov *et al.*, 1995, because we have replaced the local force picture by the more correct electrohydrodynamic approach described in Sec. II.F. In the end, we shall see that this modification only amounts to a redefinition of the reduced electric-field parameter ε. B is the random force, with the following properties:

$$\begin{cases} \langle B(n,t)\rangle = 0 \\ \langle B(n,t)B(n',t')\rangle = 2kT\xi_b \delta(n,n')\delta(t,t'). \end{cases} \tag{5.12}$$

Equation (5.12) will be more conveniently manipulated in reduced units:

[21] Actually, an analytical model of biased reptation that attempted to include internal modes was proposed by Viovy (1988b), but only the particular case of field-inversion electrophoresis was considered at that time.

$$\frac{\partial u(n,\tau)}{\partial \tau}=\frac{\partial^2 u}{\partial n^2}+\varepsilon h(n,\tau)+\beta(n,\tau), \tag{5.13}$$

where u is the curvilinear coordinate in units of blob size ($u=s/b$), $\tau=t/\tau_b$, $h=\cos\theta(n,t)$, and β is the reduced random noise,

$$\langle\beta\rangle=0$$
$$\langle\beta(n,\tau)\beta(n',\tau')\rangle=2\delta(n-n')\delta(\tau-\tau'). \tag{5.14}$$

The boundary conditions reflecting the entropic penalty due to the tube constraints are

$$\left.\frac{\partial u}{\partial n}\right|_{n=0}=\left.\frac{\partial u}{\partial n}\right|_{n=1}=1. \tag{5.15}$$

The subtleties of biased reptation lie entirely in the second term of the second member of Eq. (5.13), which involves the same two features as already introduced in the biased reptation model: first, the motion is in general biased by the electric field, since ε is nonzero, and second, this bias is coupled with chain conformation by h, which plays the role of a local orientational order parameter. As we shall see, however, this coupling is more delicate than first anticipated in the biased reptation model and is the source of serious difficulties in the theoretical treatment. Formally the macroscopic electrophoretic mobility can be derived from Eq. (5.13) by projection of the motion on the direction of electric field,

$$v_x(t)=\frac{b}{\tau_b}\int_0^N \frac{\partial u(n,\tau)}{\partial \tau}h(n,\tau)dn. \tag{5.16}$$

It was shown by Semenov *et al.* (1995), that the velocity can be expressed as

$$\langle v_x\rangle=\mu_0 E H^2[1+O(n^*/N)], \tag{5.17}$$

in which

$$H^2=\langle R_x^2/N^2b^2\rangle \tag{5.18}$$

and n^*, a number between 1 and $N^{1/2}$, will be defined self-consistently below. This expression essentially has the same shape as Eq. (5.9) in the biased reptation model. The difficulty lies in the calculation of the orientational order parameter. Several levels of approximation can be used, in order to calculate this quantity. The first is to remark that Brownian drift is always dominated by electrophoretic drift in the long-time limit and to ignore possible correlations between fluctuations in the orientation and position of segments. Then the first and last terms in the second member of Eq. (5.13) can be dropped, the probability distribution function of h is evaluated on the scale of one blob, and Eq. (5.16) can be averaged over time; this is the BRM approach. The problem with this is that *correlations between position and orientation of segments are indeed important*. This coupling involves considerable analytical difficulties (Semenov *et al.*, 1995), but the correct result (at scaling level) can be obtained by a rather simple argument. As

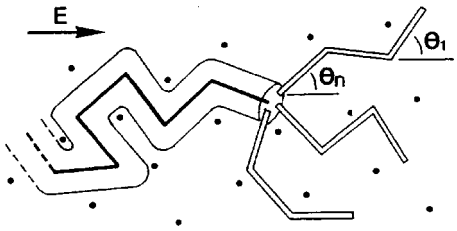

FIG. 8. Tube representation of the head of a flexible polyelectrolyte migrating in a gel. The bold line represents part of the molecule inhabiting the permanent tube ($n>n^*$). The double lines represent the various possible conformations sampled by the end section ($n<n^*$) during the rapid length fluctuations of the chain.

mentioned previously, we expect that, for $\varepsilon\ll 1$, fluctuations in the tube length will occur rapidly due to Rouse motion of the end blobs (i.e., Brownian activation of longitudinal modes of order greater than one). These modes are only weakly affected by the field. We can then apply the results previously derived by Doi and Edwards (1986) for Brownian diffusion: after a time t, the number n_{fluct} of tube segments that have been modified by length fluctuations is of order

$$n_{\text{fluct}}\approx\begin{cases}(t/\tau_0)^{1/4}, & t/\tau_b<N^2\\ N^{1/2}, & t/\tau_b>N^2\end{cases}. \tag{5.19}$$

During the same time, the chain has been drifting along the tube with an as yet unknown curvilinear velocity ds/dt, i.e., on a number of tube segments

$$n_{\text{drift}}=|t(ds/dt)/b|=t\mu_0 E|H|/b. \tag{5.20}$$

Note that the drift can have a positive or negative value, depending on the arbitrary choice of numbering for the blobs. Here, we are interested in the drift counted downfield, which is positive by definition, hence the absolute value. The critical time t^*, at which $n_{\text{fluct}}=n_{\text{drift}}=n^*$, marks the boundary between two time (and distance) domains: for shorter times, fluctuations dominate, so that tube segments at a distance smaller than n^* from the end will be visited several times by the chain end and have a small probability of survival. Tube segments at a distance larger than n^*, in contrast, are permanently ''memorized'' in the tube conformation. Thus the chain can be schematically pictured as an inextensible ''heart'' section, advancing steadily along its permanent tube, preceded by a fluctuating section of length n^*, exploring numerous configurations (Fig. 8). Therefore it is the orientation of the n^*th segment which defines the overall tube orientation, and it is this orientation (rather than that of the end segment) which should be Boltzmann averaged in order to yield the tube orientation. This average depends on the total force exerted on the n^*th segment by the n^* head segments. Since hydrodynamic interactions are screened over distances larger than the blob size b, this force is of order $n^*\xi_b\mu_0 E$, and the average orientation is given by

$$|H|=\langle\cos\theta\rangle=L(n^*\varepsilon), \tag{5.21}$$

where L is the inverse Langevin function. For weak fields, then, $|H| \sim n^* \varepsilon$. This relation, combined with Eqs. (5.19) and (5.20) allows a self-consistent determination of the orientation factor, which yields $H^2 \sim \varepsilon$, a result completely different from the original prediction of the biased reptation model without fluctuations. A more rigorous approach, based on a perturbative treatment of Eq. (5.13) (valid in the limit $\varepsilon \ll 1$, $N\varepsilon \gg 1$), leads to the same result, together with an evaluation of the prefactor (Semenov *et al.*, 1995; Subbotin and Semenov, 1996):

$$\frac{\mu}{\mu_0} = \begin{cases} 1/3N, & N\varepsilon < 1 \\ H^2 \approx 0.5\varepsilon, & N\varepsilon > 1 \end{cases}. \tag{5.22}$$

This result has been confirmed by several experimental results (Heller, Duke, and Viovy, 1994; Yan *et al.*, 1996; Pluen *et al.*, 1998) and by direct numerical simulation of the repton model (see Sec. VII.B, Duke, Semenov, and Viovy, 1992, and Barkema *et al.*, 1994). Barkema *et al.* proposed an interpolation formula very close to Eq. (5.22):

$$\frac{\mu}{\mu_0} = [(3N)^{-2} + (2\varepsilon/5)^2]^{1/2}. \tag{5.23}$$

The crossover from unoriented reptation ($N < N^*$), in which size fractionation occurs, and oriented reptation ($N > N^*$), in which the mobility is field dependent and independent of size, occurs around

$$N^* = (\tfrac{5}{6})\varepsilon^{-1}. \tag{5.24}$$

One can check that these results are consistent with the assumptions made at the beginning of the argument, i.e., that in the oriented regime $1 < n^* < N^{1/2}$. Analytically, the model also predicts that, for $\varepsilon \sim 1$, the mobility should saturate for all chains and become independent of the field, in qualitative agreement with experiment. This latter prediction is not a very strong one, however, since obviously the mobility in a gel cannot exceed the free-flow mobility, which is field independent, and since we already suspect that several assumptions of the reptation model, including the tube itself, dramatically fail for $\varepsilon \sim 1$.[22] Since this saturation exists, however, it is convenient for applications to introduce it phenomenologically (Viovy, 1996),

$$\mu/\mu_0 = \left[(3N)^{-2} + \left(\frac{2\varepsilon}{5 + 2\alpha\varepsilon} \right)^2 \right]^{1/2}, \tag{5.25}$$

where α is the limiting ratio of free mobility to in-gel mobility for large chains and large fields. This ratio is rather consistently found (both in experiments and in computer simulations) to be of order 3 (Akerman, 1996a; Long, 1996; Lee *et al.*, 1996).

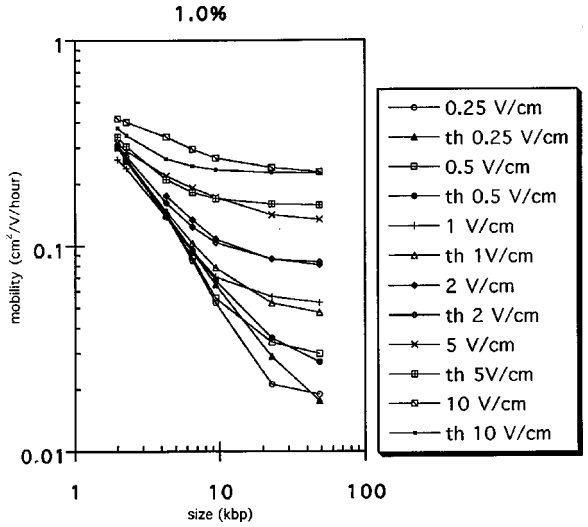

FIG. 9. Comparison of experimental and theoretical values for the mobility of duplex DNA fragments in 1% agarose, 1X TBE, at different field strengths. Data are from Heller *et al.*, 1994. The corresponding theoretical curves are obtained using Eq. (5.26), an effective pore size of 230 nm, and independently measured molecular parameters (see text for details).

2. Comparison with experimental mobilities

At scaling level, the BRF predictions are in rather good agreement with experimental measurement of the electrophoretic mobility. A more quantitative comparison concerning duplex DNA was performed by Heller *et al.* (1994). The mobility of DNA fragments with sizes ranging from 2 kb to a few hundreds of kbp, under fields covering two orders of magnitude, was measured in agarose gels ranging from 0.5 to 2%. An example of the results is provided in Fig. 9. At relatively low electric fields, two regimes with $\mu \sim N^{-1}$ and $\mu \sim N^0$, respectively, are actually observed. The scaling with electric field is presented in Fig. 10 for different sizes and different gel concentrations. The E^1 scaling is observed for large enough chains. The same type of scaling was reported by Slater and Drouin (1992), Yan *et al.* (1996), and Pluen *et al.* (1998) for single-stranded DNA in polyacrylamide gels.

Since the BRF model is based on a molecular approach, it should, in principle, be possible to perform quantitative predictions in terms of independently measured molecular parameters. For that, it is useful to express Eq. (5.25) in terms of the ratio of pore size to Kuhn length (b/l), number of Kuhn segments N_k, and "molecular" reduced field ε_k [see Eq. (5.7)]:

$$\mu/\mu_0 = \left\{ [(b/l)^2/3N_k]^2 + \left[\frac{2\varepsilon_k (b/l)^2}{5 + 2\alpha\varepsilon_k (b/l)^2} \right]^2 \right\}^{1/2}. \tag{5.26}$$

A comparison of the mobility of duplex DNA, the physical parameters of which are well known, is pro-

[22] Also note that, in deriving Eq. (5.23), we made use of Eq. (2.24) for evaluating the electrohydrodynamic force per blob. For strong chain stretching, hydrodynamics interactions are different and the force is not expected to obey the same expression.

posed by Viovy (1996).[23] The number of Kuhn segments of a given DNA fragment is easily derived, knowing that DNA has a curvilinear length of 0.34 nm per base pair and a Kuhn length of about 100 nm in the buffers usually utilized in electrophoresis, such as $1X$ TBE. Therefore $N_k \approx N_{bp}/300$. The free-liquid mobility of DNA, which also depends on the buffer, has been determined to rather good accuracy (Olivera *et al.*, 1964; Barron *et al.*, 1994). In $1X$ TBE (Tris 89 mM, borate 89 mM, EDTA 2 mM), it is evaluated as 3.4 $(+/-0.4)\times10^{-8}$ $m^2\,V^{-1}\,s^{-1}$. The limiting mobility of large DNA in strong fields was also measured. In 1% agarose, it is of order 1.1×10^{-8} $m^2\,V^{-1}\,s^{-1}$ (Akerman, 1996a), fixing the parameter α in Eq. (5.26) at 3. Experimental values also provide an evaluation of $\varepsilon_k/E \sim 1.8\times10^{-4}$ V/m. As discussed in Sec. III.B, the least certain parameter in the model is probably the pore size. Since the reproducibility that can be obtained in fitting Eq. (5.26) to electrophoresis data, in a given gel system, appears much better than the experimental uncertainty on the pore size obtained by diverse independent means, we chose to use the pore size as a single adjustable parameter in the fit. The theoretical curves in Fig. 9, corresponding to DNA between 1.5 and 48 kb, and field strengths ranging from 0.25 to 10 V/cm were obtained with a pore size of 230 nm in the local force model. A more recent investigation in the electrohydrodynamic frame yields, instead, a pore size of order 500 nm (Meistermann, 1999).[24] This value is compatible with earlier evaluations of the pore size in 1% agarose. We must emphasize, however, that this evaluation cannot be generalized to other types of molecules or particles.

Expressing mobilities in terms of molecular parameters also leads to interesting predictions for the dependence upon pore size of the limit of separation (expressed in absolute values), $N_k^* = N^*(b/l)^2$. For the BRF model with electrohydrodynamic friction (i.e., taking into account hydrodynamic coupling with counterions), the prediction is

$$N_k^* = \varepsilon_k^{-1}, \tag{5.27}$$

i.e., independence of pore size, whereas the predictions for the BRF model in a local force picture and for the BRM with local force would be $(b/l)^{-1}$ and $(b/l)^{-4}$, respectively. Figure 11 (from Heller *et al.*, 1994) shows that the limit of separation seems to tend asymptotically (for small fields) to a universal curve, independent of gel concentration and scaling as E^{-1}, in agreement with the predictions of the BRF model with electrohydrodynamic force [Eq. (5.26)]. Note that the scaling behaviors in Figs. 10 and 11 are qualitatively different from the predictions of the biased reptation model (square dependence). Therefore these figures provide a clear discrimination between the BRM and BRF.

The BRF model with electrohydrodynamic force, finally, predicts a mobility scaling with $(b/l)^2$, in both the

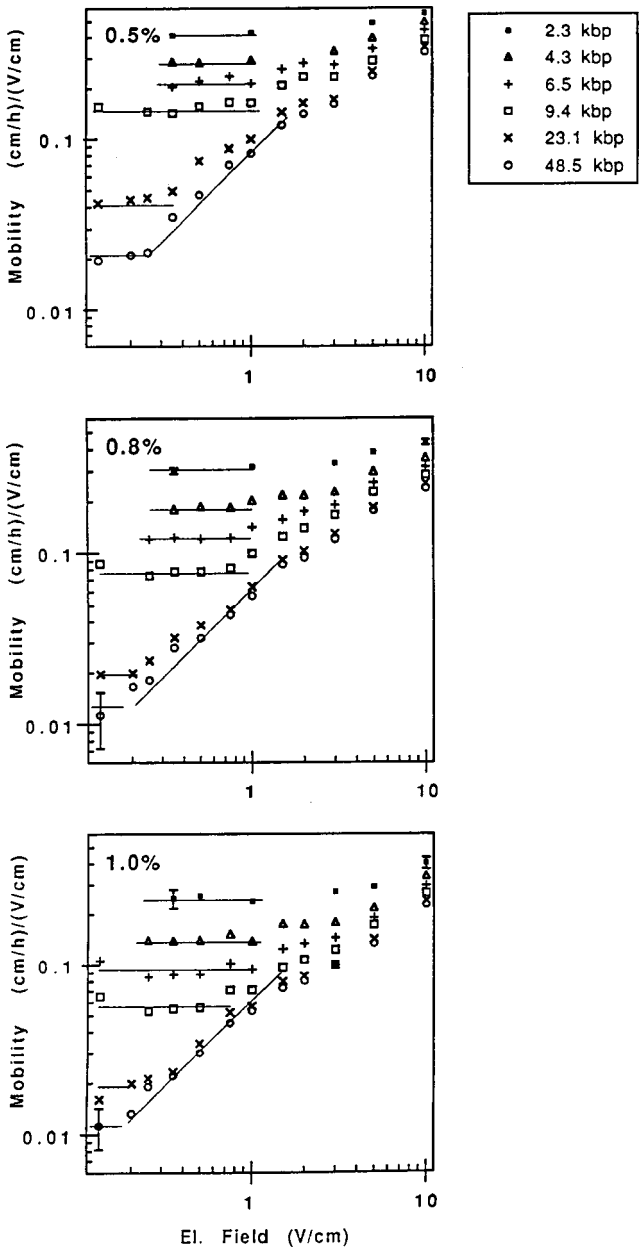

FIG. 10. Mobility of duplex DNA fragments in agarose at different concentrations and $1X$ TBE, vs field strengths. Different curves correspond to different DNA sizes (in box). The tilted line, drawn as a guide for the eye, corresponds to a slope of 1. Data from Heller *et al.*, 1994.

[23]Note that Eq. (5.26) is slightly different from the one proposed in Viovy, 1996, as far as pore size dependences is concerned: This is because of the introduction of the electrohydrodynamic picture of the force on a blob, in replacement of the local force: The electrohydrodynamic force scales as b^2 [see Eq. (5.5)], whereas, from Eqs. (5.1) and (5.6), the local force picture yields b^3. This does not affect significantly the conclusions of this particular comparison, however, because the way the "effective charge" was measured in a local force approach in some sense adapted it to yield the correct electrophoretic mobility (for a discussion of this rather subtle point, see Long, Viovy, and Ajdari, 1997).

[24]Note that, since the change from local force to electrohydrodynamic force only affects the pore size dependences, only the fitted pore-size value and not the quality of the fit will be affected by this change for data involving a single pore size.

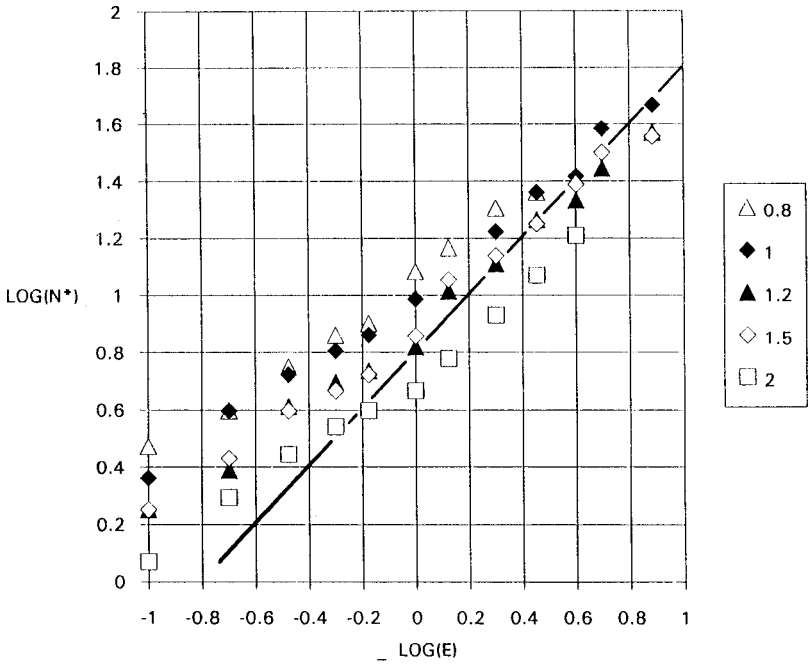

FIG. 11. Dependence of the theoretical limit of separation N^* vs electric field (log-log scale) for different agarose concentrations (see box). The solid line corresponds to a slope of 1. Data from Heller *et al.*, 1994.

regime of reptation without orientation and that with orientation. This is in contrast with other models, which predict a higher exponent in the regime of reptation with orientation (3 for BRF local force and 6 for BRM). Comparison with experiments is rather difficult in this case, because it requires an accurate knowledge of the dependence of pore size on gel concentration: this variation depends on gel architecture. For a network of flexible chains, one expects $b \sim c^{-0.75}$, i.e., $\mu \sim c^{-1.5}$. Detailed studies of the mobility and dispersion of DNA is gels, undertaken by Tinland and co-workers (Tinland *et al.*, 1997), are in better agreement with the BRF-electrohydrodynamic force prediction than with any other model of gel electrophoresis.

Finally, a very complete discussion of the application of reptation models to single-stranded DNA, involving measurements of the orientation, of the dispersion coefficient, and of the orientational dynamics of single-stranded DNA chains in acrylamide, was provided by Pluen (1996); Pluen *et al.* (1998). The general conclusions of this study are the same as reported here: At scaling level, the BRF model [Eq. (5.26)] provides a good description of electrophoresis in low constant field, except for the dependence on gel concentration, where it predicts exponents in better agreement than previous models but still overestimated as compared to experiments. Another point of disagreement appears at high gel concentrations, in the domain $N \sim N^*$. In such situations, the mobility seems significantly smaller than predicted, and a minimum in the mobility can even be observed. We now discuss this point.

D. Mobility minimum around N^*

The calculations presented above are not expected to describe correctly the velocity in the crossover region $N \sim N^*$ because the two regimes $N \ll N^*$ and $N \gg N^*$ were actually treated separately and joined by a phenomenological combination of the analytical results corresponding to the two asymptotic regimes. As remarked by Slater *et al.* (1987), evaluating the mobility around N^* requires a careful account of the dynamic sampling of conformations. It had been recognized by Noolandi *et al.*, 1987 (within the BRM assumptions) that preaveraging conformations on the ensemble of all thermodynamically available configurations (as was done earlier by Lumpkin *et al.*, 1985, in the context of the BRM) and ignoring the coupling between long-lived fluctuations in the end-to-end distance and the velocity could lead to significantly erroneous results. In particular, these authors showed that a numerical solution of the BRM without a preaveraging approximation yielded a mobility minimum around N^*, which was not predicted in the preaveraging approximation. This minimum was observed experimentally in conditions close to those prescribed by the theory (Noolandi *et al.*, 1987). This work was followed by several analytical studies, which differ in detail and formalism but employ the same physical idea (Doi *et al.*, 1988; Viovy, 1988a; Déjardin, 1989):[25] The relevant average for deriving the mobility is the time average, not the thermodynamic average over available states. There may be a difference between the two, of kinetic origin, since chains will remain longer in conformations with a lower mobility. For $N \gg N^*$ the orientation is strong, so that its relative fluctuations are small: motion is expected to be relatively uniform, and corrections to preaveraging are also small. In the region $N \sim N^*$, however, the fluctuations of the orientation factor H have the same order of magnitude as the average

[25]Also note an attempt by Lumpkin, Levene, and Zimm (1989) to remove the initial preaveraging assumption in orientational correlation functions made in the Lumpkin *et al.* paper of 1985, at the expense of a numerical solution.

value, so U-shaped conformational states of the tube, in which the orientation factor of the chain is essentially zero, are rather probable. The chain can leave these states only by Brownian curvilinear motion, which is very slow. This leads to a higher weighting of these states in the time average of conformations than in the thermodynamic average. Indeed, the distribution of the order parameter H^2 becomes double peaked around N^*, with one peak at the preaveraged position ($\approx\varepsilon$) and a second peak around 0, related to the slow dynamics of conformations with an end-to-end distance close to 0.[26] For $N \ll N^*$, conformation fluctuations are even larger, but the Brownian exchange rate between conformations is also large, so that the correction to the preaveraged result is again small. The quantitative predictions of these early papers are now somewhat obsolete, since they were developed in the frame of the BRM, but the underlying physics remain valid. In other words, Noolandi *et al.* correctly accounted for the coupling of slow fluctuations of the end-to-end distance with the velocity, but ignored the fast fluctuations. Duke *et al.* (1992) in contrast, accounted for the fast fluctuations, but ignored the slow ones. The two levels of fluctuations were finally combined in the framework of the BRF model by Semenov *et al.* (1995). It was then confirmed that the leading correction to the scaling prediction, at the approach to N^* starting from large N, is dominated by large-scale fluctuations in the curvilinear mobility (related to fluctuations in the order parameter H), and that the correction is negative:

$$\frac{\mu}{\mu_0}(N \geqslant N^*) \approx 0.5\varepsilon(1 - N^*/2N). \tag{5.28}$$

Thus the effect initially predicted by Noolandi *et al.* survives in the BRF model, although shifted to smaller N.

E. Enhanced band broadening

The possibility of nontrivial enhanced band dispersion during gel electrophoresis was mentioned first by Adolf in 1987, in an article that unfortunately remained relatively unnoticed by experimentalists. It was discussed later by Viovy (1989) and finally studied in more detail by Slater (1993), Slater, Mayer, and Drouin (1993a, 1993b) Mayer *et al.* (1994b), Duke, Viovy, and Semenov (1994), and Semenov and Joanny (1997). Only the two last articles in this series were treated within the frame of the BRF model, but otherwise all rely on the same physics. In essence, this is the observation that, when $\varepsilon \ll 1$, fluctuations in the end-to-end distance (projected on the direction of migration) remain of order $b\,N^{1/2}$, whether in the oriented or unoriented reptation regime. The dispersion coefficient is then obtained as

$$d_c = Nb^2/t_{\mathrm{dis}}, \tag{5.29}$$

in which t_{dis} is the disengagement time. In the limit of vanishing fields, d_c should reduce to the Brownian reptation diffusion coefficient,

$$d_1 = D_b/N^2 = D_k N_k^{-2}(l/b)^3, \quad E \to 0, \tag{5.30}$$

where we have defined the diffusion coefficient of a blob

$$D_b = b^2/\tau_b = kT/\eta b \tag{5.31}$$

and that of a Kuhn segment

$$D_k = D_b(b/l) = kT/\eta l. \tag{5.32}$$

The important point, however, is that the disengagement time can be reduced by reptation down to values much lower than the equilibrium one, thereby leading to enhanced dispersion (this is very different from the situation encountered for small compact molecules: for those, diffusion on their own size in the absence of external force is in general faster than electrophoretic drift over the same distance).[27] For polyelectrolytes in the oriented regime ($N > N^*$), the disengagement time is:

$$t_{\mathrm{dis}} = bN/\mu_0 E\varepsilon^{1/2}. \tag{5.33}$$

Using Eq. (5.29), this leads to a dispersion that is now field dependent and independent of molecular size,

$$d_3 = D_b\varepsilon^{3/2} = D_k\varepsilon_k^{3/2}(b/l)^2, \quad N > N^*. \tag{5.34}$$

An even more striking prediction of the model is that between the two limits represented by Eqs. (5.30) and (5.34), an intermediate regime exists, in which the disengagement time is smaller than the equilibrium reptation time t_{rep}, but the conformation remains Gaussian. The corresponding dispersion coefficient is

$$d_2 = D_b\varepsilon N^{-1/2} = D_k\varepsilon_k N_k^{-1/2}(b/l)^2,$$
$$N^{**} \approx \varepsilon^{-2/3} < N < N^*. \tag{5.35}$$

In this regime, dispersion departs from Brownian diffusion, whereas the mobility remains driven by the Einstein relation.[28] These different expressions for the dispersion coefficient, corresponding to different regimes [Eqs. (5.30), (5.34), (5.35)] can be inserted in Eq. (3.5), in order to determine the migration-related bandwidth at a given migration time. In turn, this bandwidth can be combined with the expression for the mobility [Eq. (5.26)] and with Eq. (3.4) to yield the theoretical (or maximum achievable) resolving power.

[26] Incidentally, this effect was called by Noolandi *et al.* (1987) "self-trapping," an expression that should rather be avoided, since these slow conformations are absolutely unstable and cannot constitute traps.

[27] Enhanced dispersion also occurs in the direction perpendicular to the field, but it is less important for applications and can be worked out the same way as in the longitudinal direction (Semenov and Joanny, 1997).

[28] Note that Eqs. (5.30), (5.34), and (5.35) are different from those proposed in Viovy (1989) and Slater (1992), because of the use of the BRF model, but also different from the results quoted in Duke, Viovy, and Semenov (1994), because they include electrohydrodynamic effects, introduced in Sec. II.F. These electrohydrodynamic corrections affect the dependence of the results on the pore size b, but not on the field and molecular size.

The mechanism of enhanced dispersion, which is related to the nonlinear nature of transport equations, is very specific to the reptation process. It has also been studied by Slater (1993), using computer simulation (in the BRM frame). The experimental study of mobility dispersion by direct electrophoretic measurements is difficult, because of dispersion effects associated with the presence of a "band" (i.e., a finite zone in which DNA concentration varies). Recently, however, the use of fluorescence recovery after photobleaching (Wu *et al.*, 1990) has permitted accurate investigations of this effect, for single-strand DNA in acrylamide (Pluen *et al.*, 1998) and for duplex DNA in agarose (Tinland, 1996; Pernodet and Tinland, 1997; Tinland, Pernodet, and Pluen, 1998; Meistermann, 1999). Three regimes for dispersion were actually observed, corresponding to field and DNA size scaling, in very good agreement with the BRF predictions [Eqs. (5.30), (5.34), and (5.35)]. As was the case for the mobility, the agreement with the predictions for dispersion scaling with size is less satisfying (the observed (b/l) scaling exponent is about 2, 2, and 1 for regimes 1, 2, and 3, as compared with predicted values of 3, 2, and 2. As previously discussed, however, the measurement, and the concept of a "pore size" itself, is a delicate matter, and these results (and predictions) may remain a matter of debate until separation media with uniform pore architectures can be constructed and studied.

Leaving aside this complication, it remains true that dispersion plays an important role in applications, and that the formulas proposed in this section, combined with Eq. (5.26) for the mobility, can be used to optimize experimental conditions for a given application, along the lines developed by Slater and Drouin (1992), Slater, Mayer, and Drouin (1993a, 1993b), Slater (1993), and Slater *et al.* (1994).

F. Persistent chain in tight gels

The migration of polyelectrolytes in the regime $l>b$ (polyelectrolyte Kuhn length larger than the pore size) has not received as much attention as the flexible chain, probably because it does not seem to correspond to DNA in agarose, the favorite paradigm of physicists. This is rather unfortunate, however, because this situation certainly has an experimental relevance: it corresponds for instance to the migration of duplex DNA in acrylamide gels and to many situations encountered in capillary electrophoresis (in which entangled polymer solutions with a relatively small mesh size are used—see, for example, Viovy and Heller, 1996). The BRF model has been applied to this regime by Semenov *et al.* (1995). In this situation, the tube length is of the order of the contour length of the polyelectrolyte, and there are important orientational correlations between consecutive tube segments. Actually, in the absence of field, the tube conformation is controlled by the persistence length, and its mean-square end-to-end distance is lN_k. In this case Eq. (5.1) should be replaced by

$$N=N_k\frac{l}{b}. \tag{5.36}$$

For vanishing fields, the averaged orientational order parameter of the chain is now

$$|H|=\frac{l}{b}\frac{1}{3N} \tag{5.37}$$

and the mobility in this regime is

$$\frac{\mu}{\mu_0}=\frac{l}{b}\frac{1}{3N}=\frac{1}{3N_k}. \tag{5.38}$$

It becomes independent of pore size.[29] In a tight gel, the bending elasticity prevents excursions out of the tube: Eq. (5.5) does not need to be fulfilled for the reptation model to be applicable, and ε can exceed 1. Field-induced orientation still occurs, though, and at large enough fields we expect a departure from the linear unoriented regime and a field-induced orientation of the chain. For $l\gg b$, length fluctuations are frozen, and one recovers the BRM asymptotic prediction,

$$\mu/\mu_0(N\to\infty)\approx\varepsilon^2=\varepsilon_k^2(l/b)^{-4}. \tag{5.39}$$

This freezing of length fluctuations occurs only progressively: the longitudinal modulus K does not jump abruptly to infinity when $l=b$, but rather scales as $(l/b)^2$. This implies that the effect of fluctuations on chain orientation do not disappear abruptly either. Actually, it was shown by Duke, Semenov, and Viovy (1992) and Semenov *et al.* (1995) that the mobility evolves through several regimes before reaching that represented by Eq. (5.39). The calculations are rather cumbersome, and I reproduce here only the results. Figure 12 represents the full phase diagram of reptation regimes, in the plane $[\varepsilon_k,(l/b)]$, for an arbitrary value of N_k, larger than 1. The equations of the regimes and of the transition lines are given in Tables II and III, respectively, as a function of ε, N, and l/b, as well as in a (ε_k,N_k) representation (all numerical factors of order 1 are absent, since they are not known in the tight-gel regime). This diagram shows that the regime of oriented reptation tends to disappear rapidly in tight gels. For large values of l/b, it can be recovered only by increasing the field strength dramatically. Probably, the only experimentally available regimes for $l/b>1$ are 4, 5, and 6. Regime 7, which corresponds to very high fields and represents a narrow domain between regimes with a much weaker field exponent of the mobility (0.4 and 0, respectively, for regimes 6 and 3), would be very difficult to observe. This may explain why an E^2 dependence of the mobility, which has been actively sought since its prediction by the BRM, has never been convincingly observed experimentally. In contrast, a regime with $\mu\sim E^{0.4}$, consistent with our regime 6, has been observed by Mitnik, Salomé, *et al.*, 1995, for DNA in entangled solutions of hydroxypropylcellulose at concentrations

[29]Note that, for $l>b$, the electrohydrodynamic and local force expressions for the driving force are equal at scaling level. Therefore the expressions provided by Semenov *et al.* (1995) for a tight gel are also consistent with an electrohydrodynamic treatment.

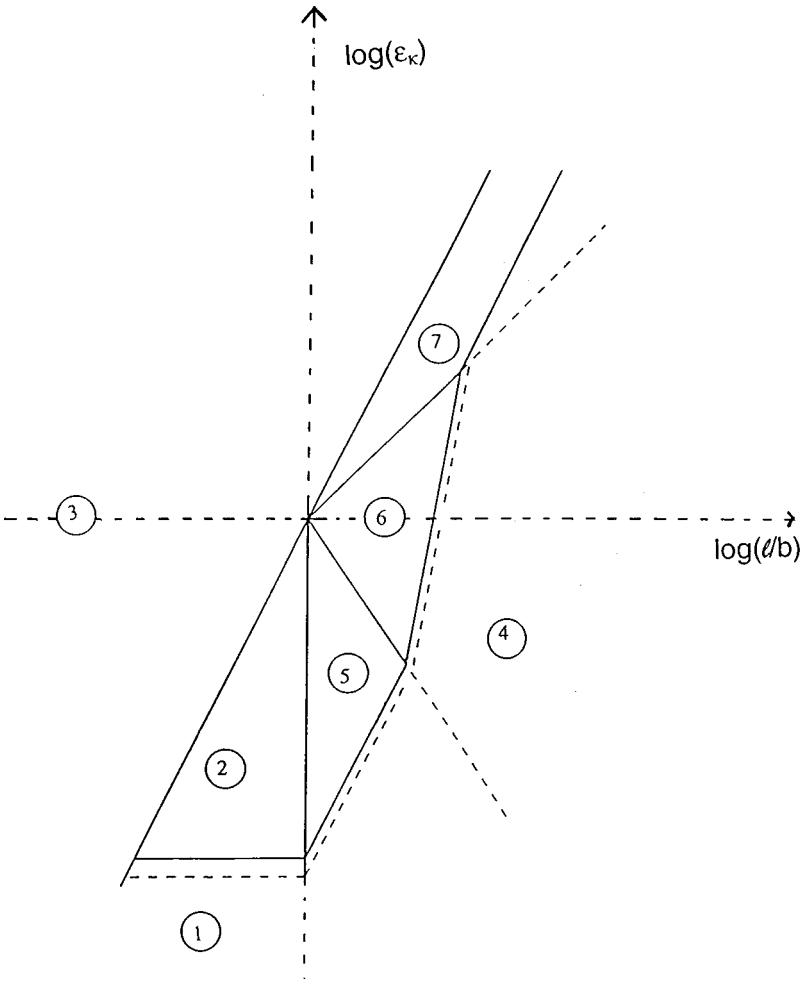

FIG. 12. Diagram of the seven dynamic regimes for the mobility of a polyelectrolyte in a gel, in absolute reduced units. The left part of the diagram corresponds to flexible chains, for memory, and the right-hand side to persistent chains (compared with the pore size). The vertical axis corresponds to increasing electric fields. The numbers in circles are indexes for the different regimes, described in Tables II and III. The corresponding expressions for the mobility are given in Table II. The equations of the transition lines are given in Table III. Transitions 1/2, 4/5, 4/6, and 4/7 actually depend on N (the dotted line indicates how they would shift for a larger value of N).

higher than 0.4%. A similar exponent $E^{0.5}$ was also observed by Magnusdottir, Isamhert, *et al.* (1998). If we identify the screening length of this solution with an effective pore size, as suggested by Grossman and Soane (1991) and Viovy and Duke, (1993), this would indeed correspond to a regime $l/b>1$ and to a confirmation of the BRF predictions. However, this reduced exponent may also be a consequence of a field-dependent defor-

TABLE II. Reduced mobility in the seven different regimes displayed in Fig. 12. Columns 2 and 3 represent the scaling predictions (in "per blob" and "per Kuhn segment" reduced units, respectively. Column 4 contains more detailed predictions when available. The last column gives the type of migration.

Regime	$\mu/\mu_0(\varepsilon,N)$	$\mu/\mu_0(\varepsilon_k,N_k)$	Eq.	Type
1	$(N)^{-1}$	$(3N_k)^{-1}(l/b)^{-2}$	$\mu/\mu_0=\left[(3N)^{-2}+\left(\frac{2\varepsilon}{5+2\alpha\varepsilon}\right)^2\right]^{1/2}$	unoriented; $l<b$
2	ε	$\varepsilon_k(l/b)^{-2}$	$\mu/\mu_0=\left[(3N)^{-2}+\left(\frac{2\varepsilon}{5+2\alpha\varepsilon}\right)^2\right]^{1/2}$	oriented; $l<b$
3	1	1	$\mu/\mu_0=\left[(3N)^{-2}+\left(\frac{2\varepsilon}{5+2\alpha\varepsilon}\right)^2\right]^{1/2}$	saturated
4	$(N)^{-1}(l/b)$	$(N_k)^{-1}$	$\frac{\mu}{\mu_0}=\frac{l}{b}\frac{1}{3N}=\frac{1}{3N_k}$	unoriented; $l>b$
5	$\varepsilon(l/b)^{1/2}$	$\varepsilon_k(l/b)^{-3/2}$		oriented; $l>b$
6	$\varepsilon^{2/5}(l/b)^{-8/5}$	$\varepsilon_k^{2/5}(l/b)^{-12/5}$		oriented; $l>b$
7	ε^2	$\varepsilon_k^2(l/b)^{-4}$		oriented; $l>b$

TABLE III. Equations of the transition lines between the dynamic regimes displayed in Fig. 12, in reduced units (per blob in column 2 and per Kuhn length in column 3.

Transition	Transition line	Transition line
1/2	$N=\varepsilon^{-1}$	$N_k=\varepsilon_k^{-1}$
2/3	$\varepsilon=1$	$\varepsilon_k=(l/b)^2$
1/4	$(l/b)=1$	$l/b=1$
2/5	$(l/b)=1$	$l/b=1$
4/5	$N=\varepsilon^{-1}(l/b)^{1/2}$	$\varepsilon_\kappa=(N_\kappa)^{-1}(l/b)^{3/2}$
4/6	$N=\varepsilon^{-2/5}(l/b)^{13/5}$	$\varepsilon_k=(N_\kappa)^{-5/2}(l/b)^6$
4/7	$N=\varepsilon^{-2}(l/b)$	$\varepsilon_k=(N_\kappa)^{-1/2}(l/b)^2$
7/3	$\varepsilon=1$	$\varepsilon_k=(l/b)^2$
5/6	$\varepsilon=(l/b)^{-7/2}$	$\varepsilon_k=(l/b)^{-3/2}$
6/7	$\varepsilon=(l/b)^{-1}$	$\varepsilon_k=(l/b)$

mation of the polymer matrix (which is not properly speaking a gel). An investigation of the mobility of persistent chains in real cross-linked gels of small pore size would be very interesting and could remove this doubt. Another conclusion from these studies is that for polyelectrolytes in tight gels there is not a single scaling variable, playing the same role as $N\varepsilon$ in more open gels.

We should point out that the possibility of specific friction between the polyelectrolyte and the gel fibers, and the enthalpic contributions due to coupling of chain elasticity with the randomness of the gel, have been totally ignored so far. This assumption, which is reasonable for flexible chains in a dilute gel (see Viovy and Duke, 1994, in response to Burlatsky and Deutch, 1993), becomes questionable when the ratio l/b is large and when both the gel and the polyelectrolyte become rigid. For instance, the mobility of rodlike viruses in agarose is strongly pore-size dependent (Griess and Serwer, 1990). Retardation due to increasing persistence length has also been observed in a computer modeling of the migration of persistent nonlinear bead-spring chains in a network of obstacles (Guerry *et al.*, 1996). Finally, note that frictional effects due to polyelectrolyte bending were investigated by Levene and Zimm (1989) on the basis of a numerically solved reptation model.

To summarize, the motion of persistent chains in tight gels appears to be particularly relevant for reptation models, since the tube constraint in this case is hardly disputable. This chain motion is also increasingly pertinent experimentally. Unfortunately, our level of understanding of the tight-gel regime is not as good as for flexible chains. Analytically, the treatment of the crossover zone, in which persistence length and pore size are of the same order of magnitude, is particularly difficult. Since small pore sizes also correspond in general to higher gel concentration and flexibility, additional theoretical difficulties related to analyte-gel friction and gel deformability come into play. These different questions have not received a thorough examination, and efforts to better understand this range of pore sizes are very much needed, in particular, in consideration of its importance for sequencing and capillary electrophoresis.

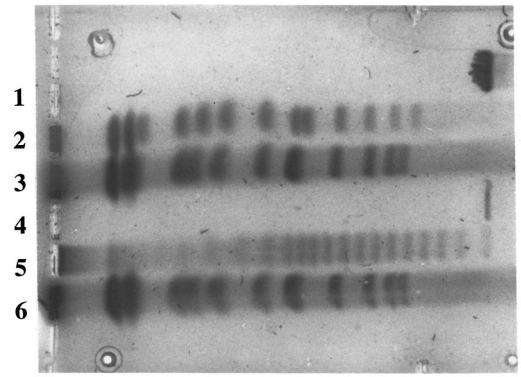

FIG. 13. Separation of various DNA standards in pulsed-field conditions (agarose 1.5%, TBE 0.5*X* buffer (45 mM tris, 45 mM borate, 1 mM EDTA, *p*H 8.3). This separation was performed in a homemade gel rotation apparatus used at 120°, pulse duration 60 s. Lanes 1 to 6, from top to bottom, correspond to: 1, 4/Lambda bacteriophage strain *c*1857*S*7 48.5 kb (lane 1 was deliberately overloaded); 2,3,6: chromosomes of yeast Saccharomyces Cerevisiae strain YPH80 (purchased from FMC Bioproducts, Rockland, ME). Dark bands (right to left): band 1 (I): 250 kb; band 2 (VI): 280 kb; band 3 (III): 360 kb; band 4 (IX): 440 kb; band 5 (VIII, V): 600 kb; band 6 (XI): 680 kb; band 7 (X, XIV, II): 790 kb; band 8 (XIII, XVI): 930 kb; band 9 (VII, XV): 1100 kb; band 10 (IV, XII): 1700, 2200 kb; 5/concatemers of Lambda bacteriophage strain *c*1857*S*7 (purchased from FMC): (all multiples of 48.5 kb, up to 21).

G. Pulsed-field electrophoresis

The principle of this technique, proposed for the first time in two famous papers by Schwartz and Cantor (1984) and Carle and Olson (1984; i.e., two years after the first publications on biased reptation), amounts to periodically changing the direction or the orientation of the electric field. Biased reptation ideas provide a natural framework for interpreting pulsed-field data, especially considering direct experimental evidence for a strong correlation between mobility and orientational behavior in a pulsed field (Akerman and Jonsson, 1990). In the previous section, we have shown that long charged chains in gels orient in the direction of the field when they reptate. This orientation, however, is only progressively built up by reptation after the onset of the field. Therefore, a chain initially oriented at random starts its motion at a size-dependent velocity and reaches its steady state, size-independent, velocity only after a time of the order of the reptation time. Since the reptation time is itself size dependent, by pulsing the field at a given frequency, one can discriminate between ''long'' chains that cannot reach the steady-state velocity during one period and ''short'' ones that travel most of the time at the steady-state velocity.

By increasing by about two orders of magnitude the size of DNA molecules that could be separated in gel electrophoresis (Fig. 13), pulsed-field electrophoresis revolutionized molecular genetics, and bridged the gap between the genetic mapping and *in situ* hybridization

techniques previously available,[30] having a resolution of several Mbp, and detailed analyses of small DNA fragments, down to the ultimate single base resolution necessary for sequencing. The implications for molecular genetic were so important at that time[31] that frantic developments of experimentations around the pulsed-field electrophoresis principle readily followed Schwartz and Cantor's first papers, leading to a large number of variants. Pulsed-field electrophoresis methods can be classified into three "families" recalled below in order of decreasing technical complexity:

- *Crossed-field gel electrophoresis* in which at least two field orientations are used. The first variants of this kind, using inhomogeneous fields (Carle and Olson, 1984, 1985; Schwartz and Cantor, 1984; Gardiner *et al.*, 1986; Smith and Cantor, 1986, 1987; Smith *et al.*, 1987), have been gradually abandoned in favor of the use of two homogeneous electric fields at a fixed angle (generally around 120°), generated by a series of electrodes clamped to regulated potentials. This is the *clamped homogeneous electric-field method* (CHEF): Chu *et al.*, 1986; Sor, 1987; Vollrath and Davies, 1987; Clark *et al.*, 1988; Birren *et al.*, 1989). Homogeneous crossed fields can also be applied to the gel by a mechanical rotation of the gel in a fixed field (Anand, 1986; Serwer, 1987; Southern *et al.*, 1987; Serwer and Hayes, 1989a), or by a mechanical rotation of electrodes at a fixed potential (Gemmil *et al.*, 1987). Finally, methods using more than two fields (Bancroft and Wolk, 1988) in which a crenel-type migration is obtained by applying three different fields, have been proposed.
- Field-inversion gel electrophoresis methods (Carle *et al.*, 1986, Carle and Olson, 1987a, 1987b, Turmel and Lalande, 1988, Crater *et al.*, 1989, Heller and Pohl, 1989), in which the field alternately applied in the two directions along a single orientation. One can distinguish unbiased field-inversion electrophoresis (Carle *et al.*, 1986), in which the field amplitude is the same in the two directions (but the durations of the forward and backward pulses are different, to create a nonzero average field), and biased field-inversion electrophoresis (Lalande *et al.*, 1987), in which the forward and backward pulses have different amplitudes ["Zero-Integrated Field" or ZIFE (Turmel *et al.*, 1990) is a particular case of the latter, in which the product of pulse time by field amplitude just compensates between the forward and the backward pulses.].
- Intermittent-field methods (Fesjian *et al.*, 1996, Jamil *et al.*, 1989, Lai *et al.*, 1988) in which the field is just interrupted periodically.[32]

The applications of pulsed-field electrophoresis are now well documented in several reviews, such as those of Smith and Cantor, 1987, Olson, 1989a, 1989b, Gardiner, 1991, Sor, 1992, and textbooks (e.g., Birren and Lai, 1993, for practical recipes, or Burmeister and Ulanovsky, 1992, for more general considerations and theory). See also a special issue of the review "Electrophoresis" (Smith, 1993) dedicated to this subject. The general phenomenology of pulsed-field electrophoresis is that it opens a *separation window*, in which the mobility of large chains is size dependent. The pulsing period optimal for separation around a given DNA size N depends on the size and on the electric field E and scales approximately as (Cantor *et al.*, 1988, Mathew *et al.*, 1988a, 1988b, 1988c)

$$\tau_{\mathrm{opt}} \propto N^{1} E^{-1.5\sim 2}. \tag{5.40}$$

In crossed fields, the separation power is good for field angles above 90° and decreases rather abruptly below 90°. Finally, a spectacular nonmonotonic dependence of the mobility with size ("band inversion"), in the vicinity of the separation region, is observed in unbiased field-inversion electrophoresis (some band inversion can also occur in other modes, but with a much lower amplitude).

The equations of the BRM or BRF models, which have been discussed only in the steady state in previous sections, can also be solved in the time-dependent regime, in order to describe the progressive evolution of the orientation for a chain starting in an arbitrary conformation, and the various dynamic situations encountered in pulsed fields. Neglecting logarithmic corrections, the orientation time t_{or} is predicted to be proportional to the reptation time, i.e., scaling as $NE^{-1}H^{-1}$ (Slater and Noolandi, 1985, 1986a; Viovy, 1989; Heller, Pakleza, and Viovy, 1995; Long and Viovy, 1996, 1997). The size dependence of this orientation time is at the heart of the pulsed-field method, and a qualitative picture giving useful scaling predictions can indeed be gained without detailed calculations (Viovy, 1987a, 1987b).

Let us consider, for example, crossed fields (Fig. 14). When two fields with the same amplitude E along directions A and B at an angle ϕ are alternately applied during a time t_p to a mixture of DNA molecules, the smaller chains with $t_{\mathrm{or}} \ll t_p$ rapidly reach steady-state mobility at the beginning of each pulse [Fig. 14(c)]: they spend most

[30]Genetic mapping is based on a statistical analysis of the traits inherited by the progeny of a pair of individuals: the probability that two traits of a given parent will be passed together to a child during sexual reproduction increases when the distance between the genes coding for this trait in the genome decreases; *In situ* hybridization uses the direct observation by microscopy of fluorescent "gene labels" on condensed metaphase chromosomes.

[31]Today, new "shotgun sequencing" strategies and powerful clone alignment softwares have rendered this technique less attractive for massive gene analysis projects, but it remains useful for various applications such as cariotyping of microorganisms or diagnosis of large-scale genetic rearrangement.

[32]For completeness, we should note that hybrid methods combining several of these effects (for instance, introducing field interruptions in crossed-field or field-inversion gel electrophoresis, or field inversion in crossed-field or field-inversion gel electrophoresis), now very easy to attempt using computer-controlled apparatuses, have been proposed for specialized applications (Turmel *et al.*, 1990; Zhang *et al.*, 1991; Birren and Lai, 1993).

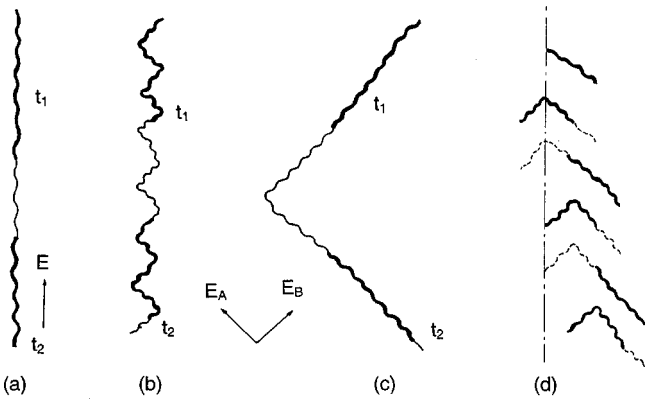

FIG. 14. Different regimes of migration in crossed fields. Bold lines represent chain conformations at different times t_1 and t_2, while the fine lines represent the tube. (a) Permanent field; (b) short-pulse regime ($t_{or}>t_p$), for field angles up to 90°. The chain cannot reorient fully during one pulse; (c) long-pulse regime ($t_{or}<t_p$), showing the path as a sequence of fully oriented sections; (d) Ratchet migration mechanism for crossed fields at obtuse angles, when head/tail exchange occurs at the end of each pulse. Subfigures from top to bottom alternatively represent the position of the chain at the end of pulses pulling to the right, then at the end of the next pulse to the left, etc. Dashed lines are guides for the eye, representing the position at earlier stages. Straight dot-dashed line represents the direction of average field.

of the duration of pulse A (resp. B) oriented, and migrate at the steady-state, constant-field velocity v_c (which can be easily derived, in each regime, from the mobilities given by Table II). The same is true of pulse *B*. The macroscopic velocity along the diagonal *x* is obtained by projecting the zigzag path onto *x*, that is,

$$v(t_{0r}\ll t_p)=v_c(E)\cos(\phi/2)\approx EH^2(E)\cos(\phi/2). \tag{5.41}$$

Longer chains with $t_{or}\gg t_p$ do not have enough time to reorient completely during a single pulse [Fig. 14(b)], so that their nonlinear behavior is sensitive to the effective field:

$$v(t_{0r}\gg t_p)=v_c[E\cos(\phi/2)]$$
$$\approx E\cos(\phi/2)H^2[E\cos(\phi/2)]. \tag{5.42}$$

Therefore there is a drop in mobility at the crossing of $t_{or}=t_p$ which should be of order

$$\rho_v=\frac{v(t_{0r}\gg t_p)}{v(t_{0r}\ll t_p)}=\frac{H^2[E\cos(\phi/2)]}{H^2[E]}. \tag{5.43}$$

The scaling predictions for t_{or} and for r_v are summarized in Table IV. Pulsed-field effects are expected to be useful in the reptation-with-orientation regimes (2, 5, 6, 7). The predictions for the optimal pulse time for separating molecules of a given size *N* [which should be of order $t_{or}(N,E)$] are in good agreement with the experimental behavior of duplex DNA in agarose (regime 2), at scaling level. More quantitative predictions for the evolution of the velocity have been derived analytically, e.g., by Slater and Noolandi (1989b; see also Viovy, 1989).

TABLE IV. Scaling predictions of the biased reptation with fluctuations (BRF) model for the orientational parameter, orientation time, and velocity ratio, in the different regimes displayed in Fig. 12. BRM=biased reptation model.

Regime	H^2	t_{or}	r_v
1,4,3	E^0	$\propto N^3E^0$, $N<N^{**}$ $\propto N^{3/2}E^1$, $N^{**}<N<N^*$	0
2,5	E^1	$\propto NE^{-3/2}$	$[\cos(\phi/2)]^1$
6	$E^{0.4}$	$\propto NE^{-6/5}$	$[\cos(\phi/2)]^{2/5}$
7 (and BRM)	E^2	$\propto NE^{-2}$	$[\cos(\phi/2)]^2$

These calculations, which take into account the possibility of backward motion (for an obtuse angle), in which head and tail exchange at the instant of field alternation, predicted some further conspicuous qualitative features, such as a mobility minimum in the vicinity of t_{or}, or symmetry breaking in the direction of migration. These features have actually been observed experimentally [for example, by Akerman and Jonsson (1990), for the correlation between t_{or} and the mobility minimum, and Gunderson and Chu (1991) and Gurrieri *et al.* (1996) for symmetry-broken migration]. In general, however, the quantitative comparison with data was disappointing. For instance, the experimental mobility versus size curve presents a narrow region of enhanced selectivity, which is not apparent in analytical predictions, and a larger drop than predicted. The most troublesome discrepancy between predictions and experiments, however, is the behavior of very large chains. The theory suggests that the separation of arbitrarily large DNA molecules can be performed by suitably increasing the pulse time. In practice, however, only chains up to a given size can penetrate the gel at a given field strength, and the field must be decreased to separate larger chains (we shall reconsider this point in Sec. VIII.A.3).

The biased reptation approach to field-inversion electrophoresis, developed by Lalande *et al.* (1987) and Viovy (1989), closely follows the one developed for crossed fields. A drop in mobility around t_{or} is expected if the forward and backward field amplitudes are different. This prediction accounts rather well for the experimental separations of duplex DNA in field-inversion electrophoresis, when the forward and reverse-field amplitudes are different (typically a factor of 2 or more; Lalande *et al.*, 1987). The scaling of the optimal pulse time for separation with size and field also seems in agreement with experiments, in the flexible-chain limit (regime 2) represented by duplex DNA in agarose (Doi *et al.*, 1988; Crater *et al.*, 1989; Heller and Pohl, 1989). Experiments performed more recently at high fields in entangled polymer solutions, which should correspond to regime 5, also yielded a scaling close to $NE^{-1.2}$, in good agreement with the predictions summarized in Table IV (Heller *et al.*, 1995; Magnusdottir, Isambert *et al.*, 1998). The interest of field-inversion electrophoresis for sequencing (i.e., for the separation of single-stranded DNA) has also been explored (Brassard *et al.*,

1991; Heller and Beck, 1992). In this case, though, the improvement over duplex DNA is minor, because the usual sequencing conditions correspond to a weak alignment of chains and thus to weak nonlinear effects (N^* is of the order of 1 kb or larger).

Both the biased reptation model and the BRF model, however, predict that pulsed-field effects should vanish for field inversion with equal field amplitudes, in striking contradiction with the well established separation power of unbiased field-inversion electrophoresis, and with the strongly non-monotonic dependence of the mobility on chain length which has been reported in numerous experiments (Carle, Frank, and Olson, 1986; Crater *et al.*, 1989; Heller and Pohl, 1989; Kobayashi *et al.*, 1990). This failure of the original biased reptation model to explain field-inversion results and the renewed interest of biologists in electrophoresis triggered by large-scale genome programs were incentives for experimental studies of a new type, aimed at testing the theoretically proposed mechanisms of migration at the molecular level.

VI. EXPERIMENTS ON THE MOLECULAR LEVEL

A. Orientation measurements

Following the reptation model's prediction of molecular orientation during gel electrophoresis of DNA and the suggestion that this orientation plays an essential role in pulsed-field electrophoresis, experimental efforts have been directed at the quantitative determination of the alignment of chains under a variety of field conditions. One of the earliest approaches (Holzwarth *et al.*, 1987) measured the polarization of light emitted by DNA intercalated with a fluorescent dye, but most current studies rely on the strong optical anisotropy of the double helix itself, which is a result of the disposition of the bases in planes perpendicular to the axis. After orientation of the chains, one measures either the linear dichroism (Akerman *et al.*, 1985, 1989; Jonsson *et al.*, 1988; Magnusdottir *et al.*, 1994; Akerman, 1996a, 1996b) or the electric birefringence (Stellwagen, 1985, 1988; Sturm and Weill, 1989; Wang and Chu, 1989; Mayer, Strum, *et al.*, 1991, 1993) of a gel loaded with DNA. These techniques are sensitive to the difference in the absorption (for dichroism) or in the refraction (for birefringence) of light polarized in directions parallel and perpendicular to the field direction. In these experiments, attention has been paid to the steady-state value of the orientation, to its response to sudden changes in the applied field, and to the way the orientation relaxes when the field is switched off. A thorough review of early studies of DNA orientation in gel electrophoresis can be found in Norden *et al.*, 1991.

The response of relaxed chains when a field is suddenly turned on is probably the most striking result of these studies. The characteristics of this behavior have been examined in great detail (Holzwarth *et al.*, 1987; Akerman *et al.*, 1989; Sturm and Weill, 1989; Norden *et al.*, 1991; Magnusdottir *et al.*, 1994): The orientation signal rises from zero and displays an overshoot, usually followed by a small undershoot, or even several damped oscillations, before attaining the steady-state value. The relative size of the overshoot increases with chain length and with field strength. The orientation time, i.e., the time taken to reach the overshoot, increases approximately linearly with chain length and decreases approximately inversely with field strength. The preeminent role of reorientation in pulsed-field techniques is emphasized by the observation that the switch time that gives good resolution of fragments scales with molecular size and field strength in the same way (Birren *et al.*, 1988; Heller and Pohl, 1989; Akerman and Jonsson, 1990). Reptation models indeed predicted an orientation, but no overshoot. They also predicted an orientation independent of chain length, in disagreement with the observations (Holzwarth *et al.*, 1987; Jonsson *et al.*, 1988). Similar effects were also observed in the birefringence of DNA in a biased sinusoidal electric field, and could be correlated to size fractionation in this mode of field-inversion electrophoresis (Starchev *et al.*, 1996).

A clue to the origin of this discrepancy is provided by studies of the relaxation of the orientation when the field is turned off (Stellwagen, 1988; Sturm and Weill, 1989). The decay has two components, one fast, and the other slow. The rapid process, which is highly nonexponential, is responsible for the major part of the relaxation for long molecules. The slow process is exponential, with a rate that decreases with the cube of the molecular size, in accordance with the gradual randomization of an oriented tube by Brownian reptation. The slow component could be reconciled with reptation in an oriented tube [Eq. (5.3)] but not the fast one.

These results were quite strong evidence against the fixed-tube-length hypothesis, and they argued in favor of a search for analytical and numerical models more realistic than the original biased reptation model (see Sec. VII). Around the time these improved reptation models were proposed, however, a technical development made possible perhaps the most sensational advance in DNA electrophoresis after the invention of sequencing and of pulsed-field electrophoresis.

B. Watching the real thing happen: Videomicroscopy

Imaging techniques allowing real-time observation of DNA molecules as they moved under an optical microscope and recording of the images on video tape for detailed study were initially developed by Yanagida *et al.* (1983). They were applied to DNA electrophoresis simultaneously by Smith *et al.* (1989) and Schwartz and Koval (1989). These authors published striking images of the behavior of DNA chains in continuous and pulsed fields, soon followed by others (see, in particular, Gurrieri *et al.*, 1990, 1996). These videomicroscopy observations have provided the most direct experimental evidence of the motion of DNA in gel electrophoresis.

When a field is suddenly applied to a set of chains in thermal equilibrium, they extend both ends to form a narrow U-shaped conformation, which, after a pro-

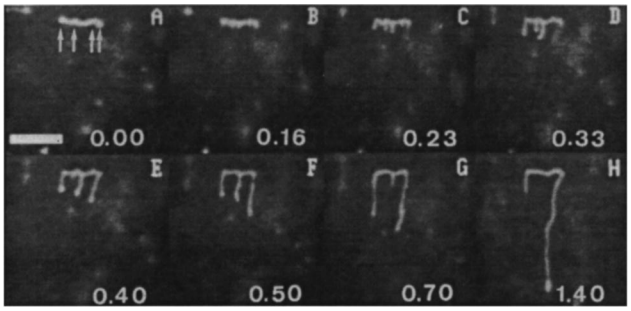

FIG. 15. Evolution of a *T*2 molecule (160 kb) subjected to an electric field in the vertical direction starting at time 0, after having been aligned in the horizontal direction. Bar=4 microns. The molecule does not move as a whole, reflecting the existence of topological (tube) constraints. However, several loops along the path start to grow in (B) and (C). The number of loops progressively decreases, at the same time as the length of the loops increases. Finally, the chain ends up in a Γ shape, before becoming fully aligned in the field and retracting to a conformation comparable to state *A*, but aligned in the vertical direction (these last two steps are not shown in this sequence). Reprinted with permission from Gurrieri *et al.*, 1990.

tracted tug of war between the two arms, resolves into an oriented configuration. During migration in constant field, fragments of λ bacteriophage DNA, of size 48.5 kbp, display a cyclic motion, with frequency strong contractions that usually lead to the formation of U-shape configurations. These configurations are actually very similar to those predicted two years earlier (Deutsch, 1987) in pioneering computer simulations of a flexible chain among obstacles (see Sec. VII.A).[33] When the field is turned off, chains that are in U-shaped or oriented configurations contract rather rapidly to a globule; the same occurs when the field is suddenly reversed, although more rapidly. For large fragments, however, compact conformations never occur, and chains seem to move in a curvilinear manner reminiscent of reptation. Major differences from the original reptation model remain, however: the tube length is certainly not constant, and the leading end is generally the brightest part of the molecule, suggesting that the DNA density along the tube is uneven. Even more strikingly, one can see loops of the chain branching off the main tube and growing in the field, and others retracting.

These studies also provided valuable insights into the mechanism of electrophoresis in crossed fields. When a chain is aligned in one direction by the field, and the field is turned by 90° (Fig. 15), reorientation does not occur from one end, as anticipated in the reptation model: in general, several loops protruding from the initial tube start to grow and, after a rather confused competition, one of these loops wins and the chain finally retracts significantly. This process was anticipated by Deutsch (1987, 1988) in light of his computer simulations. The behavior of large DNA was later observed in various pulsed-field situations. At first, these observations were rather qualitative. More quantitative studies now exist (Matsumoto *et al.*, 1992; Masabuchi *et al.*, 1993, 1996; Oana *et al.*, 1994; Larsson and Akerman, 1995; Larsson, 1995; Gurrieri *et al.*, 1996), but even the first qualitative studies provided direct evidence strong enough to motivate a thorough rethinking of theoretical ideas. In particular, they suggested that a generalized tube model, incorporating internal modes that allow the chain to extend and contract, might be a good representation of the motion of DNA in gel electrophoresis. They also revealed that the formation of loops branching out of the tube had to be taken into account. These loops, currently called *hernias*, seem to occur only above a certain field threshold (Akerman, 1996b; see also theory in Long and Viovy, 1996), resolving to a large extent the controversy raised by Deutsch's simulations: At low fields, loops are rare, and the linear tube model should be valid, but at high fields these loops cannot be ignored. The situation commonly encountered in pulsed-field electrophoresis corresponds to the high-field case described above, thereby explaining why the reptation model was not very successful in its attempts to describe pulsed-field electrophoresis quantitatively. Rather strikingly, however, the latest videomicroscopy studies (Gurrieri *et al.*, 1996), did show that in some cases, such as pulsed fields at an obtuse angle (the most common mode of pulsed fields) the reorientation behavior is actually dominated by a ''ratchet'' mechanism in which head-tail exchange leads to a reversal in direction of migration, as anticipated very early by Southern *et al.* (1987) and studied in more detail by Viovy (1989) and Slater and Noolandi (1989). In this case, as in the constant-field regime, and in contrast with field inversion, hernias affect the predictions quantitatively and not qualitatively.

In complement to orientation studies and videomicroscopy at the single-molecule level, detailed information on the average motion of monodisperse populations of DNA molecules with high time and space resolution (typically 1*s* and submicrometer) were also obtained by the Holzwarth group.[34]

VII. BEYOND BIASED REPTATION: MODELS FOR MIGRATION IN HIGH FIELDS

Discrepancies between videomicroscopy experiments and the predictions of the biased reptation model (presence of an orientation overshoot and of hernias, mobility minimum in field inversion) are actually not so surprising, considering that the electric fields of ~5–10 V/cm at which most of these experiments are performed (as are most agarose gel electrophoresis separations except pulsed-field electrophoresis separations of Mb

[33]Note that this process for the creation of U shapes by extension, starting from a collapsed state, is different from the one proposed in the tube model of Noolandi *et al.* (1987), in which the U shapes are expected to arise from random fluctuations of the tube orientation.

[34]See, for example, Whitcomb and Holzwarth, 1990; Howard and Holzwarth, 1992; Keiner and Holzwarth, 1992; Neitzey *et al.*, 1993, 1995; Hutson *et al.*, 1995; Platt and Holzwarth, 1998.

DNA) correspond for duplex DNA to reduced fields ε of order 1 (see Sec. V.C.2), i.e., to high-field conditions in which the tube constraint [Eq. (5.5)] may be violated. Orientation and videomicroscopy experiments were both a strong incentive and a powerful guide in the search for new models. These models generally rely heavily on computer simulations, due to the need to account for numerous degrees of freedom and to the impossibility of using near-equilibrium expansions.

A. Direct simulations of a chain in an array of obstacles

The most direct type of simulation of DNA electrophoresis (Olvera de la Cruz *et al.*, 1986; Deutsch, 1987, 1988; Deutsch and Madden, 1989; Shaffer and Olvera de la Cruz, 1989) does not impose the constraint of a tube and so avoids the main assumptions inherent in the biased reptation model. Instead, it places a test chain, made of charged beads connected by either freely hinged links or springs, in an array of obstacles and sets up systems of equations for the motion of each bead, taking into account the electric force, the chain tension, and thermal noise. These equations are solved numerically with the condition that the chain may never penetrate the obstacles. To reduce computing time, most of the simulations to date have been performed in two dimensions. It is indeed reasonable to assume that 2D chains in an array of pointlike obstacles will obey essentially the same qualitative physics as 3D chains in an array of connected linear obstacles. [Some 3D simulations, such as those of Norden *et al.* (1991), and electrophoresis experiments performed in quasi 2D geometry (Volkmuth *et al.*, 1992) seem to confirm this expectation.]

The first simulations of this type (Olvera de la Cruz *et al.*, 1986) used harmonic entropic springs to simulate the chain, and a Monte Carlo algorithm. In relatively high fields, this choice led to artificially large extensions of the chain (the length of an harmonic chain can extend to infinity in a strong field) and also to artificial trapping effects due to the discrete nature of the Monte Carlo algorithm. These difficulties were analyzed by Deutsch, who proposed more realistic simulations based on a freely jointed chain and a set of 3D Langevin equations,

$$\xi \frac{\partial \mathbf{r}_i}{\partial t} = t_i(\mathbf{r}_{i+1} - \mathbf{r}_i) - t_{i-1}(\mathbf{r}_i - \mathbf{r}_{i-1}) + q\mathbf{E} + \mathbf{F}_i + \mathbf{B}_i , \tag{7.1}$$

where $\mathbf{r}_i$ is the position of bead i, t_i is the tension between beads i and $i+1$, q is the bead charge, $\mathbf{F}_i$ is the interaction potential between the bead and the obstacles, and $\mathbf{B}$ is the random (Brownian) force. The choice of a freely jointed chain avoids problems with spring extension. It imposes, however, a self-consistent calculation of the tensions at each step, to comply with the condition

$$(\mathbf{r}_{i+1} - \mathbf{r}_i)^2 = l^2 . \tag{7.2}$$

This requires a number of steps of order only N. To avoid divergences at extreme fields and crossing of obstacles, Deutsch represented the gel by discs with a diameter larger than l and combined a hard-core and a soft-core repulsion of finite width.[35]

Simulations of these 2D chains in a continuous field (Deutsch, 1987, 1988, Deutsch and Reger, 1991; Deutsch and Madden, 1989) yielded cyclic motions at odds with the reptation "credo" of that time and actually very similar to the types of motion that were to be discovered two years later by videomicroscopic studies of agarose gel electrophoresis of λ phage (see Sec. VI.B) and by Monte Carlo simulations (Fig. 17 below). In view of the apparent success of the biased reptation model at explaining the saturation of mobility in constant fields, this completely different picture was rather startling. But numerical results indicated that in this model, too, the mobility becomes independent of chain length at high molecular weight. Since fragments of different size cycle in distinct manners, a theoretical explanation of this feature was less evident. This picture also provided a qualitative explanation of two results that the biased reptation model failed to address. First, the anomalous mobility in field-inversion electrophoresis can be interpreted as a resonance effect (Deutsch, 1989): when the pulsing frequency is comparable with the natural cycle frequency the molecule has a tendency to oscillate between U-shaped and compact configurations without progressing. This causes a reduction in the mobility. Second, since the molecules are all initially in random-coil configurations, they start with their cycles in phase and begin to orient in unison. This explains why the orientation at the onset of the field presents an overshoot, since the chain orientation is maximum in the U-shaped configuration. The orientation peak corresponds to the moment when the majority of chains forms oriented configurations. As time progresses, randomness causes the cycles of different molecules to become uncorrelated and the orientation signal settles at the steady-state value, which is the average over many cycles. Last but not least, Deutsch's prediction of cyclic "geometration" motions were confirmed by videomicroscopy studies of the migration of DNA in agarose, at field strengths of about 10 V/cm, i.e., strengths comparable to those used in gel electrophoresis. Further direct comparison of orientation time constants with the distribution of cycle durations measured by microscopy (Larsson and Akerman, 1995) confirmed Deutsch's interpretation of the orientation overshoot.

On mechanistic grounds, Deutsch (1988) and Deutsch and Madden (1989) suggested that the field could draw

[35]Simulations of chains in arrays of obstacles have also been performed on 2D lattice chains (see for example, Kremer, 1988; Batoulis *et al.*, 1989) by a Monte Carlo method. These simulations avoid the "pathological" extensions of Olvera de la Cruz (1986), but they remain limited to rather low fields by both computational time and the problems raised by Monte Carlo simulations for systems far from equilibrium.

loops of the molecule out of the tube to form long sections where the chain is doubled up. These simulations, then, directly challenged the validity of the tube picture for electrophoresis. Application of the model to crossed-field electrophoresis (Madden and Deutsch, 1991) also stressed the importance of loops or hernias, but here the simulations were restricted by the relatively time-consuming nature of the algorithm to chains smaller than 50 kbp (shorter than those most relevant for pulsed-field electrophoresis), and to relatively high fields (corresponding to $\varepsilon > 1$). To avoid this problem, several groups tried to salvage the principle of one-dimensional motion for its analytical and computational simplicity, and at the same time allow for arbitrarily large variations in tube size.

B. Tube models with internal modes of arbitrary amplitude

1. Lakes-straits model

The lakes-straits model, proposed by Zimm in 1988 (see also Zimm, 1991) was the first one to bridge the gap between the biased reptation model and the direct computer simulations of chains among obstacles briefly described just above. It conveyed important new physical ideas and remains a milestone in our understanding of gel electrophoresis in strong fields.

In this model, the polyelectrolyte chain is assumed to occupy a sequence of large pores or lakes, connected by narrower straits. Motion proceeds by exchange of chain segments between different lakes across the straits joining them. It remains a tube model, in the sense that obstacles are gathered into a one-dimensional series of topologically constraining objects (here, the straits) and that the detailed arrangement of these obstacles can be ignored (it can actually be viewed as a biased version of the "slip-link" model introduced by Doi and Edwards in 1986).

Assuming that the chain portion contained in a lake is in thermal equilibrium, and neglecting excluded-volume interactions, the free energy of this chain portion (of entropic origin) can be calculated using the classical theory of entropic elasticity. In the Gaussian limit, the expression is

$$S = k \ln\left[C^n \left(\frac{3}{2\pi n b^2} \right)^{3/2} \exp\left(-\frac{3b^2}{2nl^2} \right) \right], \tag{7.3}$$

where l is the Kuhn length and b is the size of the lakes (more precisely, the distance between the incoming and the outgoing strait), in analogy with the notations chosen earlier for the tube model. When a length dl of chain is pulled from one lake, the entropic free energy changes by TdS. Therefore the tension exerted by the chain portion in the lake on the portion in the strait can be derived:

$$f_i = T \frac{dS_i}{b\, dn_i} = \frac{3kT}{2n_i l} \left(\frac{b^2}{n_i l^2} - 1 \right) + \frac{kT}{l} \ln C, \tag{7.4}$$

where i is the lake index. In Zimm's articles, the constant C is set equal to 1, based on the argument that dynamics are related only to differences between tensions.[36] Equation (7.4) presents the usual "pathological" behavior of the Gaussian approximation for strong forces, i.e., it allows a divergence of the chain size. To correct for this problem, which is relevant to the electrophoresis of long polyelectrolytes (Olvera de la Cruz *et al.*, 1986), Zimm subsequently replaced Eq. (7.4) in his computer simulations by a truncated empirical formula interpolating towards the Rayleigh (1919) result for a finite random flight.[37] The current of segments between lakes, J_i, is then calculated by a balance of electric forces, entropic forces, and Brownian forces:

$$J_i = \frac{(x_{i+1} - x_i)F}{lb\xi} + \frac{f_{i+1} - f_i}{b\xi} + B_i, \tag{7.5}$$

where x_i is the position (in the direction of the field) of the center of lake i, F is a field-dependent constant representing the electric force on the segment in the strait (note that the force on the segments in the lakes is not taken into account), and B_i is a local Brownian force. In the low-field limit, assuming that the current across all straits is equal (i.e., neglecting internal modes of the tube) and summing up all Eqs. (7.5), the model can be solved analytically, and the biased reptation model result is recovered. It is not in this limit however, that the lakes-straits model is the most interesting. For large fields, Zimm (1988) could describe the behavior of the velocity in field inversion and the transient evolution of the orientation. Since other models with comparable physical ingredients were proposed shortly after the lakes-straits model, for the sake of economy Zimm's results will be discussed together with these other models in Sec. VII.B.3.[38]

---

[36] Actually, this is more subtle than it may appear at first sight. In the slip-link model of Doi and Edwards, an entropic tension must be applied on the end blobs, to account from the fact that they have more degrees of freedom (they can orient in 3D) than the in-tube blobs that are constrained to follow the tube axis. Without this end force, the chain would collapse into one single pore. Equation (7.4), in contrast, leads to a null force when the equilibrium average end-to-end distance of the chain portion contained in the lake is equal to the lake size. So, in some sense, it contains the Doi-Edwards end force built in. This is because the free-energy minimization of Zimm is performed on a single lake (implicitly assuming an infinite bath of segments all contained in lakes around it), whereas Doi and Edwards considered the total free energy of a finite chain. This point is discussed in detail by Loomans *et al.* (1995).

[37] Other choices, such as the inverse Langevin function, would probably lead to similar results (see Flory, 1969).

[38] Another model, based on an anharmonic chain of springs in a tube, was proposed by Noolandi *et al.* (1989). The results are actually very similar to those of the lakes-straits model, suggesting that the use of lakes or of a continuous tube is more a question of computational convenience than a physically significant difference.

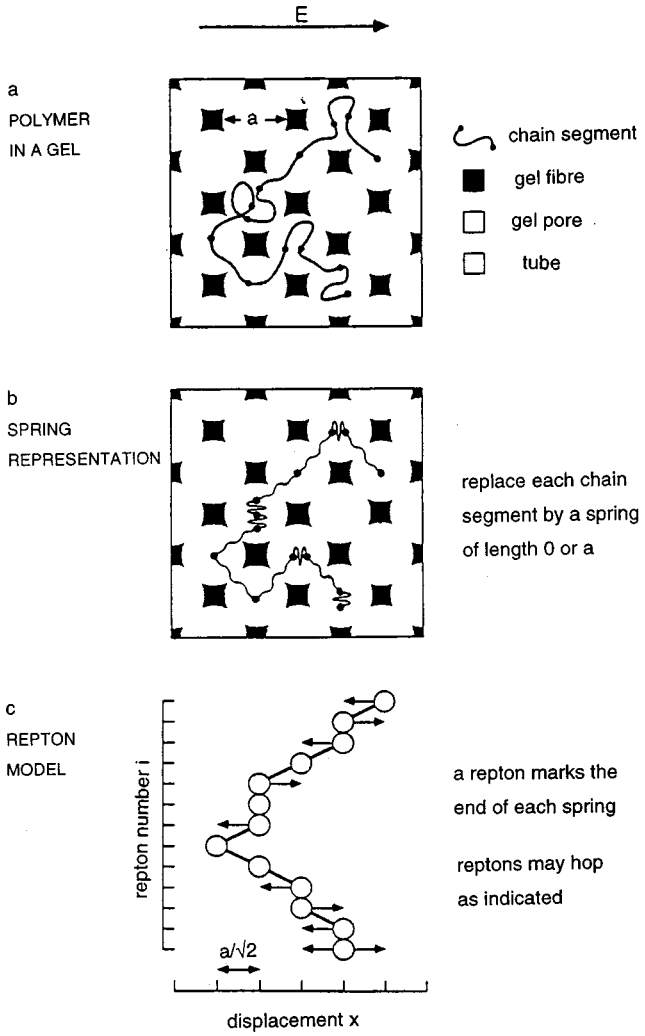

FIG. 16. Schematic representation of the simplification steps leading to the repton model: (a) flexible chain in a model array of obstacles; (b) "all-or-nothing" representation of stored length in the pores; (c) binary repton mapping. Reprinted with permission from Duke, 1990a.

2. Repton model

The biased repton model (Duke, 1989) is based on a rather different strategy for taking into account internal modes, originally proposed by Rubinstein (1987) for entangled polymers. The chain [Fig. 16(a)] is represented as a series of segments (reptons) that can be either collapsed (slack) or fully extended (taut) [Fig. 16(b)]. The slack reptons play the role of "stored length" or defects in the original de Gennes reptation model. The conformation of the chain in the tube can be mapped onto an Ising model (e.g., with spin 0 for slack and 1 for taut). The dynamics are simulated by random exchanges of spins, taking into account the potential energy of the reptons in the external field and following a Monte Carlo algorithm based on local detailed balance. One can see an example of this mapping in Fig. 16(c). The allowed moves are marked by arrows. Special treatment is reserved for the ends, which possess more degrees of freedom. Actually, the end reptons can be viewed as being in equilibrium with an infinite thermal bath of zeros and ones. The relative proportion of slack and taut segments in the reservoir imposes the equilibrium degree of stretching of the chain (since stored length can change only at the chain ends). In the simulations, it is tuned to represent at best the actual ratio of pore size to Kuhn length, i.e., the length stored in the tube at equilibrium. This mapping to a binary problem is a minimalist approach to internal modes, but it was nevertheless expected to retain the correct dynamics of modes larger than the pore size. It makes the model very efficient from a computational point of view, since it reduces to a minimum the number of calculations to be done in floating point (indeed, the longest part of the calculation is the choice of random numbers). Simulations of the repton model have been applied by Duke (1989, 1990a, 1990b) to electrophoresis at moderate fields, in the constant-field and field-inversion modes.

3. Results of tube models with internal modes

The different studies recalled in Secs. VII.B.1 and VII.B.2 emphasized different aspects of the polyelectrolyte dynamics, but overall they provided a very consistent and unified picture. Therefore I present here a synthesis of the results obtained by Zimm (1988), Noolandi *et al.* (1989), and Duke (1989, 1990a, 1990b).

As far as the constant-field mobility was concerned, the main predictions of the BRF model were recovered. Indeed, the E^1 dependence of the mobility versus electric field was reported by Duke (1990a) prior to the analytical development of the BRF model, but it was at that time interpreted as a crossover effect. The band inversion predicted by both BRM and BRF was also recovered. At a molecular level, though, models with internal modes yield cycling motion of molecules in a continuous field. The amplitude of these motions is less pronounced than in the direct simulations (Deutsch, 1987, 1988), but both bunching of the chain and very substantial tube-length fluctuations are observed, and frequently induce the molecules to take up hook-shaped configurations (Fig. 17). As a result, the chains are, on average, stretched within the tube and the degree of stretching increases with molecular size (Noolandi *et al.*, 1989; Duke, 1990a). This accounts for the dependence of the steady-state orientation on chain length. In fact, for large molecules, the greater degree of alignment caused by chain extension is responsible for the major part of the orientation signal, a feature which also explains relaxation after the field is switched off (Sturm and Weill, 1989; Mayer, Sturm, *et al.*, 1991, 1993). The fast decay is due to relaxation of the internal modes as the chain contracts in the tube, while the subsequent slow decay follows the molecule's reptative escape from the oriented tube into a new, random one (Duke, 1990b).

An overshoot at field onset or field reversal was also observed in the simulations, and it could be attributed to a correlated stretching of chains very similar to that proposed by Deutsch (Sec. VII.A). The simulations displayed the same variation of the overshoot time with

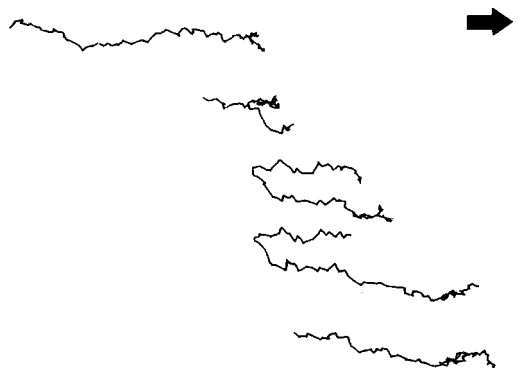

FIG. 17. Simulation of the migration of a 100-kbp molecule in a constant electric field. The gel fibers constrain the chain's motion: (a) The molecule is initially oriented along the field direction (arrowed); (b) it starts to bunch at the head and a hernia begins to grow; (c) the hernia unravels to leave the molecule stretched in a U-shaped conformation; (d) the chain slides like a rope around a pulley; (e) the molecule is once again oriented. After Duke, 1989.

chain length and field strength as observed experimentally, although the amplitude of the overshoot was somewhat smaller.

Finally, these models also provided explanations of the anomalous mobility in field-inversion electrophoresis which were qualitatively similar to Deutsch's description. The reduction in mobility occurs when the pulse time is close to the orientation time. It is caused by the occurrence of field cycles during which the molecule makes no progress (Zimm, 1988; Duke, 1989). The mechanism is as follows: Starting from a compact state, the chains extend during the longer, forward pulse to form a U-shaped configuration, but do not have time to pull free into a fully oriented tube before the field is reversed. Because of tension accumulated along the chain, the field switch causes a recoil of the molecule down the arms of the U, which is faster than the elongation. Therefore, at the end of the short, reverse pulse, the chain is once more in a compact state. During an individual field cycle, the chain does not migrate, but merely changes configuration. Clearly, this mechanism is rather sensitive to the ratio of forward and backward pulse times, with the most significant effect occurring when this is equal to the ratio of the extension and recoil times. Such a sensitivity is borne out experimentally (Heller and Pohl, 1989), where a pulse ratio of 3:1 gives superior separations than higher or lower values.

A comparison of these results with those of direct simulations shows that the internal modes of the molecule in the tube, as well as the extension and recoil of the chain according to the field direction, are primarily responsible for the nonmonotonic mobility in field-inversion electrophoresis. Nonreptative loop formation may amplify this behavior, but it is not the origin of the effect.

C. Critique of modified tube models

In summary, the three models called here "tube models with internal modes" confirmed the initial suggestion by Deutsch that large fluctuations of internal modes were essential to an understanding of gel electrophoresis at relatively high fields. They also showed that these features could be included in a tubelike representation, while keeping an apparently good level of realism. This is much less time-consuming than the direct approach of Deutsch, because the details of the dynamics inside one pore, which consume most of the computer time in direct simulations, are ignored, and also because interactions with obstacles are built into the 1D nature of the problem.

These models also in some sense bridge at least part of the gap existing between direct simulations and the oversimplified reptation approaches presented so far, and offer hope for further analytical progress and general predictions.

The lakes-straits, 1D Langevin, and repton models present specific difficulties and advantages:

- From a computational point of view, the management of time steps in numerical versions of the lakes-straits model is rather delicate [as in all models involving bonded continuous potentials, such as those of Noolandi *et al.* (1989) or Deutsch (1987, 1988)] and is a major limitation to the range of chain sizes that can be simulated in these models.
- As discussed by Zimm (1991), the evaluation of effective friction coefficients in the lakes-straits model involves some assumptions and may be rather delicate.
- In the lakes-straits model, only the electric force on the segments in the straits has been taken into account. Forces are exerted on segments in the lakes too, and it is not obvious that they should play no role, in particular in the case of strong fields.
- The confinement due to the lake "walls" was not taken into account in Zimm's treatment of the lakes-straits model. This question was reconsidered recently by Loomans *et al.* (1995) and Disch *et al.* (1996). These authors showed that changes in the details of the confinement could affect the mobility significantly but apparently do not affect the qualitative conclusions of the model.
- Finally, it is worth mentioning that, in order to save computational time, the Brownian contribution to exchange between lakes in the lakes-straits model were ignored, except at end lakes and branching lakes. I suspect that this amounts to freezing the fast part of length fluctuations, which is important for deriving the correct mobility in the low-field limit (Duke, Semenov, and Viovy, 1992). To my knowledge, however, the dependence of the mobility upon field in the lakes-straits model has not been worked out in detail, so it is not clear at present whether this approximation is a source of problems. In any case, it is not intrinsic to the model and could be removed from further simulations (at the expense of a longer computing time).
- On the positive side, the lakes-straits model provides the most natural framework for investigating the effect of pore-size fluctuations, and the inclusion of hydrodynamic interactions (see Sec. II.F). To my knowl-

edge these possibilities have not yet been explored.

- The 1D Langevin approach raises less delicate questions, but this is at the expense of a significant loss of physical insight, since the difficulties mentioned above are not really solved but simply ignored by the assumption of a uniform tube.
- The repton model presents two advantages over the two previous models: its computational simplicity, and the connection it allows with a large corpus of earlier theoretical work based on the Ising model, in the area of phase transitions and critical phenomena. These two reasons are probably responsible for the attention it has received in the past few years. Indeed, after the first three articles by Duke mentioned above, work based on the biased repton model diverged into two streams. The first, under the impulse of Widom, van Leeuwen, and others, was a thorough theoretical physics investigation of the model in its purest mathematical form. The second, driven by Duke and Viovy, was more interested in practical applications and consisted in modifications of the model aimed at making it more realistic for the high-field conditions in which pulsed-field experiments are performed. The price to pay was a partial sacrifice of the mathematical simplicity of the original model.
- For long chains and high fields, however, the repton model shares with standard Monte Carlo approaches a major conceptual difficulty, discussed by Deutsch and Madden (1989). In the Monte Carlo method in general, motion can only occur by finite-size steps. In the repton model, if a chain adopts a U-shaped conformation, for instance, as represented in Fig. 17, passage of a repton from one side of the U to the other corresponds to the crossing of a potential energy barrier. The height of this barrier increases with both chain size and field, and yields a mobility that artificially decays exponentially to 0 (as reported by Olvera de la Cruz, 1986). Therefore standard Monte Carlo simulations should never be used to describe systems involving free-energy differences significantly larger than kT. This limitation of Monte Carlo simulation was overcome by Duke and Viovy (1992a, 1992b), as we shall now see.

D. Branched tube simulations and nonlocal Monte Carlo

1. Principle and predictions for constant field

Following the observation by videomicroscopy of loop formation during electrophoresis at relatively high fields several tube models with internal modes were generalized in order to account for such tube branching.

In a second version of the lakes-straits model (Zimm, 1991), branching was included by the possibility of overflow out of an internal lake (i.e., a lake anywhere along the chain path, rather than an end lake), resulting in the development of a lateral loop. A general formula for the rate of such overflows (as a function of segment density in the lake) was calculated using a Kramers (1940) reaction-path approach and included in the simulations. A rather similar model was proposed in parallel by Smith *et al.* (1991). The general features of the linear-tube version were recovered, with the following differences:

(a) The conformations of the chains looked very different, with a significant number of loops branching off the tube and pointing in the field direction.

(b) The overshoot and the mobility minimum in field-inversion electrophoresis were enhanced, in better agreement with experiment, suggesting that the presence of loops favors the formation of U shapes.

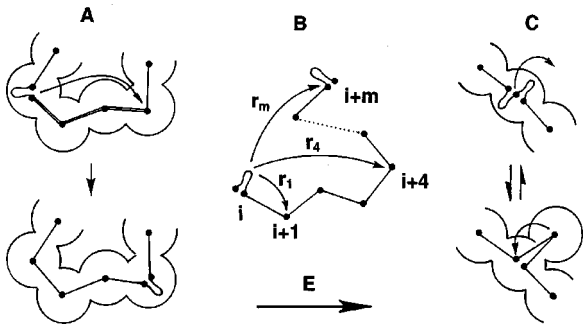

FIG. 18. Move rules used in the nonlocal repton model (Duke and Viovy, 1992b); (a) slippage of taut segments along the tube; (b) possible defect jumps along a taut chain portion; (c) creation of a tube branch (hernia) by annihilation of two defects (slack segments).

The most detailed numerical study allowing for the formation of branched tubes was proposed in a series of articles by Duke *et al.* (1992a, 1992b, 1994; Hutson *et al.*, 1995; Neitzey *et al.*, 1995). Branching is included in a manner comparable to that in the lakes-straits model. A pair of slack reptons is allowed to exchange into a pair of taut segments (pointing in a new direction chosen at random), with an entropic penalty [see Fig. 18(c)]. Before applying this generalized model to the large-fields/long-chains case in which loops or hernias are actually relevant, however, the intrinsic failure of the Monte Carlo approach for high fields had to be cured. This was done by introducing the concept of nonlocal Monte Carlo.[39]

One can remark that, in real situations, a taut section of chain is able to slide bodily along its contour under the action of tension or of an electric force, if it is followed by a defect [see Fig. 18(a) where such a taut segment is shown moving to the right]. After some time, the taut segment has moved over a distance b, the defect has disappeared, and a new defect has been created at a remote distance. This is equivalent to long-range hopping of the defect (the hopping distance along the chain can be arbitrarily long, making the algorithm nonlocal,

[39]A related model, also based on the repton model and including the possibility of branching, was proposed by Deutsch and Reger (1991). This model, however, presented some problems of consistency between the low-field and high-field limits and has not been compared with experiments as thoroughly as Duke's. Therefore I shall restrict the present discussion to the model of Duke *et al.*

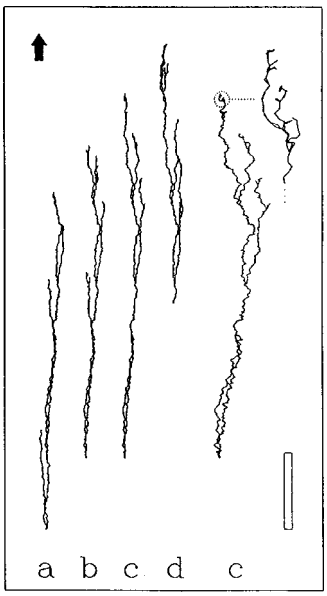

FIG. 19. Successive snapshots of the conformation of a 1000-repton DNA molecule (corresponding to 1 Mb in 1% agarose) under constant field ($\varepsilon=1$), modeled using the nonlocal repton model. On the right, state *c* is laterally expanded for easier visualization. The scale bar represents 100 pores. From Duke and Viovy, 1992a.

in contrast with conventional Monte Carlo in which hopping can occur on neighboring sites only). The problem now is to derive the correct hopping rate, i.e., the one that yields, in the long-time limit, the same result as the continuous Langevin equation. This is done using the same method as for analyzing reputation steps in the biased reptation model (Slater and Noolandi, 1986a, following Feller, 1968), i.e., calculating the mean passage time and the probability of jumps forward and backward for a particle diffusing between two potential barriers:

$$\begin{cases} \tau_{0\pm}=\left[\dfrac{\tanh\gamma}{\gamma}\right]\tau_b \\ p^{\pm}=[1+\exp(\mp 2\gamma)]^{-1}. \end{cases} \tag{7.6}$$

Here the bias between up-field and down-field jump probabilities, p, just reflects the Boltzmann weight, and τ_0 reflects the overall enhancement of the jump rate (for small fields, it is similar to τ_b, and at large fields it becomes linear with E, as the overall drift). The bias γ is given by the end-to end projection of the sliding section of size x ($\gamma=\varepsilon x/b$).

Combining the jump time and the hopping probability [Eq. (7.6)], one derives the hopping rate

$$r(n,x)=\frac{1}{n\tau_b}\frac{\gamma}{[1-\exp(-\gamma)]}. \tag{7.7}$$

Hopping events over different ranges have probabilities that depend on the range (longer hops are less favored due to friction) and on the energy gain/loss due to the hopping.

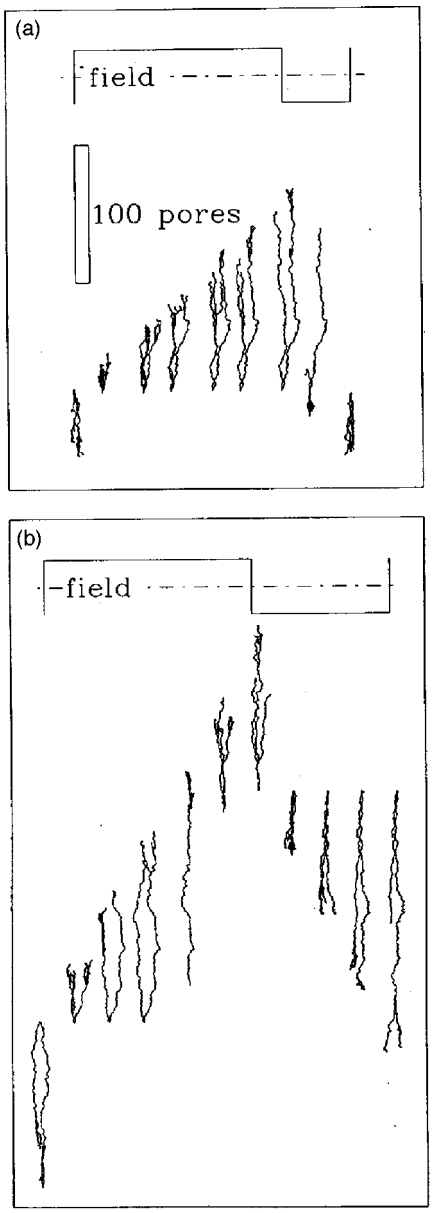

FIG. 20. Time sequence of the configurations of a $N=600$ chain during field-inversion electrophoresis: (a) pulse ratio 3:1 and forward pulse time 3000 computer units, corresponding to the mobility minimum; (b) forward/reverse ratio of 3:2 and 6000 units, corresponding to maximum mobility. From Duke and Viovy, 1992b.

This algorithm is no longer plagued by spurious potential barriers, since the transmission of tension over arbitrarily long distances along the chain, a property of the real polyelectrolyte, is built into Eq. (7.7). It is also much faster than simulations based on the Langevin equation. The discrete nature of the simulation reduces dramatically the number of calculations on real numbers, and in addition the long-range hopping "trick" precludes the need for short time steps in highly stretched conformations. The nonlocal repton model allowed the simulation of very large chains, in the Mb range, and detailed comparisons with videomicroscopy

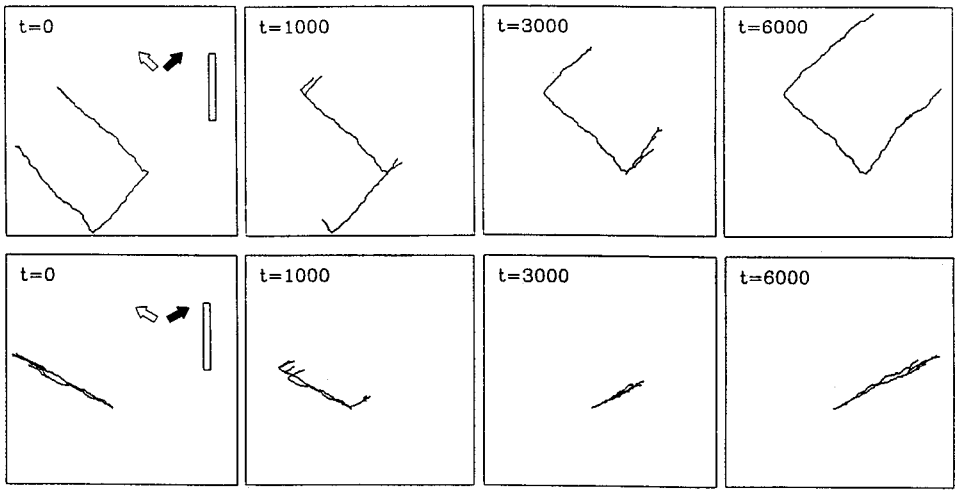

FIG. 21. Successive snapshots of the conformation of a 1000-repton DNA molecule during a single pulse in pulsed-field electrophoresis ($\varepsilon = 1$). Switch time 6000 units, corresponding to the separation domain. Top row, 90°, bottom row, 120°. The scale bar represents 100 pores. From Duke and Viovy, 1992b.

studies and mobility measurements.

First, these simulations provided a clarification of chain motion in continuous fields, demonstrating that the cyclic motion revealed by the direct simulations of Deutsch (1987, 1988) occurs only in an intermediate-size regime (Duke and Viovy, 1992a, 1992b). Longer chains, in the Mb range, adopt configurations in which the main tube is oriented, but hernias (also aligned with the field) branch off it at intervals (Fig. 19). The overall motion is similar to biased reptation, but with a ''renormalized'' tube that fluctuates widely in length as individual hernias unwind at the tail end. Branched configurations of megabase DNA have actually been observed in videomicroscopy experiments. The cycling motion of shorter fragments corresponds to the case in which the chain is not long enough to support the growth of many hernias at the same time. The behavior observed in field-inversion electrophoresis resembles closely that described by Zimm (1991): the effect of tube excursions is to accentuate the anomalous dip in the mobility by increasing the probability that U-shaped configurations will be generated (Fig. 20).

2. Application to pulsed fields

It is in crossed fields, however, that hernias play the most unexpected role (Fig. 21): the way that they help to reorient the molecule explains why the resolution does not vary gradually with field angle, but improves sharply above 90° and remains even for a wide range of obtuse settings. Simulations have shown (Duke and Viovy, 1992a) that when the pulse time is equal to the molecular reorientation time the chains typically alternate between U-shaped conformations aligned along the different field directions. When the fields are orthogonal, the U is broad based and the chain remains extended and advances along the gel during its reorientation, so that the pulse has very little effect on the average mobility. In obtuse settings, on the other hand, the U is usually very narrow and, following the switch, the component of the new field acting back along its arms forces the molecule to retract rapidly and gather in a ball at the base. One or more hernias are pulled out of the bunch to extend in the new field direction as the new head of the molecule, which typically has a forked appearance as observed in videomicroscopy experiments. Finally, the hernias unravel so that, at the end of the pulse, the molecule is once again in a narrow U-shaped configuration. During this reorientation process, the molecule makes little progress along the gel. It is this feature that provides the resolution in obtuse-angle techniques, since fragments of different size are held up for different periods as they change direction. This process is actually much closer to the one at play in field-inversion electrophoresis than was previously anticipated, providing a good basis for the fact that crossed-fields and field-inversion electrophoresis overall present very similar behavior and similar limitations. A quantitative comparison between measurements of the center-of-mass displacement of DNA molecules during crossed-field electrophoresis and predictions of the nonlocal repton model was carried out by Hutson *et al.* (1995) and Neitzey *et al.* (1995). The agreement was better than 50% on absolute values in all cases, and the qualitative behavior was very closely reproduced (see Fig. 22).

Overall, the nonlocal repton model has now been applied to a number of situations involving duplex DNA in agarose (small and large chains, low and high fields, constant and pulsed-field situations, orientation and displacement measurements), and in all these cases the agreement was very satisfying, especially considering the rather strong assumptions involved in the model, such as discretization in reptons and the choice of a uniform pore size. This suggests that the essential features of gel electrophoresis of large flexible polyelectrolytes are captured in this model. Of course, not all situations have been investigated, and one can anticipate that other systems will resist description by a repton image more stubbornly. This could for instance be the case for sieving media with very large pores or large pore-size distributions (when the number of blobs is small, the discretization may become more and more troublesome, and the gathering of electrohydrodynamic effects into an effective force per repton will also become more and more disputable). The repton model may also be inadequate

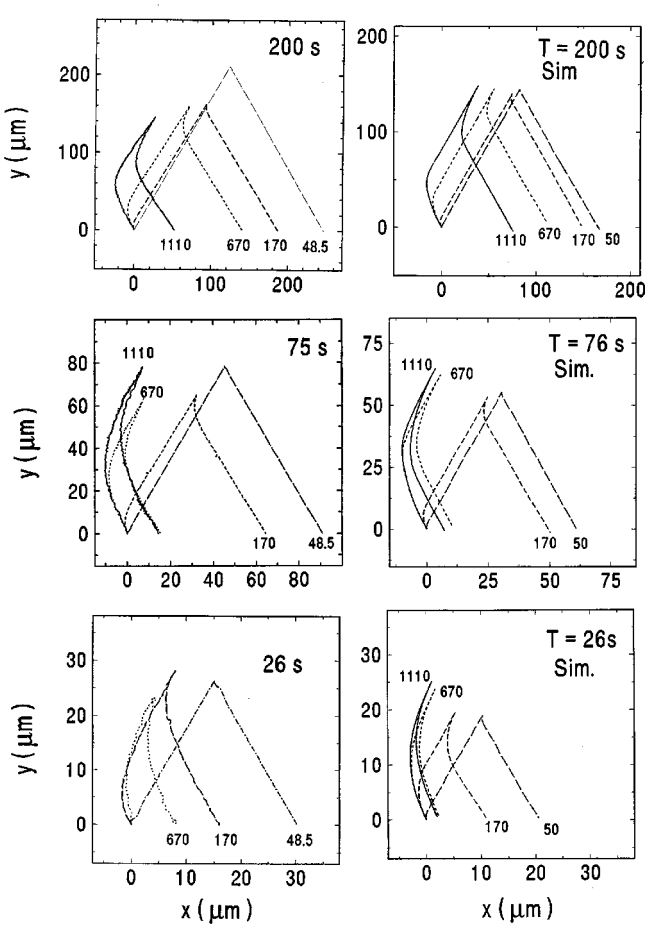

FIG. 22. Trajectories of a DNA band (averaging the center-of-mass displacement of many molecules), as determined experimentally (left) and by the nonlocal repton model using absolute parameters (right). The time corresponds to a complete pulsed-field electrophoresis cycle at 120°, for various molecular sizes (in kbp on the figure). Small molecules instantaneously follow the field, whereas large ones undergo reversed motion, by the ratchet mechanism. From Hutson *et al.*, 1995.

for situations in which the pore size is smaller than the persistence length: the low-field limit has been treated by Semenov *et al.* (1995), but a full understanding of tube constraints in general is not yet available.

E. Return to analytics

Recently, several theoretical efforts have been aimed at using the information gained in simulations to construct simplified, analytically solvable models valid when the reptation models fail, i.e., essentially at high fields ($\varepsilon \sim 1$).

1. Investigating the repton model in depth

A new series of studies of the repton model was launched when Widom *et al.* (1991), remarked that the model's dynamics could be formally written as a set of coupled rate equations on configurations:

$$dp_{xy}(t)/dt = \sum_x \sum_y [W_{xy;x'y'} p_{x'y'}(t) - W_{x'y';xy} P_{xy}(t)], \tag{7.8}$$

where p_{xy} is the probability of occupancy of configuration y at time t and position x (precisely, x is the position of an arbitrarily chosen "label repton"). $W_{xy,x'y'}$ is the transition rate from state xy to state $x'y'$. These rates depend on the external field and follow detailed balance. Because of the move rules specific to the repton model, however, most of these rates are nil, and the others are proportional to G or G^{-1}, where $G = \exp(\varepsilon)$. The x dependence can be described by a standard Fourier transform, so the problem is, so to speak, reduced to the diagonalization of a $3^{N-1} \times 3^{N-1}$ transition-rate matrix for each mode. This problem remains terrible in the general case, because the matrix is not Hermitian for general $\mathbf{q}$, not symmetric in the long-wavelength limit $\mathbf{q} = 0$, and not even symmetrizable when the field is nonzero ($B \neq 1$). Some general theorems have nevertheless been demonstrated, such as the independence of the results from the choice of marker repton for the position (Kolomeisky and Widom, 1996) and the satisfaction of the Einstein relationship between drift and diffusion for the $\mathbf{q} = 0$ mode (van Leeuwen, 1991). Exact results were obtained analytically for chains up to four reptons in Widom *et al.*, 1991, but further progress required use of numerical solutions, or the introduction of simplifying assumptions. To take full computational advantage of the binary nature of the repton model, Barkema *et al.* (1994), wrote the code representing repton transitions in bit operations and were able to perform an extensive simulation of the model. This simulation confirmed in quantitative detail the prediction of the BRF, and the rather unusual scaling of the velocity with $E|E|$ in the limit ($N \to \infty, E \to 0, N\varepsilon > 1$). It also provided accurate evaluations of the prefactors [already included in Eq. (5.25)].

A strong theoretical effort was undertaken by van Leeuwen and co-workers to derive analytical results in the long-chain limit.[40] The latest versions in this series are based on two approximations: the first one is to assume that the number of reptons does not remain fixed to N exactly, but only on average. This approximation is in some sense the counterpart of the assumption of approximately fixed tube length made in the BRM and BRF treatments, but it seems to have fewer consequences for theoretical predictions and to be rather harmless, provided N is large enough. The advantage of this approximation is that it allows the application of standard (grand-canonical) thermodynamics and the use of chemical potentials for the density of *extrons* (in the

[40]See van Leeuwen and Kooiman, 1992; Kooiman and van Leeuwen, 1993; Leegwater and van Leeuwen, 1995; Leegwater, 1995; Aalberts and van Leeuwen, 1996. The last-named paper also contains an interesting discussion of similarities between the repton model and phase transitions in magnetic systems.

nomenclature of this group, a slack repton). The second simplification is called the *fast-extron limit*. In this approach, it is assumed that the density of extrons along the chain changes rapidly as compared to the creation of new extrons at chain ends. The analytical and computational advantage of this assumption is important, since it allows one to focus on the orientational processes occurring at chain ends in the presence of the field, and treat what happens along the chain in a mean-field manner. Therefore this model could be pushed very deep into the scaling regime (at present numerically) and provided very accurate results and scaling laws. The results are quite complex, and there is no unique combination of the variables ε and N leading to collapse of all observables onto a single master curve. For instance, the tube length seems to scale as

$$\frac{L}{L_0}=\left[1+\frac{\varepsilon^2\langle H^2\rangle}{16d}\right], \tag{7.9}$$

where d is the dimensionality of the lattice, L is the tube's curvilinear length (number of ''introns''), L_0 is the equilibrium value of L, and H the order parameter (reduced end-to-end vector projection on field direction), which plays a role similar to that provided in Eq. (5.21) for the BRF model. Interestingly, then, this model is able to account for the dependence of the average tube length on the field (quadratic), which was predicted by computer simulations but was not present in original biased reptation models. A crossover to enhanced diffusion is also observed, but it appears at smaller fields than the deviation from equilibrium tube length: it is asymptotically universal in the scaling variable ε^2N^3. This result is in agreement with the prediction made by both the BRM and BRF model for enhanced dispersion [Eq. (5.35)].

These calculations also revealed the existence of a bifurcation in the probability distribution $p(L,H)$, which becomes bimodal above a critical field. Physically, this transition can be associated with the critical field at which the field-induced orientation of the chain becomes larger than random fluctuations of the end-to-end distance. This should also correspond to the onset of ''reptation with orientation'' in reptation models. Above the transition, the bimodal distribution implies that head-tail exchange becomes improbable. This bifurcation is closely related to the mobility minimum investigated in the framework of the biased reptation model (Doi *et al.*, 1988; Viovy, 1998a; Déjardin, 1989). The development of a shallow saddle point around $H\sim 0$ corresponds to the trapping of chains in conformations of low mobility; Head-tail exchange has also been investigated in the context of the nonlocal repton model by Long, Neltner, and Viovy (1995), and the probability of exchange was shown to decrease with N at fixed reduced field, in agreement with Aalberts and van Leeuwen (1996). Interestingly, however, Aalberts and van Leeuwen find for this bifurcation a combination of variables with a noninteger exponent:

$$\varepsilon_c N^{1.19\pm 0.01}. \tag{7.10}$$

Considering the high degree of accuracy in the exponent provided, the discrepancy remains thought provoking. Actually, it lies between the BRF scaling variables for the transition to an oriented regime for a flexible chain (regime 2 in Fig. 12), εN, and those for a semiflexible chain in regime 6, $\varepsilon N^{5/2}$ (although much closer to the first). It is interesting to note that the repton model as treated by Aalberts and van Leeuwen corresponds from the point of view of the longitudinal modulus to a ''marginally flexible chain'' [$(L-L_0)/L_0$ is of order 1]. Could this noninteger exponent be an effect of crossover to the persistent-chain regime? It has also been suggested (van Leeuwen, personal communication) that these ''unusual'' scaling variables might be specific to the vicinity of the bifurcation. Finally, a third interpretation would be to associate them with perturbations introduced by the fast-extron simplification. Further investigations, for instance, modifications of the dimensionality of the lattice to vary artificially the longitudinal modulus, or numerical simulations with and without fast-extron exchange, might be useful to clarify this question.

Another interesting reexamination of the repton model was recently presented by Widom and Al-Lehyani (1997). By assuming that the tube conformation remains fixed on the time scale of the fluctuations of end segments responsible for the orientation (an hypothesis very similar to the separation of time scales made in the BRF approach to derive the orientation factor self-consistently) these authors obtained an expression for the instantaneous velocity essentially identical to Eq. (5.22), thus confirming this fundamental equation of BRF theories. This work also investigates finite-size corrections, using the scaling variable $N\varepsilon$ introduced by Barkema *et al.* (1994). It confirms that the tube length ratio $L/(N-1)$ remains of order $\frac{2}{3}$ (the exact numerical value depends on the choice made for the thermal bath of reptons, or, in other words, on the entropy cost of staying in the tube), with finite-size correction falling off with E^1.

An interesting question that remains is that of the transmission of tension, already discussed in Sec. VII.D. For long chains in relatively high fields (e.g., $N\varepsilon\gg 1$), the phase space of the repton model should be corrugated into numerous subsets of configurations separated by high potential barriers (associated with U shapes). This phenomenon, which is considered as a spurious effect of discretization when one views the repton model as a tool for representing a real continuous polyelectrolyte, is a real property of the model as a mathematical object. It may be expected to lead to trapping events and ultimately to exponential slowing down of the dynamics, as observed in several models of dynamics in random fields. Why is such slowing down not observed in the works presently published? It would be interesting to check, in particular, if this is a consequence of the simplifying assumptions discussed above, which artificially smooth the phase space, or a more fundamental property of the repton model, which might dynamically avoid

trapping conformations. An interesting and original point in the biased repton model (and in biased reptation in general) taken as particular realizations of diffusion in a random potential, is that the disorder is ''annealed'' because the tube is in permanent renewal, but only over a long time scale, because there is some memory frozen in the tube conformation.

2. Analytical models for high fields

As discussed in Sec. VI, the weak-field condition expressed by Eq. (5.5) is easily violated, and fields yielding to strong stretching are easy to obtain with semiflexible polyelectrolytes like duplex DNA. For instance, measurements of the orientation and mobility of *T*2 DNA (166 kbp) showed that the full-extension characteristic of the high-field limit is reached at 15 V/cm in 1% agarose (Akerman, 1996a). An interesting model for such situations, proposed by Lim *et al.* (1990), was based on a chain of anharmonic springs with finite extensibility in a tube. It addressed the problem of transient orientation of chains at the field onset. The evolution of the conformation, starting from a state with a small order parameter H, was solved in the high-field limit ($\varepsilon > 1$). The authors argued that in this limit Brownian motion becomes irrelevant, and the problem becomes deterministic. Essentially, chain segments start to protrude from both ends of the tube in the direction of the field and create new tube sections, which grow simultaneously at the expense of the stored length initially contained in the tube. The authors also assumed that, apart from a negligibly small transition region, the chain segments (anharmonic springs in the model) abruptly jump from their relaxed state to a fully stretched state. After some time, the entire chain is fully stretched, after which curvilinear slippage (triggered by the initial asymmetry in the tube) occurs, following the well-known rope-over-a-pulley process. This finally leads to a full disengagement of the chain in an oriented state followed by a longitudinal (Rouse-type) relaxation. This process qualitatively accounts for orientation overshoot. The time of maximum stretching (overshoot time) was predicted to scale as $\sim N \ln NE^a$ where the exponent a is equal to 1 in strong fields and 2 in weak fields. This model, however, did not include the possibility of loops growing sideways from the tube (an easy process in the limit $\varepsilon > 1$).

A detailed analysis of this latter process was recently made by Long and Viovy (1996, 1997). This work can actually be viewed as a synthesis of the Lim-Slater-Noolandi (1990) model, and of a model proposed by Deutsch (1987) for pulsed-field electrophoresis. Deutsch's idea was that, when a chain is oriented in a given direction and a field is suddenly applied perpendicular to it, numerous hernias of random sizes immediately nucleate and start to interact, the larger ones ''eating'' their smaller neighbors by the rope-over-a-pulley process, until only one hernia remains. Long and Viovy reconsidered the same situation, in a more detailed study allowing for stored length along the tube (in the form of anharmonic springs, as in Lim *et al.*, 1990). An interesting prediction of this more complete model is that there are two possible regimes for the disengagement: below a size N_c, which depends on the nucleation and growth rate of hernias, disengagement occurs mainly by the ends (as in Lim *et al.*, 1990), while above N_c, competition between hernias, as in the Deutsch model, is the dominant process. The model also predicted that the shape of the orientation overshoot is actually more complex than previously expected. For large enough chains, it should present a shoulder, corresponding to a time independent of molecular size (this shoulder marks the full extension of the chain in its tube and the beginning of the Deutsch process), followed by a larger maximum with a time proportional to chain length (corresponding to the disappearance of the last hernia). Interestingly, the existence of hernias wipe out the logarithmic term predicted in the Lim model, i.e., stretching time is linear in size. These predictions concerning the overshoot were confirmed experimentally (Akerman, 1997). The experimental nucleation rates also exhibit the predicted exponential field dependence, and decreasing the pore size slows down hernia nucleation.

Other recent theoretical efforts have been aimed at describing the evolution of chain conformations and of the mobility in a steady field, in the high-fields regime in which hernias are frequent. The first one (Obukhov and Rubinstein, 1993, and Lee *et al.*, 1996) is, like the Lim model, based on the idea that the evolution of large chains in strong fields should obey deterministic rules. The model takes inspiration from the observation made by Duke and Viovy 1992a, 1992b, that large chains in a steady field progress in an elongated treelike conformation with the tip of the branches in the downfield direction (Fig. 19). In this model the creation and coalescence of hernias is the leading process of the dynamics. Hernias are permanently created at the tips of the branches by a local tip-splitting process. This process is actually the only place in which randomness enters the model. The conformation subsequently evolves by purely deterministic equations of motions, modeling the chain as an inextensible uniformly charged rope with uniform friction. In spite of its simplicity, this model yields very interesting conclusions:

(i) A self-similar structure of the conformation is recovered, with an average number of hernias proportional to $\ln(N)$.

(ii) The average velocity is independent of molecular weight (a consequence of the local character of the tip-splitting process) and equal to 30% of the free-liquid velocity. This prediction is in remarkable agreement with the experimentally observed value [$\alpha = 3$ in Eq. (5.26) and Akerman, 1996a].

(iii) The quasicyclic motion apparent in computer simulations is also recovered.

(iv) The model seems to depend rather weakly on the precise value of the tip-splitting probability, a phenomenological parameter in the model that is difficult to evaluate directly from molecular properties.

(v) Finally, it is worth noting that the model predicts quantitative but no qualitative differences between the

behavior of a linear and of a ring polymer. This prediction is at odds with experimental evidence, as discussed in Sec. VIII.B.1, probably because of the possibility that rings may hang around protruding fibers of the gel, not considered in the model.

Semenov and Joanny (1997) have also proposed an analytical model for the electrophoresis of large DNA involving hernias (called ''hairpins'' in this publication). Like Lee *et al.*, the authors make use of the expected convergence of linear and ring polymers when hernias come into play, but Semenov and Joanny focus more on the moderate field limit (ε of order 1). They show, in particular, that the rate of hairpin nucleation in this domain should be dominated by fluctuations in the tube orientation and can be given by

$$\Gamma = \exp(-C_{st}/\varepsilon^{1/2}), \tag{7.11}$$

where C_{st} is a constant that depends on the gel structure and polymer persistence length. The exponential is typical of an activated process. The field exponent is more unusual and is related to the fact that the field affects the height of the barrier directly, via force exerted on one chain segment, and indirectly, by increasing the orientation of the tube and decreasing its conformation fluctuations. For chain orientation, the authors use quasiequilibrium arguments on the conformation of ring (or folded) polymers. They picture the chain in the course of migration as a linear sequence of fractal ''Pincus blobs.'' Below a critical size, scaling as $N^{1/2}\varepsilon^{1/5}$, the local conformation is that of a ''lattice animal'' (Derrida and Herrmann, 1983), without excluded volume. Above this size the chain is essentially stretched. The model also predicts that, due to the onset of hairpin formation, the mobility should increase by a factor of order $N^{1/6}$, around a reduced value of the electric field $\varepsilon^{**} \sim N^{-5/6}$. Finally, this model leads to the prediction, nontrivial and at odds with the conventional reptation *credo*, that in the limit of N and experimental time tending to infinity, the linear tube conformation is absolutely unstable for any value of ε. For experimentally reasonable numbers, however, the scaling predictions are rather close to those of the BRF model (i.e., a model without hernias), so they may be difficult to check experimentally. This may be why the fractal-blobs structure predicted by this model has never, to my knowledge, been observed either in videomicroscopy or in computer simulations: it may correspond to an asymptotic regime that is experimentally or numerically inaccessible. A similar question is also raised by the conditions (and time) necessary to observe the predicted low-field breakdown of reptation. For high fields ($\varepsilon > 1$), finally, Semenov and Joanny predict an almost fully stretched chain, but do not consider the dynamics of hernias in detail.

In complement to these rather involved theoretical studies, it is worth mentioning a simple treatment of the ''geometration'' mechanism in terms of steps, recently proposed by Gisselfält *et al.* (1997), which provides a convenient and intuitive framework for the design and interpretation of experiments. The question of band broadening in the high field regime was also addressed recently by Popelka *et al.* (1999), using a generalization of the ''geometration'' model of Deutsch (1989).

VIII. OFF THE MAIN TRACK: LESS COMMON SEPARATION MECHANISMS

During the last 10 or 20 years, the main interest of physicists in electrophoresis has been in problems posed by the separation of large DNA and the concepts of reptation. There are, however, mechanisms that do not resort to this approach. We have already considered one, the sieving of globular particles, in Sec. IV. We shall now review a series of mechanisms that can be gathered into the general category of ''trapping phenomena.'' These include all types of polyelectrolytes, either globular or flexible, so it might have been more logical to discuss them earlier in this review. However, this discussion is much easier to do now, because trapping events invoke concepts that have been introduced when discussing various dynamic and thermodynamic properties of flexible chains involved in reptation. I shall also briefly mention some interesting mechanisms specific to particular polyelectrolyte architectures.

A. Trapping mechanisms

1. Entropic trapping

In the interest of linearity in the presentation, I claimed in Sec. I.C.2 that the BRF model agreed almost quantitatively with experimental data in the low-field limit. This was somewhat oversimplified, however. For instance, careful examination of the lowest-field data in Fig. 9 reveals that the experimental mobility-versus-size curves present a steeper slope than the theoretical ones. Other data from the same article, obtained in more concentrated gels, present a more pronounced deviation from BRF prediction, with slopes lower than -1 in a size range that should correspond to unoriented reptation. Even more dramatic behaviors, with local slopes exceeding -2, were reported by Smisek and Hoagland (1990) and Arvanitidou and Hoagland (1991) for polystyrene sulfonate and by Mayer, Slater, and Drouin (1994a) for single-stranded DNA. This behavior seems favored by concentrated gels, low fields and flexible polyelectrolytes, and it is very reproducible. The groups of Hoagland and Slater attributed it to a process called *entropic trapping*, first reported after computer simulations of polymer diffusion in random environments (Baumgartner and Muthukumar, 1987; Muthukumar and Baumgartner, 1989).

The physical basis of this phenomenon is actually very simple. When a flexible polymer is located in a random environment with a distribution of pore sizes and an average pore size comparable to the polymer radius of gyration or somewhat smaller, there is competition between distribution of the chain length among several pores (the formation of a ''tube,'' responsible for reptation and discussed at length in this review) and squeezing of the whole chain into a single pore. In the latter

process, of course, the entropy loss will be minimum in the largest pores, and generally there is a range of polymer sizes for which a finite fraction of the pore-size distribution is able to ''house'' the whole chain at an entropy cost smaller than that of a tube conformation (and also, obviously, smaller than in other smaller pores). In general, these larger pores are localized, so their centers constitute local minima for the part of the free energy that is of entropic origin (hence their name ''entropic traps'').

If the field is weak enough as compared to the entropic trapping effect (i.e., if the traps survive when the free-energy profile is tilted by addition of a potential-energy contribution of electric origin), we expect significant slowing down of the electrophoretic mobility. The size dependence of this slowing down (for a given pore-size distribution) is difficult to evaluate from these simple qualitative arguments and has been the object of both numerical (Baumgartner *et al.*, 1987; Slater and Wu, 1995; Nixon and Slater, 1996) and analytical work (Muthukumar and Baumgartner, 1989). These studies effectively show a general but nonuniversal slowing down of the mobility, with nonscaling behavior and local exponents dependent on the randomness of the structure. The entropic nature of this trapping well explains why it is most pronounced for flexible chains that present, at equal radius of gyration, a stronger entropic contribution to the free energy.

From a polymer physics point of view, entropic trapping is actually a very natural process (related to the well-studied mechanism of size-exclusion chromatography), and it is somewhat surprising that is has been overlooked for quite a long time in the context of gel electrophoresis. This is probably due to the conditions necessary for its appearance, and in particular the requirement of low fields: such conditions are not very interesting as far as separation is concerned, and they were avoided by experimentalists on a pragmatic basis.

2. Enthalpic trapping and random potentials

Several theoretical attempts have been made to analyze biased diffusion in a random 1D potential (de Gennes, 1982; Loring, 1988; Bouchaud and Georges, 1988; Lumpkin, 1993; Zimm and Lumpkin, 1993). Roughly speaking, random unbounded 1D potentials should always yield anomalous diffusion and exponential slowing down in the long-time limit (Bouchaud and Georges, 1990), a behavior not common in gel electrophoresis of linear polyelectrolytes (we shall see that the situation is different for other objects). An interesting article by Zimm (1996) probably provides the clue to this divergence. In this article, random potentials in two dimensions, with or without lateral channels, are compared. Migration in the model without channels leads to a sharp slowing down, whereas the laterally connected matrix yields finite mobility in the limit of low electric fields. This is due to a unique property of the 1D potential, that of having no way to circumvent the highest potential barrier in the whole distribution. Zimm argues that this particularity makes 1D random potentials very poorly adapted to the modeling of motion in random 3D gels, but shows that a ''clipped'' potential in which the high bumps of the distribution are erased provides results very similar to a model of higher dimensionality (in this particular case 2D), while remaining easier to handle.

3. Irreversible trapping

When presenting pulsed-field electrophoresis (Sec. V.G), I mentioned that separating larger and larger molecules by this technique requires lower and lower electric fields. This leads to inconveniently long separation times and ultimately to an absolute limitation of the method, which probably lies around 10 Mb. This limitation is not explained by current models of migration. Several articles (Smith and Cantor, 1987; Carle and Olson, 1987a, 1987b; Olson, 1989a; Turmel *et al.*, 1990; Gemmil, 1991) have associated it with a field-dependent trapping phenomenon. An experiment specifically designed to study field-dependent mobility anomalies (Viovy *et al.*, 1992) has demonstrated that this trapping is irreversible. The experiment uses a programmable rotating gel pulsed-field electrophoresis apparatus. Starting with a Mb DNA molecular weight standard, a conventional crossed-fields gel electrophoresis is performed, in a low field E_1 optimized for the separation of the different bands in the standard. Then a cycle at a different voltage E_2 is performed. In a third step, the gel is turned by 90°, and crossed-fields gel electrophoresis in the initial conditions is resumed. When $E_2=E_1$, the bands corresponding to the different sizes in the standard are resolved and aligned on a tilted axis, with an angle depending on the relative duration of the first and third steps [Fig. 23(a)]. When $E_2>E_1$, however, the bands corresponding to smaller sizes continue to behave as with equal fields, but molecules larger than a given threshold are unable to resume motion during the third step at low field [Figs. 23(b)–(d)]. This demonstrates that they have been irreversibly trapped in the gel by the higher-field sequences. The transition to this trapping behavior is rather sharp, and the critical size for trapping scales roughly as $E^{1.5\sim2}$. (Considering the E^2 dependence of electrophoretic velocity, this means that doubling the size of the DNA to be separated increases by a factor of 8–16 the duration of the experiment!)

This irreversible trapping has been attributed to the formation of tight knots, following the formation of topologically interpenetrating loops by a hernia growth process. The predicted scaling for the critical trapping size (within the BRF model in the limit of strongly extended chains) is $E^{1.5}$, in good agreement with experiment, but a more direct proof of this mechanism is still missing. It is worth noting that at low gel concentrations (typically $<1\%$), the well-defined arrested bands for large chains are progressively replaced by horizontal smears, suggesting that the arrest of chains also induces chain breakage. The breakage is more pronounced for more dilute gels, a reasonable result considering that en-

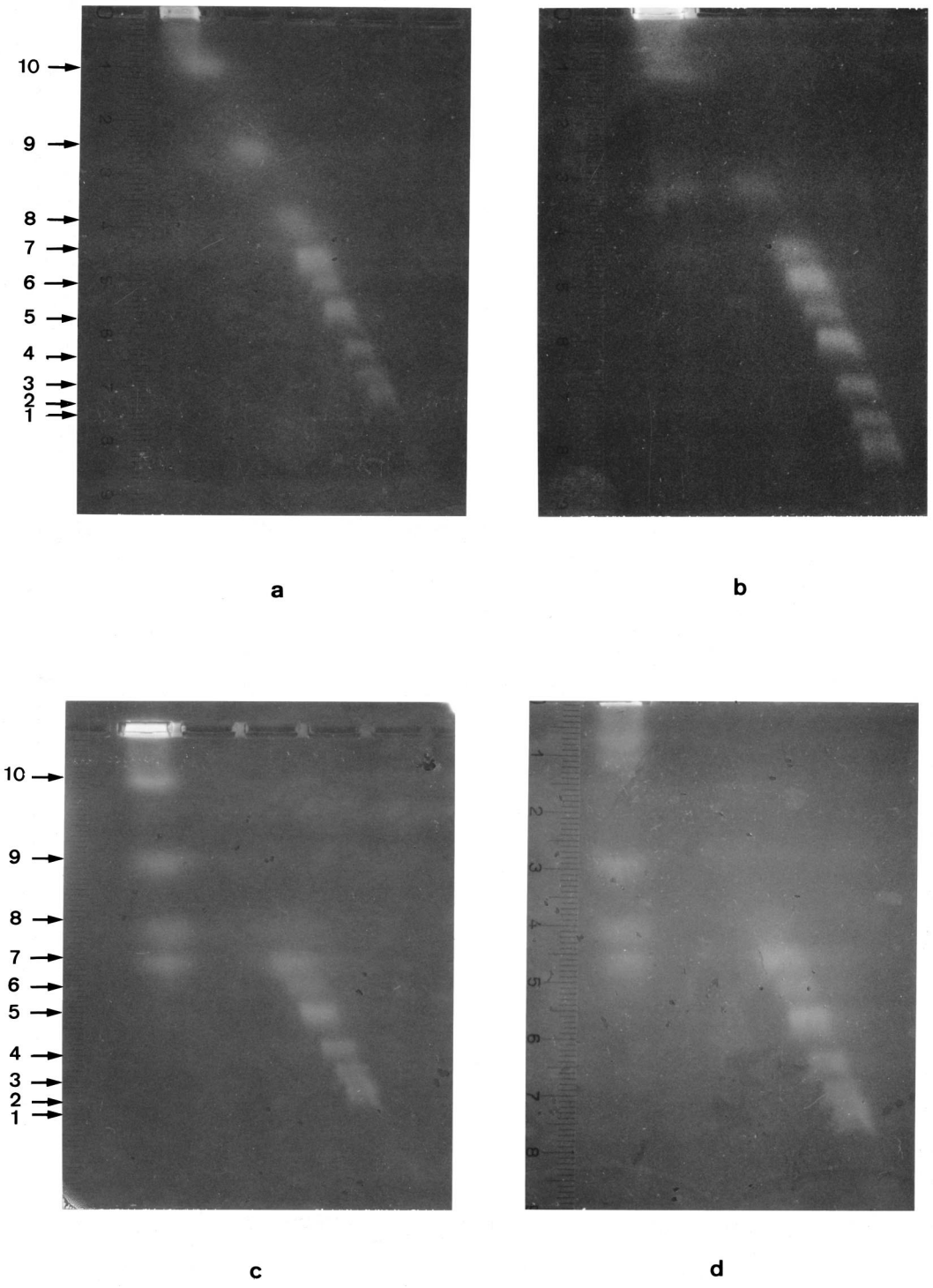

FIG. 23. Demonstration of irreversible trapping of *Saccharomyces Cerevisiae* chromosomes during pulsed-field electrophoresis in 1.5% agarose. In both cases, a field of 6.7 V/cm, 90 s was applied for 22 h in the vertical direction and 12 h in the horizontal direction. Between these two steps, a pulsed field was applied: (a) at 6.7 V/cm, (b) at 7.8 V/cm, (c) at 9.1 V/cm, and (d) at 10.6 V/cm. High fields during the second step lead to irreversible trapping of the largest chromosomes, which are therefore unable to resume their motion sideways. Chromosome sizes are the same as in Fig. 13. From Viovy *et al.*, 1992.

tanglements with the gel are able to prevent tension along a trapped chain from being fully transmitted to the trapping point (we have seen in the BRF model that larger pores yield larger orientations).

4. Trapping of rigid particles

In contrast with flexible polyelectrolytes, rigid particles easily get trapped in a gel and produce mobility

curves with cutoffs (mobility decreasing to 0) at finite particle size (Griess *et al.*, 1990; Griess, Guiseley, and Serwer, 1993; Griess, Harris, and Serwer, 1993). As suggested by these authors, the cutoff is very probably due to trapping of particles in ''dead ends'' of the gel, against openings in the structure too small to be penetrated. Particles larger than 100 nm, i.e., larger than proteins, can easily be in a regime in which the electrostatic barrier to migration exceeds the thermal energy, thereby inhibiting thermal detrapping. As remarked by Slater and Guo (1996a, 1996b), this trapping challenges the free-volume model, by indicating loss of ergodicity in gel electrophoresis. Griess and Serwer (1990) and To *et al.* (1993) showed that mobility could be restored to some extent using field-inversion electrophoresis to detrap particles periodically, and to help them in finding the largest pores in the structure (in the case, field pulses play the same role as Brownian forces for smaller particles). By combining long pulses of low intensity and short pulses of high intensity, these authors were even able to move in opposite directions large and small particles bearing charges of the same sign and to obtain a strongly enhanced resolution for particles with a size corresponding to the threshold between these two behaviors (Serwer and Griess, 1998).

B. Polyelectrolytes with nonlinear architectures

Specific migration mechanisms also exist for polyelectrolytes with a structure or topology different from that of the linear, uniformly flexible and uniformly charged polyelectrolytes.[41]

1. Circular polyelectrolytes

Circular polyelectrolytes are probably the most commonly encountered nonlinear flexible polyelectrolytes, as far as applications are concerned. This is because numerous chromosomes, and notably the plasmids extensively used for cloning, naturally occur in a circular form. Because of the particular double-helix form of DNA, a further distinction must be made: When a double helix is closed on itself, the number of turns is frozen, and so is the twist (number of turns per unit length). Since changes in the environment can change the equilibrium twist, it can easily happen that the frozen state does not correspond to the equilibrium twist, i.e., the helix bears a torsion. In that case, most of this torsion is relaxed by *supercoiling*, i.e., making a helical superstructure (a phenomenon that can be experienced daily with telephone chords, at least until cellular phones become widespread enough to deprive physicists of this convenient pedagogical tool). Another way to relax torsion is to change the number of turns, by the action of an enzyme (the topoisomerase) or by the presence of a single-strand nick (a nick is a rupture in the backbone in one of the two strands of the double helix—it allows relaxation of the torsion; the DNA in that case is called ''open-circular'').

The macroscopic structures of supercoiled and relaxed DNA differ markedly: the open-circular molecule resembles (for long enough chains) the Gaussian ring familiar to polymer physicists, whereas supercoiled DNA presents a more compact rodlike (possibly branched) structure (see Dubochet *et al.*, 1992, for a review of this subject, and Marko and Siggia, 1994, 1995, for a theoretical analysis). These structures can interact differently with a gel, and gel electrophoresis is indeed the tool most commonly used to analyze the twist of circular DNA. For supercoiled DNA molecules, which are relatively compact, some qualitative aspects of the migration are reasonably well described by Ogston-like sieving mechanisms, and the more compact (i.e., the more supercoiled) the molecule, the faster it is. It is possible to use this property in combination with the fact that intercalators modify the twist of DNA, to elegantly analyze all the topoisomers of a circular DNA by simple gel electrophoresis experiments (Depew and Wang, 1975). The orientation of supercoiled DNA is also weaker than that of relaxed DNA, as expected (Stellwagen, 1988). Finally, it is worth mentioning that the gel electrophoresis mobility of supercoiled DNA in acrylamide seems to depend on the handedness of the supercoiling (Drak and Crothers, 1991). This is not unexpected from Curie principles, since DNA helixes with right- and left-handed supercoiling are not mirror images of each other due to the twist of the DNA molecule itself, but, as mentioned in Zimm, 1993, no molecular explanation is available at present.

The migration of relaxed rings is more easily described by statistical mechanics, and this has been undertaken by Lee *et al.*, (1996), Semenov and Joanny (1997), and Alon and Mukamel (1997). Actually the predicted migration mechanism is not dramatically different from that observed for linear chains in high fields (when hernias are present), with the difference that for rings there is no alternative linear reptation mechanism available, so that amoebalike progression by growth of hernias remains the only mechanism, even at low fields. Also, fluctuations in the conformation and in the velocity are greater for ring polymers, because for linear polymers the extremities tend to be localized upfield and downfield and to stabilize the conformation (see Lee *et al.*, 1996). In real gels and in particular in agarose, however, the situation is rather different from these predictions, and trapping with exponential slowing down of open-circular DNA is frequent (Mickel *et al.*, 1977; Serwer and Hayes, 1987). This trapping is attributed to the presence of protruding ''pillars'' or ''hangers'' in the gel structure (agarose is made of very rigid multiple helix structures), on which the ring molecule becomes caught or threaded in the course of migration. This interpretation is consistent with the strongly enhanced orientation as compared to linear DNA of similar size, the lower

[41]Taken in its most general sense, this definition involves most native proteins and compact biomolecules, which are never perfectly spherical (see Goldenberg and Creighton, 1984). Several attempts have been made in the past to extend the free-volume model to nonspherical molecules (e.g., Tietz, 1988). They are discussed in Sec. IV, and the present section will deal with flexible polyelectrolytes only.

trapping probability of the supercoiled form as compared to the relaxed circular form (Akerman, 1998), and the fact that well-chosen pulsed fields are able to restore mobility for these molecules. Pulsed-field electrophoresis is indeed one way to differentiate linear and circular DNA that have the same constant-field mobility (Louie and Serwer, 1989; Serwer and Hayes, 1989b; see also Birren and Lai, 1993).[42]

2. Bent semirigid molecules

Semiflexible linear polyelectrolytes like duplex DNA can feature local bends related to specific sequences. When these molecules are electrophoresed in a gel with a pore size smaller than the persistence length, the angle of these bends and their position along the molecule affect the electrophoretic mobility (Levene and Zimm, 1989). This phenomenon, combined with the ability to cut the DNA molecule at different locations by restriction enzymes, can be used to locate rather precisely the position of a bend along the sequence (several applications are reviewed by Stellwagen, 1987).

3. Heterogeneous polyelectrolytes

Polyelectrolytes with inhomogeneous distributions of charges are very common in biology. Proteins, in particular, generally feature very specific distributions of charges, which lead to neutrality at a well-defined *p*H (isoelectric point) and are at the basis of the isoelectric focusing separation technique. In sieving gel electrophoresis, one deliberately avoids this complication and restores a uniform charge density, ensuring that the mobility will depend on size only. This may be done by a suitable choice of *p*H or by solvating the molecule with highly charged surfactants. The combination of *pI*-based fractionation of native proteins in a first dimension, followed by size fractionation of the same denatured proteins in a second dimension is the basis of 2D electrophoresis, a major tool in biology. This technique will gain further importance in the coming years, with wider use of massive ''proteome'' analysis (entire books and special issues of reviews are regularly dedicated to this domain. For a recent account see Dunn, 1994, 1997). I shall not consider this application further here, because it appeals to completely different mechanisms (chemical equilibria in polyampholytes) that are beyond the scope of this review. I discuss only studies concerning gel electrophoresis of charged *flexible* block copolymers. Free-flow behavior will be discussed briefly in Sec. IX.C.

Gel electrophoresis of block polyelectrolytes was pioneered and studied in detail by Slater, Noolandi, and co-workers (Slater and Noolandi, 1986b; Slater, 1992; Slater, Noolandi, and Eisenberg, 1991; Wu and Slater, 1993). Two general ideas underlie these studies. The first, which came directly from the reptation model, is that the orientation of the tube is due to the local orientation of the head segment, so that a small length of uncharged or differently charged polymer at the chain ends could dramatically change the orientation and consequently the dynamics. In particular, self-trapping was predicted in some cases, and improved resolution in others (see Slater, 1992). It would probably be interesting to reconsider these predictions in depth in the light of recent work on nonreptative processes. In particular, it is now recognized that, at high fields, hernias play an essential role in the dynamics (see, in particular, the discussion of high fields in Secs. VII.B and VII.D and Lee *et al.*, 1996). In low fields, the hernia nucleation rate is low, but for block polyelectrolytes one may expect significant accumulation (or depletion) of stored length at the boundary between blocks, even in the $\varepsilon \ll 1$ regime.

Another interesting idea (Wu and Slater, 1993) is that for a neutral chain carrying small amounts of localized charges (e.g., at the end, as in telechelic ionomers), easily available electric fields are able to dramatically affect the conformation of the chain in a manner that depends heavily on the details of the charge distribution.

4. End-labeled polyelectrolytes and trapping electrophoresis

The last category of polyelectrolytes discussed here (which may formally be considered as a particular case of block polyelectrolytes), is that of uniformly charged chains labeled at their ends with a bulky component (for simplicity, we shall consider this labeling component to be neutral, although most of the remarks that follow would also apply to a differently charged label). Interest in this construct was triggered by an article of Ulanovsky *et al.*, 1990, in which the mobility of single-stranded DNA molecules end-labeled with streptavidin was reported to have a striking dependence upon size and field. For small DNA sizes, the protein simply reduces the mobility by a moderate factor, as was already known in various cases of DNA protein interactions; such cases were attributed to increased friction. Above a given size, however, the mobility drops abruptly, and important deviations from the behavior of naked DNA are observed. Strikingly, this threshold shifts to smaller sizes when the field is increased, leading to a mobility that actually decreases with increasing field, in contrast to the usual reptation behavior. A similar behavior was observed independently by Serwer *et al.* (1992) on *T*7 capsid-DNA complexes. Ulanovsky *et al.* suggested that this reduction in mobility was due to trapping of the bulky streptavidin against pores large enough to be threaded by the DNA but too small to let the protein pass. This idea was developed into an analytical model by Défontaines and Viovy (1991, 1992, 1993, 1994). The model is based on reptation with internal modes and allows for random trapping of the protein in gel fibers. The electric force pulling the DNA prevents the protein from escaping the trap. Detrapping can occur by a thermally activated process countering the electric force and can be treated following the Kramers method (1940). The model was extended to include the possibility of detrapping by

[42]Finally, note that efficient separation of DNA based on topology has recently been reported using polymer solutions instead of gels (see Sec. IX.D).

reversed-field pulses, as was also suggested by Ulanovsky *et al.* Taking into account the possibility of chain stretching leads to a rather complex variety of regimes,[43] but the general predictions are in qualitative agreement with experimental observations. These studies motivated several theoretical works (Slater and Villeneuve, 1992; Desruisseaux and Slater, 1994, 1996, Slater, Desruisseaux, *et al.*, 1995). Rather surprisingly, though, to my knowledge they have not been followed by further experimental work. Probable reasons for this apparent lack of interest can be found in theoretical studies of trapping by Slater, Desruisseaux, *et al.* (1995) and Desruisseaux and Slater (1996). These authors ignored the possibility of chain extension, thereby reducing the complexity of the model, but they investigated the distribution of detrapping times. They could show that the trapping process leads to long tails in the distribution, anomalous diffusion, and considerable band broadening as compared with conventional reptation electrophoresis. Ultimately, one loses by band broadening more than one gains in band spacing, explaining why this technique has not yet lived up to the expectations it raised when first introduced.

The electrophoretic mobility of a labeled polyelectrolyte in a gel in the absence of trapping has been investigated theoretically by Aalberts (1995). Considering the difficulty of completely avoiding specific label-gel interactions, and the fact that such molecules can be separated in free liquid (Heller, Slater, *et al.*, 1998), this approach will probably remain restricted to small (molecular) labels.[44]

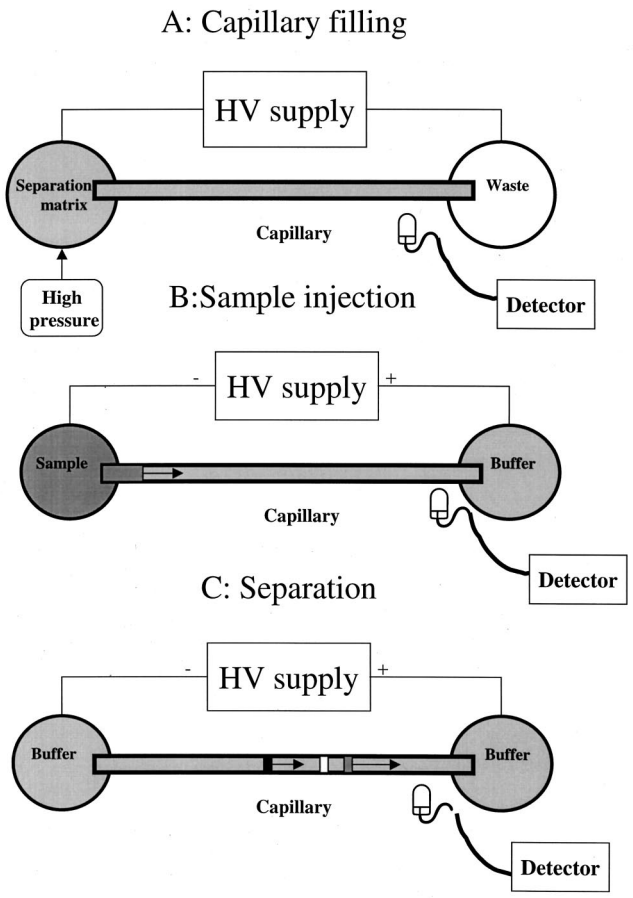

FIG. 24. Schematic representation of a capillary electrophoresis experiment: A, the capillary is dipped in a vial containing the separation matrix and filled by high pressure; B, the inlet vial is replaced and a small plug of sample is injected electrokinetically; C, the inlet vial is replaced by a buffer vial. The different analytes migrate, separate into ''bands'' according to their mobility, and are detected close to the capillary outlet.

IX. CAPILLARY ELECTROPHORESIS AND ''ELECTROPHORESIS ON CHIPS''

A. Presentation

A recently developed technique, which became recognized in biology only a few years ago, involves performing separation in a narrow channel [typically a fused-silica capillary with an internal diameter between 50 and 100 μm and a length between 10 and 50 cm (Fig. 24)]. A simple change from macroscopic to microscopic format of the electrophoresis chamber has little to do with the molecular mechanisms that are the main subject of this review, but the smaller capillary formats requires a rather drastic reevaluation of supporting media and separation mechanisms. In particular, putting permanent gels inside of small capillaries such as those currently used in slab apparatus causes endless problems, such as clogging, gel breakage, and bubble formation. On the other hand, capillaries offer the possibility of using fluid media that are impossible to use in macroscopic format. In sum, most of the physics of separation has to be reinvented for capillary electrophoresis. Another reason for interest in this technique is the hope that it will revolutionize within a few years the electrophoresis of biomolecules. For instance, it is now clear that the human genome sequencing project will be completed much faster than initially anticipated, thanks to the launching of capillary-array automated sequencers with a throughput increased by a factor of at least 10 as compared to slab-gel sequencers. Diagnosis (Righetti and Gelfi, 1997; Landers, 1997) and forensic (McCord, 1998) applications are also developing rapidly. Capillary electrophoresis is now a research field in its own right, and it has been the subject of several books (Grossman and Colburn, 1992; Righetti, 1996; Heller, 1997) and numer-

[43]The details of these predictions are now rather obsolete due to the current picture of chain orientation and electrohydrodynamic effects, but the underlying principles should remain valid.

[44]DNA-protein complexes were recently used successfully for size separation by end-labeled free-solution electrophoresis (Mayer, Slater, and Drouin, 1994b; see Sec. IX.C). Another approach, using complexation occurring behavior in the course of electrophoresis in free solution, was also proposed by Carlsson *et al.* (1996) for the detection of mutations. These interesting methods do not involve topological interactions and will not be considered further here.

ous reviews [see, in particular, Beale, 1998, for a terse but complete review of the field, and several special issues of the journal *Electrophoresis* (edited, respectively, by El Rassi, 1997; Fanali, 1997; Landers, 1997; Heegaard, 1998; and McCord, 1998)].

The first advantages of capillary electrophoresis are excellent heat dissipation and a reduction of convection, allowing the use of high fields (typically 200–300 V/cm) and of non-gelled supports.[45] Injection of samples is in general performed automatically, and detection is made on line (generally by UV absorption or laser-excited fluorescence), using technologies borrowed from chromatography. These advantages contribute to ease of operation, improved resolution, and higher output, so the considerable interest in this technique is not surprising. It is probable, however, that the ascendancy of capillaries as we know them at present will be temporary, and that they will soon be replaced by yet more integrated ''laboratories on chips'' prepared using the tools of microelectronics, and integrating in one planar molded device both sample preparation and electrophoretic channels (see, for example, Effenhauser *et al.*, 1997; Foret, 2000). Numerous laboratories and companies are already working intensely on these concepts. Such chips can be used to drive the same separation mechanisms as are currently used in cylindrical capillaries, only with greater speed and efficiency. A complementary trend is to use them to construct custom-made systems and invent completely new size-fractionation strategies based on the improved theoretical knowledge of electrophoretic molecular dynamics gained in the last few years. Some of these systems will be presented in Sec. IX.E (for a more complete presentation, the reader is referred to Slater, Kist, *et al.* 1998). First, however, let us consider the more ''conventional'' capillary electrophoresis applications: many of these are already quite exciting and thought provoking!

B. Factors affecting resolution in capillary electrophoresis

1. Principles

Assuming that band broadening is due only to thermal diffusion ($w^2=2Dt$), one obtains the ''ultimate'' efficiency [as defined in Eq. (3.3)] achievable in capillary electrophoresis:

$$P=16x^2/w^2=8(\mu E)^2t/D. \tag{9.1}$$

The E^2 dependence of P provides capillary electrophoresis with a considerable advantage over slab gels, which can only accommodate field strengths 10–100 times smaller. This technique, however, may be affected by the same other potential causes of dispersion as encountered in slab gels, such as inhomogeneities in the mobility due to thermal gradients, initial (injection) bandwidth, and electroconvective effects due to differences of mobility between the analyte and the ions of the buffer. Resolution may also be affected by specific dispersive effects, such as wall-analyte interactions, differences in the path traveled by different analytes due to capillary bending, and wall-induced electro-osmosis. These different questions are reviewed in detail by Grossman and Colburn (1992) and by Gas *et al.* (1997). Electro-osmosis deserves special treatment because of its dramatic importance in the separation of biological macromolecules.

2. Electro-osmosis

As discussed in Sec. II.C, electro-osmosis is due to the finite charge of the capillary wall, and it leads to a plug-flow velocity profile of the fluid contained in the capillary. All the shear is localized in the Debye layer at the wall. When analytes contained in the fluid have a finite electrophoretic mobility, their velocity is given by the algebraic sum

$$\mu_{\text{eff}}=\mu_0+\mu_{\text{EEO}}, \tag{9.2}$$

where μ_{EEO} is the electro-osmotic mobility. Diffusion is unaffected, so that the first effect of electro-osmosis is a rather trivial modification of the migration time, for a given capillary length. For silica capillaries at neutral or alkaline pH, walls are negatively charged, and the direction of electro-osmosis is opposite to the mobility of DNA. Since the absolute value of μ_{EEO} is generally larger than that of polyelectrolytes, analytes migrate from the cathode to the anode, and the order of migration of particles is reversed (those with the lowest electrophoretic mobility migrate fastest). This can be an advantage or a disadvantage, depending on the application.

A more serious problem is that electro-osmosis is extremely dependent on the surface properties of the capillary. With macromolecular samples, in particular, it is very difficult to avoid adsorption of some trace of the analytes or of unknown contaminants (proteins, for instance, are known to be very powerful and versatile adsorbers on many different solid surfaces). This results in poor reproducibility in measured migration times. In addition this spurious adsorption is in general uneven along the surface of the capillary, and heterogeneities in osmotic pumping at different places in the capillary are able to lead to catastrophic dispersion due to the development of Poiseuille recirculations (see, for example, Ajdari, 1995). The common solution to this problem is to attach hydrophilic polymers to the surface. Capillaries with polymer layers of various chemical properties, developed for gas chromatography, are commercially available, and can be used with good success for not too

[45]Current separations of polyelectrolytes use fields of typically 200–300 V/cm, but several recent articles report ultrafast separations using field strengths of the order of 1000 V/cm (e.g., Muller *et al.*, 1998). It appears that the next generation of capillary electrophoresis protocols, with separation times of the order of 1 mn, is in preparation and may soon become the norm.

demanding applications. Due to the thickness of the Debye layer, however, best results are obtained with a thick, water swollen ''brush'' of high-molecular-weight hydrophilic polymers, which can be linked to the surface either covalently (as pioneered by Hjerten, 1985, and reviewed by Dolnik *et al.*, 1998) or by physical adsorption, a process called *dynamic coating* (Fung and Jeung, 1995; Maddabhushi, 1998).

The presence of polymer in the separating medium (the most common method for obtaining size fractionation, as we shall see in Sec. D below) tends to reduce electro-osmosis, because of increased viscosity in the Debye layer. This effect depends strongly on the specific polymer-wall interaction, so that the most recent trend is to use polymers combining wall adsorbing properties with good bulk sieving properties, such as polydimethylacrylamide. It should be noted here that the polymer layer at the surface can be significantly deformed by the electro-osmosis process, as suggested by the nonlinear field dependence of electro-osmosis (Bello *et al.*, 1995). Considering its practical importance, and the increasing knowledge available on adsorbed and grafted polymers (see, for example, de Gennes, 1983; Brochard, 1993; Ajdari, Brochard-Wyart, *et al.*, 1994; Ajdari, Brochard-Wyart, *et al.*, 1995; Aubouy *et al.*, 1996) fundamental studies of electro-osmosis in the presence of adsorbed polymers certainly deserves more attention from physicists than it has received up to now.

3. Collective electrokinetic effects

In the course of an electrophoretic experiment, important collective electrokinetic effects may arise due to the presence of macroscopic gradients or discontinuities in the concentrations of charged species, which generally occur at the sample plug. At the onset of the field, these gradients lead to nonuniform electric fields along the separation channel, which evolve with time. They can be the source of spectacular and nontrivial evolutions of the initial concentration profiles; leading either to ''concentration'' or ''dilution'' effects, depending on the situation. Electrokinetic concentration, for instance, is used in *isotachophoresis*, a mode in which all components in the sample are focused into adjacent plugs with a specific conductivity, all migrating at the same velocity. These collective electrophoretic effects have been the subject of a considerable literature (see Gebauer and Bocek, 1995, 1997), but in practice they are seldom relevant to the separation of large polyelectrolytes, for which they do not lead to size fractionation (it is worth keeping in mind, though, that they may lead to spurious band dispersion if the analyte concentration is too high).

The separation of large polyelectrolytes, typically more than a few kbp for DNA, by capillary electrophoresis may also be affected by electrohydrodynamic phenomena, first described by Mitnik, Heller, *et al.* (1995) and studied in detail by Magnusdottir, Isambert, *et al.* (1998). The application of fields of typically 100 V/cm was shown to induce the segregation of an initially homogeneous and monodisperse DNA solution into

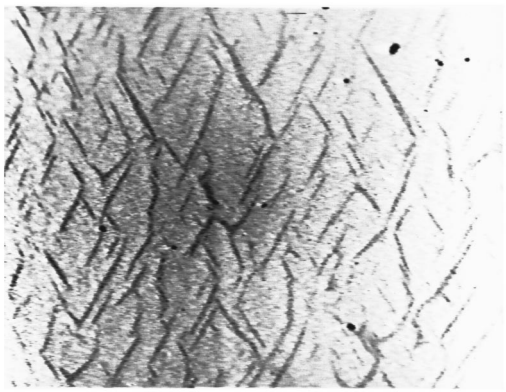

FIG. 25. Tilted DNA-rich vortexes appearing in monodisperse Lambda DNA solutions under ac fields in a planar capillary configuration (200 V/cm peak-to-peak, 100 Hz). The DNA is labeled with ethidium bromide and appears as dark streaks. The total width of the image is 500 μm.

DNA-poor regions and vortexlike DNA-rich domains (aggregates) in permanent rotation. These aggregates led to turbulent mixing of the solution ruining separation, and to spurious peaks at the detector.[46] The origin of this phenomenon was explained by Isambert, Prost, *et al.* (1997) and Isambert, Ajdari, *et al.* (1997): it is due to the development of salt-concentration gradients in the vicinity of local (spontaneous) fluctuations in the concentration of polyelectrolyte. These gradients induce space charges in the fluid, extending over distances much longer than the Debye length. In high fields these charges are able to convect the fluid, resulting in enhancement of the initial concentration fluctuations and the development of very specific dynamic tilted patterns (Fig. 25). The development of this instability from a system initially at rest has not yet been fully worked out, but a general scaling equation for the hydrodynamic velocity and the aggregation rate g, bearing numerous useful predictions, is available (Isambert, Prost, *et al.*, 1997; Isambert, Ajdari, *et al.*, 1997; Magnusdottir, Isambert, *et al.*, 1998):

$$g \propto \varepsilon_b \varepsilon_0 \frac{\mu_s}{\mu_0 c_s \eta} E^2 c_p \,. \tag{9.3}$$

Here μ_s and c_s are the mobility and concentration of background electrolyte ions, respectively, and c_p is the polyelectrolyte concentration. The model's scaling predictions are in rather good agreement with numerous experimental observations in capillary electrophoresis of large molecules (Magnusdottir, Isambert, *et al.*, 1998) or in model systems (Mitnik, Heller, *et al.*, 1995; Ladoux *et al.*, 1998). These instabilities seem quite general, and

[46] Actually, aggregation of DNA in high fields had been observed previously by Song and Maestre (1991), but its connection with resolution loss in capillary electrophoresis was not made at that time.

also appear in colloidal suspensions (Jennings *et al.*, 1990; Hu *et al.*, 1994) and in capillary electrophoresis of polysaccharides (Viovy *et al.*, 1998). The only remedies currently available to suppress this very detrimental phenomenon consist in (i) reducing the field strength or increasing the solvent viscosity, thus increasing the separation time (Sudor and Novotny, 1994; Heller, Pakleza, and Viovy, 1995); (ii) reducing the polyelectrolyte concentration, when detection limits make this possible (Kim and Morris, 1995, 1996); (iii) using isoelectric buffers (Magnusdottir, Isambert, *et al.*, 1998).

C. Free-solution electrophoresis

As discussed in Sec. II.F, there is no size fractionation of uniformly charged polyelectrolytes in free solution. It has been proposed (Noolandi, 1993) to restore size fractionation by attaching a neutral label (or more generally a particle with a different mobility) to one or two ends of the polyelectrolyte that is to be separated. The method was called *end-label free-solution electrophoresis* (ELFSE) and investigated theoretically by Mayer *et al.*, 1994b.[47] Sudor and Novotny (1995) attached a neutral fluorescent label to the end of polysaccharides and obtained in this way an extremely high resolution. This method was also applied more recently to DNA by Heller *et al.* (1998), by attachment of streptavidin to the end-biotinylated DNA. In the latter case, however, the resolution was limited by the polydispersity of the attached protein. The theory of ELFSE was generalized, in the context of electrohydrodynamic force, to arbitrary diblock polyelectrolytes (Long and Ajdari, 1996) and to more complex polyampholytes (Long, Dobrynin, *et al.*, 1998). For a diblock system, the electrophoretic velocity v is given self-consistently by

$$\frac{v}{E}=\frac{\xi_1(v-\mu_1E)\mu_1+\xi_2(v-\eta_2E)\mu_2}{\xi_1(v-\mu_1E)+\xi_2(v-\mu_2E)}, \tag{9.4}$$

in which $\mu_{1,2}$ and $\xi_{1,2}(v)$ are the free-flow (bare) electrophoretic mobility and the friction in a flow of velocity v of the isolated blocks 1 and 2, respectively. The difficult part is to evaluate the friction, which depends on the deformation of the polyelectrolyte and thus on v. In the limit of strong fields, with fully extended chains, the predictions of Mayer *et al.* (1994b) are recovered. This recent work opens the way to a unified theory of the electrophoresis of polyelectrolytes, from uniformly charged molecules like DNA to nonuniformly charged complex systems like peptides or proteins.

It was also suggested by Iki *et al.* (1996) that size fractionation of bare DNA could be obtained in ultranarrow-bore capillaries (a few μm). The suggested mechanism in this case is one that grew out of *free-flow fractionation*, in which molecules with different sizes have different residence times within the Debye layer. This mechanism needs to be confirmed, however, and in any case one suspects that, with a real-life sample, the use of such small capillary dimensions would create problems of detection, contamination of the capillary walls, and clogging.

D. Capillary electrophoresis in polymer solutions

1. Background

The idea of using polymer solutions to separate biopolymers is far from new. It was proposed years ago either in combination with a conventional gel (Bocek and Chrambach, 1991) or as a viscous solution (Burrough *et al.*, 1991). It became popular only in combination with capillary electrophoresis (see, for example, Heiger *et al.*, 1990; Nathakarnkitkool *et al.*, 1992; Grossman and Soane, 1991; Barron *et al.*, 1993). Almost every hydrosoluble polymer available on the market has been tried, often with success, for size fractionation of polyelectrolytes (for reviews see Dovichi, 1997; Quesada, 1997, Righetti and Gelfi, 1997; Madhabushi, 1998). Polyacrylamide and polysubstituted acrylamides, notably poly-dimethylacrylamide, remain favorites, especially for small DNA (sequencing fragments), but many successful separations were also achieved with polyoxyethylene (POE), polyvinyl alcohol, polyvinylpirrolidone, etc. Cellulose derivatives such as hydroxyethylcellulose, hydroxypropylcellulose, methylcellulose, dextran, glucomannan, and more generally polymers with a rigid backbone, seem to yield better results for large duplex DNA. This large number of successful polymers suggests rather universal separation mechanisms, rooted in the physics of polymer solutions.

2. Properties of polymer solutions

The properties of polymer solutions have been the object of a considerable amount of work and are now well known (see de Gennes, 1979; Doi and Edwards, 1986; and, for a more electrophoresis-oriented account Viovy and Heller, 1996). In the dilute limit, neutral polymers behave as random coils, as discussed in Sec. II.D, and their radius of gyration is given by Eq. (2.12) (for simplicity, we consider only the case $N_k > N_\nu$). Homopolymers are generally used in capillary electrophoresis in "good solvent" conditions, to avoid risks of micro or macro phase separation. Above a critical overlap concentration c^*, given by

$$c^* \approx 3M_w/4\pi N_A R g^3, \tag{9.5}$$

where M_w is the polymer molecular weight, polymer chains start to interpenetrate, leading to the semidilute

[47] Note that the model described in this reference is based on the local force picture, so that its predictions are valid only in the limit of strong chain stretching.

or entangled state, characterized by a screening length for excluded volume and hydrodynamic interactions, or blob size b, given by[48]

$$b = 1.43 R_g \left(\frac{c}{c^*} \right)^{3/4}. \tag{9.6}$$

Above c^*, chain dynamics are deeply affected by the topological constraints with neighbors, and self-diffusion of a chain is dominated by reptation, as in gels (see Sec. V.A.). The lifetime of the topological constraints is in this case the reptation time, scaling as

$$\eta_s \propto \eta \left(\frac{c}{c^*} \right)^{3.75}. \tag{9.7}$$

The macroscopic viscosity increases very rapidly with concentration ($\eta_s \sim c^{3.75}$), limiting the concentrations that can be practically injected into a capillary to about $10c^*$.

3. Separation in dilute solutions

The possibility of separating DNA using dilute polymer solutions was first demonstrated by Barron *et al.* (1993, 1994), who suggested that this separation was due to "transient entanglement coupling" of the DNA with polymer molecules encountered during its migration. This mechanism was confirmed by videomicroscopy studies (Mitnik, Salomé, *et al.*, 1995; Shi *et al.*, 1995a, 1995b; Carlson *et al.*, 1996). An analytical theory was developed by Hubert *et al.* (1996). The essential ingredients of this model are the collision rate between DNA and polymers (self-consistently depending on the cross sections of the DNA and polymer, and on the velocity of the DNA with transiently attached polymers) and the average time for disentanglement under the combined action of hydrodynamic drag on the polymer and electrohydrodynamic drag on the polyelectrolyte. Numerous regimes are possible, and only the case of strong polymer stretching (in which the local and electrohydrodynamic force pictures are equivalent) and DNA larger than the polymers was studied in detail. Comparison of the results with experiment was satisfying. Extension of the theory to other regimes is still to be done.

In practice, electrophoresis in dilute solutions leads to fast separations, a large range of separable DNA sizes (typically up to 20 kb, to be compared with about 2 kb for capillary electrophoresis gels or concentrated solutions), but rather poor resolution, due to the combination of a relatively small range of available mobilities—large chains typically migrate at half the speed of the smallest ones—and problems of analyte-wall interactions. Very fast separations of Mb DNA in dilute solutions, using pulsed-field capillary electrophoresis, were reported by Kim and Morris (1995, 1996) and Oana *et al.* (1997). These separations seem very delicate, however, probably because of the electrohydrodynamic instabilities described in Sec. IX.B.3.

4. Separation in entangled solutions

Entangled polymer solutions remain by far the most common media for capillary electrophoresis of polyelectrolytes. In general, it is much easier to obtain sharp and reproducible peaks at high polymer concentration than in the free-liquid or dilute-solution modes discussed above. This is very probably due to a reduction of the interactions between the analytes (and/or contaminants) and the capillary wall, although to my knowledge this assumption has not received direct experimental verification. The other advantage of entangled solutions lies in the separation mechanism itself.

Theoretical efforts to describe the molecular mechanisms of size separation in polymer solutions were pioneered by Grossman and Soane (1991). These authors assumed that the "mesh size" ξ of the solution plays the role of a dynamic pore size and subsequently applied gel electrophoresis theory to the polymer solutions. The underlying idea is that, for concentrated enough solutions, the lifetime of entanglement interactions between the polymer chains is long, so that they act as real crosslinks for the migrating polyelectrolyte. Therefore all the advantages (such as the N^{-1} dependence of the mobility) and disadvantages (such as the saturation of mobility for large polyelectrolytes/large fields) should be recovered. The assumption of immobile obstacles is of course critical for transposing electrophoresis theories from gels to polymer solutions, and it has been investigated theoretically by Viovy and Duke (1993; Duke and Viovy, 1994). The basis of these approaches is that the tube in which the polyelectrolyte (e.g., DNA) is moving is itself moving under the action of Brownian reptative motion of all the chains in the medium, a process called in polymer viscoelasticity *constraint release*. Assuming linear superposition of DNA biased reptation and constraint release (i.e., assuming that the latter process occurs at the same rate as in the absence of DNA), we predicted that, for a given DNA size N_k, separation is lost below a critical polymer concentration scaling as

$$\begin{aligned} (c/c^*) &\propto N_k R_{\mathrm{gp}}/l, \quad b < l, \\ (c/c^*) &\propto N_k l/R_{\mathrm{gp}}, \quad b > l, \end{aligned} \tag{9.8}$$

where R_{gp} is the polymer radius of gyration. The range of sizes that will be separable increases with the polymer concentration (and molecular weight), until it reaches the reptation limit N^* [Eq. (5.27)]. These predictions were compared with experiments by Mitnik, Heller,

[48] Actually, there are subtle and still debated differences between the screening length for excluded-volume interactions, the dynamic screening length for hydrodynamic interactions, and the blob size of the reptation model. It is also well acknowledged that the crossover to dynamic entangled behavior is shifted with respect to the static crossover c^*. There is, however, a consensus that all these lengths scale the same way in the asymptotic limit, even if prefactors are different (and possibly nonuniversal). Therefore I ignore these subtleties here, but warn the reader that numerical prefactors in this field should always be taken with caution.

et al. (1995). They seem to be reasonably verified at low fields (typically below 50 V/cm), but at higher field strengths the velocity seems to remain a nonlinear function of the field strength, even in the constraint-release regime, in contrast with predictions. More generally, experimental data appear to display a very smooth evolution of the mobility across the entangling transition, which cannot be accounted for by existing models. We believe that this is due to nonlinear constraint-release effects, driven by the strong forces exerted by the moving polyelectrolyte on the matrix.

The presence of reptation-type migration in highly entangled solutions was strongly supported by a series of videomicroscopy studies of the motion of large DNA molecules (Ueda, Yoshikawa, and Doi, 1997; Ueda and Baba, 1997; Oana *et al.*, 1997; Ueda *et al.*, 1998). Note that a very different theory, based on the a preaveraged hydrodynamic theory of polymer solutions, was recently proposed by Muthukumar (1996). A comparison with experimental data is in progress. However, since this theory does not take into account polyelectrolyte orientation, it is doubtful that it can cross over to biased reptation behavior and describe the electrophoresis of large polyelectrolytes in those aspects which are of the greatest practical interest.

Overall, it seems fair to say that the present theoretical understanding of polyelectrolyte separation in semidilute polymer solutions is rather unsatisfying, especially considering that most experiments are for practical reasons performed at high fields and moderate values of c/c^*, in which the reptation model does not work well. Fortunately, this relative weakness of the theory has not prevented capillary electrophoresis of DNA in entangled polymer solutions from becoming an extremely powerful experimental tool, rivaling gels in its efficacy for sequencing (Dovichi, 1997) and practically all analytical applications of DNA electrophoresis. Typical applications include oligonucleotides (Gelfi *et al.*, 1996), PCR fragments (Righetti and Gelfi, 1997), and detection of point mutations (Righetti, 1996). As an example, Goetzinger *et al.* (1998) reported sequencing up to 1000 bases in 80 mn, quite a remarkable achievement, using 2% linear polyacrylamide as a separation matrix. Sequencing up to 500 bases is routinely achieved in commercially available polymer solutions based on entangled linear *p*DMA. Pulsed-field capillary electrophoresis has also been applied with success to increase the available separation range of capillary electrophoresis. Magnusdottir, Heller, *et al.* (1998) separated DNA up to 166 kb with very good reproducibility in less than 10 mn (Fig. 26), as compared with the several hours necessary in agarose gels. In such applications the scaling predictions of the reptation theory apply well and provide very useful guidelines. Capillary electrophoresis in entangled solutions has also been successfully used in the separation of synthetic polyelectrolytes, such as polystyrene sulfonates (Minarik *et al.*, 1997; Cottet *et al.*, 1998).

Finally, there have been several studies demonstrating size fractionation of rigid particles in entangled polymer solutions (Radko and Chrambach, 1996, 1997; Chrambach and Radko, 1998). Interestingly, separation data can be rescaled to a universal behavior using the reduced variable R/b, suggesting that that the introduction of a new length scale (the screening length b) in an entangled system, as compared with a molecular viscous fluid, is able to invalidate the Smoluchowski result and to yield size fractionation. The detailed mechanisms of this separation are not yet understood and would make an interesting subject of research for a polymer physicist.

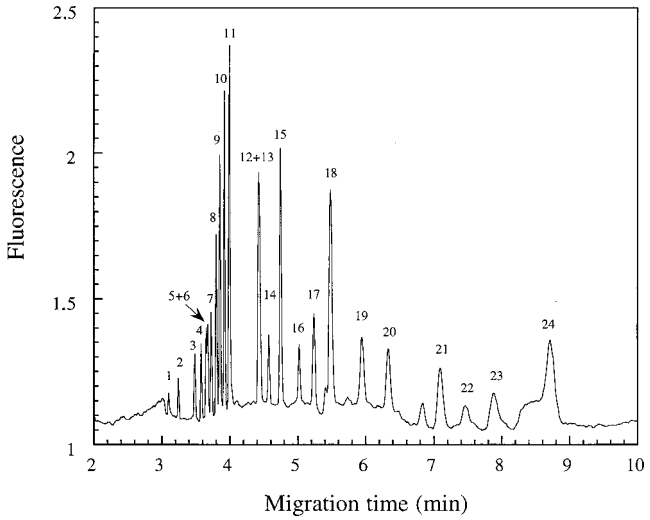

FIG. 26. Separation of a mixture of ϕx174/HaeIII (5 ng/μl), high Mw marker (Life Technologies) (16 ng/μl) and λ-phage (2 ng/μl): Running buffer, 0.7% hydroxypropylcellulose diluted in 178 mM histidine; Injection, 18.5 V/cm (dc-offset) for 70 s; FICE conditions, ac square pulse of 519 V/cm combined with a dc offset of 133 V/cm, field frequency = 30 Hz; Capillary, DB-210, 7 cm to the detector, total length 27 cm; peak assignments, (1) 72 bp, (2) 118 bp, (3) 194 bp, (4) 234 bp, (5) 271 bp, (6) 281 bp, (7) 310 bp, (8) 603 bp, (9) 872 bp, (10) 1078 bp, (11) 1656 bp, (12) 827 bp, (13) 8612 bp, (14) 10 086 bp, (15) 12 220 bp, (16) 15 004 bp, (17) 17 057 bp, (18) 19 399 bp, (19) 22 621 bp, (20) 24 776 bp, (21) 29 942 bp, (22) 33 498 bp, (23) 38 416 bp, and (24) 48 502 bp. From Magnusdottir, Isambert, *et al.*, 1998.

5. Associative polymers

The last few years have seen several successful attempts to replace entangled polymer solutions, in which the (transient) cohesion of the mesh is due to topological constraints only, by solutions of block copolymers with hydrophilic and hydrophobic parts. The hydrophobic parts self-associate in micelle-like aggregates, giving the medium its cohesion, while the hydrophilic part extends in the fluid and offers topological obstacles to the migrating polyelectrolyte. Playing with the chemical components, molecular weight, and linking structure of the different blocks presents a huge range of possibilities for tuning the properties of the solution and offers hope of overcoming the limitations presented by conventional entangled solutions. In particular, the physical gel states

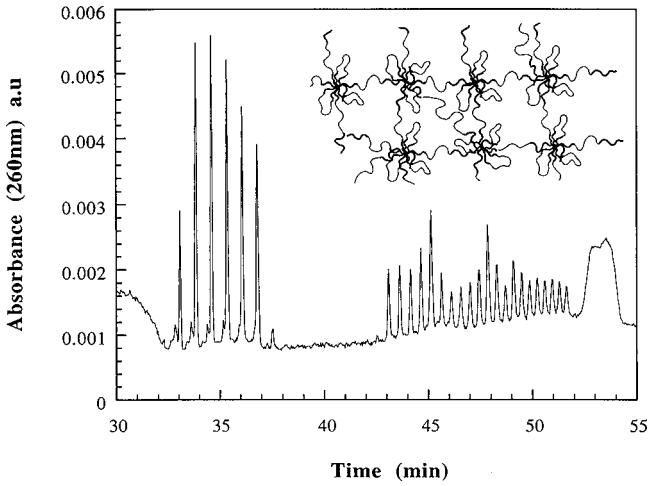

FIG. 27. Electrophoregrams for the separation of a mixture of standard poly-$d(A)$ oligonucleotides with 25–30 and 40–60 bases, in alky-POE-alkyl triblock copolymers at 10% buffer, $1X$ TBE; field strength, 200 V/cm; capillary, DB17, 100 μ ID; length to the detector, 30 cm; poly-$d(A)$ 25–30 and poly-$d(A)$ 40–60 peaks appear at 33–37 min and at 43–52 min. From Magnusdottir, Viovy, and François, 1998.

of associative polymer solutions present a much stronger shear thinning behavior than do entangled solutions (its viscosity decreases with the load), so that properly designed solutions might combine easy high-pressure loading in the capillary with good sieving properties at rest. Examples of the use of associative polymers with a hydrophilic backbone and pendant hydrophobic tails for capillary electrophoresis separations of DNA were presented by Menchen *et al.* (1996). Very high resolution of oligonucleotides was obtained by Magnusdottir, Viovy, and François, 1998, using a monodisperse triblock alkyl-polyethylene oxide-alkyl polymer. Solutions of this polymer have a low-viscosity phase induced by the formation of alkyl micelles spatially organized with cubic order and linked by polyethylene oxide blocks (Fig. 27).

Interestingly, high-resolution separations of DNA have also been achieved by Wu *et al.* (1997, 1998) and Rill *et al.* (1998) in solutions of commercial triblock polyethylene oxide-polypropylene oxide-polyethylene oxide polymers (Pluronics) in the cubic "gel" phase. The structure of this phase is not a connected array, but a colloidal crystal of PPO-rich micelles stabilized by repulsive interactions between their polyethylene oxide "hair" extending in the water. Therefore it will be interesting to learn whether separation in these media also occurs by a reptationlike mechanism (the soft entropic repulsive potentials due to the polyethylene oxide brushes would then define an effective tube) or by a completely different mechanism, related, for example, to the field-driven crossing of entropic potential barriers between regularly spaced traps. At present, this remains an open question.

E. Electrophoresis on chips and custom-made arrays of obstacles

Essentially, all the separation modes described in Secs. IX.C and IX.D can be transposed to microchannels in a planar "chip" format; the latter also allows the design of specific structures that could not be implemented in cylindrical capillaries.

1. Microlithographic arrays

In a widely cited article, Volkmuth and Austin (1992) ushered in a new generation of electrophoretic separation methods. These authors showed that DNA could be made to migrate in thin channels comprising custom-made arrays of obstacles, engraved in silicon by standard microlithographic techniques. From the point of view of the migrating particle, gels are nothing more than arrays of obstacles, and microfabricated arrays can be seen as ideal 2D "artificial gels." From the physicist's viewpoint, arrays of obstacles can be viewed as model gels that can teach us a lot about migration mechanisms thanks to their better controlled, freely tunable, and simpler structure. They offer to the imagination a practically unlimited range of possible structures and are very stimulating for both fundamental and applied research.

The work initiated by the Austin group is reported in a series of articles (Volkmuth *et al.*, 1994, 1995; Duke *et al.*, 1996, 1997).[49] The first observations concerned mobilization at relatively low fields and found several similarities with the mechanisms observed in gels: In steady field, molecules adopted conformations strongly elongated in the direction of the field and were subject to quasicyclic elongations and retractions. In contrast with gels, the obstacles could be clearly identified, and the stretching could be associated unambiguously with hooking of the molecule over a post. Disengagement occurred by a rope-over-a-pulley mechanism (in this case, though, the "pulley" is not a simplified representation of a bend in the chain's trajectory, but a real post). The dynamics of this hooking/disengagement process has been studied theoretically by Volkmuth *et al.* (1994), Nixon and Slater (1994), Sewick and Williams (1996), and André *et al.* 1998; at present, only the last group has considered hydrodynamic interactions). The main conclusion of these studies is that this disengagement mechanism can actually lead to a size fractionation of large DNA, up to the Mb range, but the size dependence is only logarithmic.

The group of Austin *et al.* also made the very interesting observation that, in these very narrow channels, the relaxation of chains is very slow, so that chains can travel many times their own length in an elongated state reminiscent of an earlier state of stretching. In a subsequent article, Duke *et al.* (1996) showed that this property could be used to avoid hooking: if the scale of the array and the electric field are large enough, and if the field is aligned along one of the principal axes of the array, lateral loops do not have time to form, so that the chain moves straight along one channel and is only weakly stretched. This is clearly illustrated in Fig. 28.

[49]Volkmuth *et al.* (1995), in particular, report an unusal and thought-provoking trapping of branched DNA.

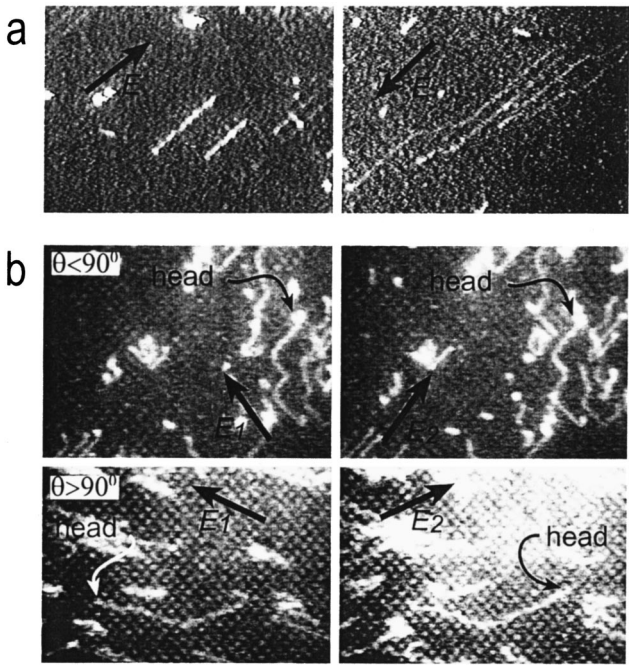

FIG. 28. Electrophoresis of bacteriophage lambda concatemers in microfabricated arrays at 3 V/cm (array spacing, 2 μm): (a) constant field (left) and just after field reversal (right); (b) in pulsed-field conditions, with a 75° angle (top), and a 135° angle (bottom). For acute angle, the same end leads the motion, irrespective of field direction. At obtuse angles, there is head-tail exchange. Also note the absence of hernias. Reprinted with permission from Duke *et al.*, 1996.

Strikingly, the behavior of DNA under these conditions resembles closely the naive predictions of the biased reptation model [compare Figs. 28(a) and 14(a)]. The molecules do not form loops or hernias, and they migrate at a rather steady velocity with uniform orientation and little stretching. In pulsed fields, too, this system seems to mimic biased reptation predictions rather closely: At acute angles, the chains follow a zigzag conformation [compare Figs. 28(b), top, and 14(b)], and at obtuse angles, they undergo a ''ratchet'' migration with head-tail reversal [Figs. 28(b), bottom and 17(d)], as discussed by Southern *et al.* (1987), Viovy (1989), and Slater and Noolandi (1989). These observations suggest that a pulsed field in such conditions might significantly improve upon the present performances of pulsed-field electrophoresis:

(a) the large pores allow fast migration;

(b) the conformation of chains fluctuate much less, so that one can expect more uniform velocities and less band broadening;

(c) since there is little chain stretching, this mechanism seems to leave very little room for chain trapping or chain breakage and should therefore allow much faster separation of large DNA.

Obviously, some technical problems such as large-scale microfabrication, sample injection, and lifetime of the cells need to be solved in order to turn this beautiful experiment into an everyday laboratory tool, but the prospect is certainly worth the effort. Mayer *et al.* (1998) have also demonstrated the possibility of separating DNA in self-assembled ferrofluid arrays with dimensions comparable with those of the microlithographic arrays of Volkmuth *et al.* This alternate way of preparing arrays might solve some of the technical problems mentioned above, although it does not allow for the same variety of structures.

2. Playing with entropy and ratchets

Other attempts to circumvent the problems inherent to gels, while using steric effects for size separation, have been made by Long, Harden, and Viovy (1995), Nixon and Slater (1996), and Slater, Guo, and Nixon (1997). The common idea underlying these attempts was to combine electric and entropic forces associated with a modulation of the steric hindrance to the molecules. Long, Harden, *et al.* (1995) used an electric field to drive molecules through a series of membranes with narrow pores. They identified several regimes. At low fields, i.e., for $E<E_c$, and for chains with a radius of gyration larger than the pore diameter of the membrane d_p, there is an entropic barrier for penetration in the pores. Depending on whether one uses a local force picture (relevant for relatively stretched chains) or the electrohydrodynamic result [Eq. (2.24)] for a coiled chain, E_c is given by

$$E_c=\begin{cases} kTl^2/q_k d_p^2, & \text{local force} \\ kT/\eta\mu_0 d_p^2, & \text{EHD.} \end{cases} \tag{9.9}$$

The threshold jumps from 0 to E_c when the polyelectrolyte radius of gyration exceeds d_p and is expected to saturate rapidly for larger chains, which is not very interesting for separation. (For $E<E_c$, only a small range of sizes could be separated with a given membrane, as in gel filtration.) At fields higher than E_c, the polyelectrolytes are readily driven through the pores. If the chains are large and pores are close enough, several pores are explored simultaneously by one chain. The membrane-crossing process is actually very similar to the reorientation mechanism treated by Long and Viovy (1996), and size fractionation is achieved thanks to the size dependence of the competition between hernias. It is predicted, however, that the most interesting separation mode corresponds to pulsed fields with a short forward pulse at $E>E_c$ and a long reverse pulse at $E<E_c$. During the forward pulse, all chains start to cross the membrane, but only those smaller than a critical size (scaling as tE^{-1}; Long and Viovy, 1996), have time to cross it completely. During the backward pulse, these chains cannot cross back (because the field is too small to overcome the potential barrier), but the large chains that are still engaged in the membrane have no barrier to cross and so can travel back. The validity of this principle was recently demonstrated experimentally by Akerman (1997). This pulsed-field mechanism actually corresponds to an *entropic ratchet effect*, to use the term introduced later by Slater, Guo, and Nixon (1997). In this latter article, the authors propose a different geometry, based on a single channel with an asymmetric modulation of the diameter. In that case, size-dependent rates for the crossing of the strictions in the channel are

expected.[50] Both approaches can be viewed as particular cases of the general rules stated by Ajdari and Prost (1992) for applying asymmetric trapping and the Curie principles to separation science.

Another idea, suggested by Chacron and Slater (1997), makes use of a temporally asymmetric field with a spatial gradient. These authors showed that this configuration should in some conditions lead to a self-focusing effect, an exciting suggestion that still deserves experimental verification. Griess and Serwer (private communication) also presented recent experimental data showing that a ratchet effect, leading to electrophoretic discrimination of DNA by their affinity for proteins, could be obtained thanks to temporally asymmetric pulses. This experiment was recently modeled by Desruisseaux *et al.* (1998). Overall, this new area of ratchet-based electrophoretic separations has not yet provided results spectacular enough to challenge more conventional gel separation methods, but it is obviously a very young, very active, and very innovative domain of research. It will certainly continue to attract the interest of physicists, and one can anticipate that the time is not far off when it will become operationally competitive.

X. CONCLUSIONS AND PERSPECTIVES

I have tried to provide in this review as complete as possible an account of the mechanisms at play during electrophoretic size fractionation of polyelectrolytes, and of the major conceptual and technical tools developed by physicists and chemical physicists to understand and describe them. The most popular paradigm in the field is DNA, well represented by a long linear polyelectrolyte. It is probably fair to say that we now have a good qualitative picture of the major mechanisms at play during electrophoretic migration of such a polyelectrolyte in a uniform gel having a pore size larger than its Kuhn length and smaller than its radius of gyration. For low fields, the reptation model provides almost quantitative analytical predictions. For high fields, we also have a good representation of the dynamics from computer models, but no quantitative analytical theory, although this latter field is progressing rapidly. There are numerous other situations of interest about which very little is known. An introduction to them was presented in Secs. VIII and IX, but it is certainly more limited than the subject deserves.

Disorder plays an essential role in gel electrophoresis, both on the dynamic side, by the importance of Brownian motion, and on the static side, by the frozen disorder present in the gels. Not surprisingly, then, modeling in gel electrophoresis relies heavily on the methods of statistical physics. More importantly, however, this field is inhabited by the ''spirit'' of soft condensed matter. This implies a strong interest in applied problems, frequent use of toy models and computer simulations, and a relative indulgence for wild simplifications. Some tolerance is rendered necessary by the complexity of the problems encountered. In addition to the difficulties inherent in the electrohydrodynamics of saline solutions, one has to deal with polymers having numerous coupled degrees of freedom. A further complication lies in the appearance not only of a large range of characteristic scales, but also of a large range of energies. During gel electrophoresis, polyelectrolytes are generally very far from thermodynamic equilibrium so that perturbation approaches are tricky to use, but Brownian motion still plays an essential role in local processes coupled to the large-scale dynamics, so that purely deterministic solutions are insufficient. Posing problems in a rigorous way and solving them analytically using only verifiable approximations is, in the large majority of cases, hopeless. As a consequence, the landscape of electrophoresis theory does not resemble a wide straight valley, steadily following the progress of mathematical tools, but a rather chaotic and hilly landscape, in which progress is made only after numerous approximations, trial and errors, and controversies. The brief account offered in the previous pages reveals several erroneous pictures that survived a rather long time, which should convince the reader that in this domain doubt is a particularly useful virtue.

Clearly, the first ''lifeguard'' of model-makers is experimental observation. We are in a much better situation for this now than we were ten years ago, with techniques able to probe many aspects of polymer dynamics on the molecular scale. The account of hernia formations is a good example of a situation in which experiments (and also in this particular case computer simulations) stimulated the development of new models. But not all molecular mechanisms are as conspicuous. For instance, the BRM prediction for the field dependence of the mobility has been steadily in contradiction with experiments for about seven years, during which one wondered if this could be a crossover effect, until a theoretical clue was provided. *A posteriori*, the critique is easy, but the coupling of fluctuations and mobility in this case was rather subtle and unusual. Indeed, the intrinsic difficulties of this field are evident in the recent history of the repton model. Theoretical investigations of this model, performed with a level of mathematical sophistication higher than that employed by the pioneers of reptation, arrived initially at the same erroneous scaling prediction and had to follow in some sense the same tortuous path to correctness.

More surprising, in my opinion, is the way hydrodynamic interactions have been overlooked and the local force picture has been universally and steadily applied by theoreticians in the field (including the author of the present review!), although ample evidence of inconsistencies in the local force approach was available in the colloid science literature, e.g., the work of Russel, Saville, Stigter, de Gennes, and others. Of course, the fact that hydrodynamic interactions are screened in gels (so that the effect on final predictions is actually rather mild) has probably contributed to the unwarranted sur-

[50]Note that the numerical application to DNA separation proposed in this article probably overestimates the field-strength range of interest.

vival of the local force picture. Only the present experimental and theoretical evolution towards more open and liquidlike structures and media makes the importance of hydrodynamics more obvious. This is particularly true for capillary electrophoresis, which adds to the conceptual difficulties listed above those of nonlinear hydrodynamics and the electrohydrodynamics of the sieving medium as a whole. This will certainly be the source of considerable theoretical difficulties, and several years will probably pass before the relatively optimistic statement I just made about our understanding of gel electrophoresis can be transposed to fluid media. Nevertheless, the immense range of applications in biology and medicine offered by capillary electrophoresis is certainly worth the effort.

The need to build on sometimes unsteady ground that characterizes the field of electrophoresis has its compensations. The first is a constant and relatively direct interaction with experiment, in particular, with the advent of videomicroscopy, the ability to watch a real molecule doing (or not doing!) what one has predicted or expected. For a polymer physicist, this is a dream come true. In this respect, I think it is also fair to say that interactions between experiment and modeling, and between biology and physics are now much more equilibrated than in the past. More than ten years ago, experiment took the lead and theorists were mainly trying to explain what experimentalists revealed (or invented). With the progress in modeling came several predictions that were later verified experimentally, such as the mobility minimum in a constant field, or the formation of hernias (observed first in Deutsch's simulations and then in videomicroscopy). At present, theory has developed enough to serve as a basis for inventing new separation tools and processes. Several of those were actually proposed recently and are still awaiting experimental trial. The second compensation is that this field constantly challenges imagination and physical sense. This may be sufficient to explain why more and more researchers are becoming interested in electrophoresis. In any case, I hope that the present review will increase the interest of physicists in this domain, which is not yet very familiar to the physics community.

ACKNOWLEDGMENTS

The view presented here relies heavily on the work of students and postdocs with whom I had the pleasure to work, most notably T. Duke, C. Heller, H. Isambert, and D. Long. I have also benefited from illuminating discussions and comments from colleagues too numerous to be cited here. It is, however, impossible not to name explicitly A. Ajdari, P. G. de Gennes, J. Prost, M. Rubinstein, A. Semenov, G. Slater, G. Thomas, B Widom, and B. Zimm. I am also indebted to colleagues, in particular B. Akerman, J. Noolandi, P. Serwer, B. Tinland, and J. M. F. van Leeuwen, for their careful reading of a first version of this manuscript and numerous comments. I wish to dedicate this review to the memory of F. Caron, who introduced me to DNA electrophoresis in 1987 and whose enthusiasm has been a key to my continuation in this field. This work was supported in part by grants from the EC (BMH4-CT96-1158 and BMH4-97-2627), and from the Association pour la Recherche sur le Cancer (No. 9372).

REFERENCES

Aalberts, D. P., 1995, Phys. Rev. Lett. **75**, 4544–4547.
Aalberts, D. P., and J. M. J. van Leeuwen, 1996, Electrophoresis **17**, 1003–1010.
Adolf, D., 1987, Macromolecules **20**, 116–121.
Ajdari, A., 1992, Ph.D. thesis (Université Paris VI).
Ajdari, A., 1995, Phys. Rev. Lett. **75**, 755–758.
Ajdari, A., F. Brochard-Wyart, P. G. de Gennes, L. Leibler, J. L. Viovy, and M. Rubinstein, 1994, Physica A **204**, 17–39.
Ajdari, A., F. Brochard-Wyart, C. Gay, P. G. de Gennes, and J. L. Viovy, 1995, J. Phys. II **5**, 491–495.
Ajdari, A., and J. Prost, 1992, C. R. Acad. Sci., Ser. II: Mec., Phys., Chim., Sci. Terre Univers **315**, 1635–1639.
Akerman, B., 1996a, Electrophoresis **17**, 1027–1036.
Akerman, B., 1996b, Phys. Rev. E **54**, 6685–6690.
Akerman, B., 1997, J. Chem. Phys. **106**, 6152–6159.
Akerman, B., 1998, Biophys. J. **74**, 3140–3151.
Akerman, B., M. Jonsson, and B. Norden, 1985, J. Chem. Soc. Chem. Comm. 422–423.
Akerman, B., M. Jonsson, B. Norden, and M. Lalande, 1989, Biopolymers **28**, 1541–1571.
Akerman, B., and M. Jonsson, 1990, J. Phys. Chem. **94**, 3828–3838.
Alon, U., and D. Mukamel, 1997, Phys. Rev. E **55**, 1783–1793.
Anand, R., 1986, Trends Genet. **2**, 278–283.
Andre, P., D. Long, and A. Ajdari, 1998, Eur. Phys. J. B **4**, 307–312.
Andrews, A. T., 1986, *Electrophoresis: Theory, Techniques and Biochemical and Clinical Applications* (Clarendon, Oxford).
Arvanitidou, E., and D. Hoagland, 1991, Phys. Rev. Lett. **67**, 1464–1467.
Arvanitidou, E., D. Hoagland, and D. Smisek, 1991, Biopolymers **31**, 435–447.
Aubouy, M., O. Guiselin, and E. Raphael, 1996, Macromolecules **29**, 7261–7268.
Bancroft, I., and C. P. Wolk, 1988, Nucleic Acids Res. **16**, 7405–7418.
Barkema, G. T., J. F. Marko, and B. Widom, 1994, Phys. Rev. E **49**, 5303–5309.
Barrat, J. L., and J. F. Joanny, 1996, Adv. Chem. Phys. **94**, 1–66.
Barron, A., H. W. Blanch, and D. S. Soane, 1994, Electrophoresis **15**, 597–615.
Barron, A. E., D. S. Soane, and H. W. Blanch, 1993, J. Chromatogr., A **652**, 3–16.
Batoulis, J., N. Pistoor, K. Kremer, and H. L. Frisch, 1989, Electrophoresis **10**, 442–446.
Baumgartner, A., and M. Muthukumar, 1987, J. Chem. Phys. **87**, 3082–3088.
Beale, S. C., 1998, Anal. Chem. **70**, 279R–300R.
Bello, M. S., P. de Besi, R. Rezzonico, P. G. Righetti, and E. Casiraghi, 1994, Electrophoresis **15**, 623–626.
Birren, B. W., L. Hood, and E. Lai, 1989, Electrophoresis **10**, 302–309.
Birren, B. W., and E. Lai, 1993, *Pulsed Field Gel Electrophoresis: A Practical Guide* (Academic, New York).

Birren, B., E. Lai, S. M. Clark, L. Hood, and M. I. Simon, 1988, Nucleic Acids Res. **16**, 7563–7582.
Bocek, P., and A. Chrambach, 1991, Electrophoresis **12**, 620–623.
Bode, H. J., 1979, in *Proceedings of 2nd International Conference on Electrophoresis, 1979, Munich* (Walter de Gruyter, Berlin), pp. 34–52.
Bouchaud, J. P., and A. Georges, 1988, C. R. Acad. Sci., Ser. II: Mec., Phys., Chim., Sci. Terre Univers **307**, 1431–1436.
Bouchaud, J. P., and A. Georges, 1990, Phys. Rep. **195**, 127–293.
Brassard, E., C. Turmel, and J. Noolandi, 1991, Electrophoresis **12**, 373–375.
Brochard, F., 1993, Europhys. Lett. **23**, 105–111.
Brochard-Wyart, F., and P. G. de Gennes, 1988, C. R. Acad. Sci., Ser. II: Mec., Phys., Chim., Sci. Terre Univers **307**, 1497–1500.
Burlatsky, S., and J. Deutsch, 1993, Science **260**, 1782–1784.
Burmeister, M., and L. Ulanovsky, 1992, Eds., *Pulsed-Field Gel Electrophoresis, Protocols, Methods, Theories*, Methods in Molecular Biology No. 12 (Humana Press, Totowa, NJ).
Buroughs, J. A., and A. Chrambach, 1991, Biochem. Biophys. Res. Commun. **180**, 1070–1074.
Calladine, C. R., C. M. Collis, H. R. Drew, and M. R. Mott, 1991, J. Mol. Biol. **221**, 981–1005.
Cantor, C. R., A. Gaal, and C. L. Smith, 1988, Biochemistry **27**, 9216–9221.
Carle, G. F., M. Frank, and M. V. Olson, 1986, Science **232**, 65–68.
Carle, G. F., and M. V. Olson, 1984, Nucleic Acids Res. **12**, 5647–5666.
Carle, G. F., and M. V. Olson, 1985, Proc. Natl. Acad. Sci. USA **82**, 3756–3760.
Carle, G. F., and M. V. Olson, 1987a, Trends Biochem. Sci. **12**, 284–287.
Carle, G. F., and M. V. Olson, 1987b, Methods Enzymol. **155**, 468–482.
Carlsson, C., and M. Jonsson, 1996, Macromolecules **29**, 7802–7812.
Carlsson, C., M. Jonsson, B. Norden, M. T. Dulay, R. N. Zare, J. Noolandi, L.-C. Tsui, and J. Zielenski, 1996, Nature (London) **380**, 207.
Chacron, M., and G. W. Slater, 1997, Phys. Rev. E **56**, 3446–3450.
Chrambach, A., and S. P. Radko, 1998, Electrophoresis **19**, 1284–1287.
Chrambach, A., and D. Rodbard, 1971, Science **172**, 440–451.
Chu, G., D. Vollrath, and R. W. Davis, 1986, Science **234**, 1582–1585.
Clark, S., E. Lai, B. Birren, and L. Hood, 1988, Science **241**, 1203–1205.
Cottet, H., P. Gareil, and J. L. Viovy, 1998, Electrophoresis **19**, 2151–2162.
Crater, G. D., M. C. Gregg, and G. Holzwarth, 1989, Electrophoresis **10**, 310–315.
Crick, F. H. C., and J. D. Watson, 1954, Proc. R. Soc. London, Ser. A **223**, 80.
Défontaines, A. D., and J. L. Viovy, 1991, in *Proceedings of First International Conference on Electrophoresis, Supercomputing and the Human Genome, 1990, Tallahasse, Florida* (World Scientific, Singapore), pp. 286–313.
Défontaines, A.-D., and J. L. Viovy, 1992, in *Pulsed-Field Gel Electrophoresis, Protocols, Methods, Theories*, edited by M. Burmeister and L. Ulanovsky, Methods in Molecular Biology Vol. 12 (Humana Press, Totowa, NJ), pp. 403–450.
Défontaines, A. D., and J. L. Viovy, 1993, Electrophoresis **14**, 8–17.
Défontaines, A. D., and J. L. Viovy, 1994, Electrophoresis **15**, 111–119.
de Gennes, P. G., 1971, J. Chem. Phys. **55**, 572–579.
de Gennes, P. G., 1979, *Scaling Concepts in Polymer Physics* (Cornell University, New York).
de Gennes, P. G., 1982, C. R. Seances Acad. Sci., Ser. 2 **294**, 827–829.
de Gennes, P. G., 1983, C. R. Seances Acad. Sci., Ser. 2 **297**, 883–886.
Dejardin, P., 1989, Phys. Rev. A **40**, 4752–4755.
Depew, D. E., and J. C. Wang, 1975, Proc. Natl. Acad. Sci. USA **72**, 4275–4279.
Derrida, B., and H. J. Hermann, 1983, J. Phys. (France) **44**, 1365–1376.
Desruisseaux, C., and G. W. Slater, 1994, Phys. Rev. E **49**, 5885–5888.
Desruisseaux, C., and G. W. Slater, 1996, Electrophoresis **17**, 623–632.
Desruiseaux, C., G. W. Slater, and T. B. L. Kist, 1998, Biophys. J. **75**, 1228–1236.
Deutsch, J. M., 1987, Phys. Rev. Lett. **59**, 1255–1258.
Deutsch, J. M., 1988, Science **240**, 922–924.
Deutsch, J. M., 1989, J. Chem. Phys. **95**, 7436–7441.
Deutsch, J. M., and T. L. Madden, 1989, J. Chem. Phys. **90**, 2476–2485.
Deutsch, J. M., and J. D. Reger, 1991, J. Chem. Phys. **95**, 2065–2071.
Disch, C., D. Loomans, I. M. Sokolov, and A. Blumen, 1996, Electrophoresis **17**, 1060–1064.
Doi, M., and S. F. Edwards, 1986, *The Theory of Polymer Dynamics* (Oxford University, Oxford).
Doi, M., T. Kobayashi, Y. Makino, M. Ogawa, G. W. Slater, and J. Noolandi, 1988, Phys. Rev. Lett. **61**, 1893–1896.
Dolnik, V., *et al.*, 1998, J. Microcolumn Sep. **10**, 175–184.
Douthart, R. J., and V. Bloomfield, 1968, Biopolymers **6**, 1297–1309.
Dovichi, N. J., 1997, Electrophoresis **18**, 2393–2399.
Drak, F., and D. M. Crothers, 1991, Proc. Natl. Acad. Sci. USA **88**, 3074–3078.
Dubochet, J., M. Adrian, I. Dustin, P. Furrer, and A. Stasiak, 1992, Methods Enzymol. **211**, 507–18.
Duke, T. A. J., 1989, Phys. Rev. Lett. **62**, 2877–2880.
Duke, T. A. J., 1990a, J. Chem. Phys. **93**, 9049–9054.
Duke, T. A. J., 1990b, J. Chem. Phys. **93**, 9055–9061.
Duke, T. A. J., R. H. Austin, E. C. Cox, and S. S. Chan, 1996, Electrophoresis **17**, 1075–1079.
Duke, T. A. J., G. Monnelly, R. H. Austin, and E. C. Cox, 1997, Electrophoresis **18**, 17–22.
Duke, T. A. J., A. N. Semenov, and J. L. Viovy, 1992, Phys. Rev. Lett. **69**, 3260–3263.
Duke, T. A. J., and J. L. Viovy, 1992a, Phys. Rev. Lett. **68**, 542–545.
Duke, T. A. J., and J. L. Viovy, 1992b, J. Chem. Phys. **96**, 8552–8563.
Duke, T. A. J., and J. L. Viovy, 1994, Phys. Rev. E **49**, 2408–2416.
Duke, T. A. J., J. L. Viovy, and A. N. Semenov, 1994, Biopolymers **34**, 239–247.

Dunn, M. J., 1994, Ed., *Proceedings of Sienna 2D Electrophoresis Conference: From Protein Maps to Genomes*, Electrophoresis **16**, 1077–1326.
Dunn, M. J., 1997, Ed., *From Protein Maps to Genomes: Proceedings of Sienna Two-Dimensional Electrophoresis Meeting*, Electrophoresis **18**, 305–662.
Edwards, S. F., 1967, Proc. Phys. Soc. London **92**, 9–16.
Effenhauser, C. S., G. J. M. Bruin, and A. Paulus, 1997, Electrophoresis **18**, 2203–2213.
El Rassi, Z., 1997, Ed., *Capillary Electrophoresis and Electrochromatography*, Electrophoresis **18**, 2121–2504.
Ernst, M. H., T. M. Nieuwenhuizen, and P. F. J. van Velthoven, 1987, J. Phys. A **20**, 5335–5350.
Fanali, S., 1997, Ed., *Capillary Electrophoresis of Chiral Compounds*, Electrophoresis **18**, 841–1044.
Fangman, W. L., 1978, Nucleic Acids Res. **5**, 653–665.
Feller, W., 1968, *An Introduction to Probability Theory and its Application* (Wiley, New York).
Ferguson, K. A., 1964, Metabolism **13**, 985–1002.
Fesjian, S., H. L. Frisch, and T. Jamil, 1996, Biopolymers **25**, 1179–1184.
Flint, D. H., and R. E. Harrington, 1972, Biochemistry **11**, 4858–4864.
Flory, P. J., 1969, *Statistical Mechanisms of Chain Molecules* (Interscience, New York).
Foret, F., 2000, Ed., *Miniaturization*, Electrophoresis **21**, 3–255.
Fung, E. N., and E. S. Yeung, 1995, Anal. Chem. **67**, 1913–1919.
Gardiner, K., 1991, Anal. Chem. **63**, 658–665.
Gardiner, K., K. Laas, and D. Patterson, 1986, Somat Cell Mol. Genet. **12**, 185–195.
Gas, B., M. Stedry, and E. Kenndler, 1997, Electrophoresis **18**, 2123–22133.
Gebauer, P., and P. Bocek, 1995, Eds. *Capillary Electrophoresis Theory*, Electrophoresis **16**, 1985–2174.
Gebauer, P., and P. Bocek, 1997, Anal. Chem. **69**, 1557–1563.
Gelfi, C., M. Perego, S. Morelli, A. Nicolin, and P. G. Righetti, 1996, Antisense Nucleic Acid Drug Dev. **6**, 47–53.
Gelfi, C., P. G. Righetti, M. Travi, and S. Fattore, 1997, Electrophoresis **18**, 724–731.
Gemmil, R. M., 1991, Adv. Electrophoresis **4**, 1–48.
Gemmil, R. M., J. F. Coyle-Morris, M. F. D. , L. F. Ware-Uribe, and F. Hecht, 1987, Gene Anal. Tech. **4**, 119–131.
Giddings, J. C., E. Kucera, C. P. Russel, and M. N. Myers, 1968, J. Phys. Chem. **72**, 4397–4408.
Gisselfält, K., B. Akerman, and M. Jonsson, 1997, Electrophoresis **18**, 663–674.
Goetzinger, W., L. Kotler, E. Carrilho, M. C. Ruiz-Martinez, O. Salas-Solano, and B. L. Karger, 1998, Electrophoresis **19**, 242–248.
Goldenberg, D. P., and T. E. Creighton, 1984, Anal. Biochem. **138**, 1–18.
Grabar, P., and C. A. Williams, 1953, Biochim. Biophys. Acta **10**, 193.
Griess, G., K. B. Guiseley, and P. Serwer, 1993, Biophys. J. **65**, 138–148.
Griess, G. A., R. A. Harris, and P. Serwer, 1993, Appl. Theor. Electrophor. **3**, 305–315.
Griess, G., E. T. Moreno, R. A. Easom, and P. Serwer, 1989, Biopolymers **28**, 1475–1484.
Griess, G. A., E. T. Moreno, R. Hermann, and P. Serwer, 1990, Biopolymers **29**, 1277–1287.
Griess, G. A., and P. Serwer, 1990, Biopolymers **29**, 1863–1866.
Grossman, P. D., and J. C. Colburn, 1992, *Capillary Electrophoresis Theory and Practice* (Academic, San Diego).
Grossman, P. D., and D. S. Soane, 1991, Biopolymers **31**, 1221–1228.
Guerry, E., O. C. Martin, H. Tricoire, R. Siebert, and L. Valentin, 1996, Electrophoresis **17**, 1420–1424.
Gunderson, K., and G. Chu, 1991, Mol. Cell. Biol. **11**, 3348–3354.
Gurrieri, S., E. Rizzarelli, D. Beach, and C. Bustamante, 1990, Biochemistry **29**, 3396–3401.
Gurrieri, S., S. B. Smith, K. S. Wells, I. D. Johnson, and C. Bustamante, 1996, Nucleic Acids Res. **24**, 4759–4767.
Heegaard, N. H. H., 1998, Electrophoresis **19**, 365–466.
Heiger, D. N., A. S. Cohen, and B. L. Karger, 1990, J. Chromatogr. **516**, 33–48.
Heller, C., 1997, Ed., *Analysis of Nucleic Acids by Capillary Electrophoresis* (Friedr. Vieweg & Sohn Verlagsgesellschaft, Braunschweig/Weinheim D).
Heller, C., and S. Beck, 1992, Nucleic Acids Res. **20**, 2447–2452.
Heller, C., T. A. J. Duke, and J. L. Viovy, 1994, Biopolymers **34**, 249–259.
Heller, C., C. Pakleza, and J. L. Viovy, 1995, Electrophoresis **16**, 1423–1428.
Heller, C., and F. M. Pohl, 1989, Nucleic Acids Res. **17**, 5989–6003.
Heller, C., G. W. Slater, P. Mayer, N. Dovichi, D. Pinto, J.-L. Viovy, and G. Drouin, 1998, J. Chromatogr., A **806**, 113–121.
Hervet, H., and C. P. Bean, 1987, Biopolymers **26**, 727–742.
Hjerten, S., 1985, J. Chromatogr. **347**, 191–198.
Holmes, D. L., and N. C. Stellwagen, 1991a, Electrophoresis **12**, 253–263.
Holmes, D. L., and N. C. Stellwagen, 1991b, Electrophoresis **12**, 612–619.
Holzwarth, G., C. B. McKeen, S. Steiger, and G. Crater, 1987, Nucleic Acids Res. **15**, 10031–10044.
Howard, T. D., and G. Holzwarth, 1992, Biophys. J. **63**, 1487–1492.
Hsu, T. P., and C. Cohen, 1989, Polymer **25**, 1419–1425.
Hu, Y., J. L. Glass, A. E. Griffith, and S. Fraden, 1994, J. Chem. Phys. **100**, 4674–4682.
Hubert, S. J., G. W. Slater, and J. L. Viovy, 1996, Macromolecules **29**, 1006–1009.
Hückel, E., 1924, Phys. Z. **25**, 204–210.
Hutson, M. S., G. Holtzwarth, T. Duke, and J. L. Viovy, 1995, Biopolymers **35**, 297–306.
Iki, N., Y. Kim, and E. S. Yeung, 1996, Anal. Chem. **68**, 4321–4325.
Isambert, H., A. Ajdari, J. L. Viovy, and J. Prost, 1997, Phys. Rev. E **56**, 5688–5704.
Isambert, H., J. Prost, A. Ajdari, and J. L. Viovy, 1997, Phys. Rev. Lett. **78**, 971–974.
Jamil, T., H. L. Frisch, and L. S. Lerman, 1989, Biopolymers **28**, 1413–1427.
Jennings, B. R., and M. Stankiewicz, 1990, Proc. R. Soc. London, Ser. A **427**, 321–330.
Jonsson, M., B. Akerman, and B. Norden, 1988, Biopolymers **27**, 381–414.
Jonsson, M., U. Jacobsson, M. Takahashi, and B. Norden, 1993, J. Chem. Soc., Faraday Trans. **89**, 2791–2798.

Katritch, V., W. K. Olson, P. Pieranski, J. Dubochet, and A. Stasiak, 1997, Nature (London) **388**, 148–151.
Keiner, L. E., and G. Holzwarth, 1992, J. Chem. Phys. **97**, 4476–4484.
Kim, Y., and M. D. Morris, 1995, Anal. Chem. **67**, 784–786.
Kim, Y., and M. D. Morris, 1996, Electrophoresis **17**, 152–160.
Kobayashi, T. K., M. Doi, Y. Makino, and M. Ogawa, 1990, Macromolecules **23**, 4480–4481.
Kolomeisky, A. B., and B. Widom, 1996, Physica A **229**, 33–60.
Kooiman, A., and J. M. F. van Leeuwen, 1993, J. Chem. Phys. **99**, 2247–2255.
Kramers, H. A., 1940, Physica (Amsterdam) **4**, 284–304.
Kremer, K., 1988, Polym. Commun. **29**, 292–294.
Ladoux, B., H. Isambert, J.-F. Léger, and J.-L. Viovy, 1998, Phys. Rev. Lett. **81**, 3793–3797.
Lai, E., B. W. Birren, S. M. Clark, and L. Hood, 1988, Nucleic Acids Res. **16**, 10376.
Lalande, M., J. Noolandi, C. Turmel, J. Rousseau, and G. W. Slater, 1987, Proc. Natl. Acad. Sci. USA **84**, 8011–8015.
Landers, J. P., 1997, Electrophoresis **18**, 1717–1906.
Larsson, A., and B. Akerman, 1995, Macromolecules **28**, 4441–4454.
Larsson, A., 1995, Ph.D. Thesis, Physics, Chalmers Univ. of Technology, Göteborg.
Lebrun, A., Z. Shakked, and R. Lavery, 1997, Proc. Natl. Acad. Sci. USA **94**, 2993–2998.
Lee, N., S. Obukhov, and M. Rubinstein, 1996, Electrophoresis **17**, 1011–1017.
Leegwater, F. A., 1995, Phys. Rev. E **52**, 2801–2806.
Leegwater, F. A., and J. M. F. van Leeuwen, 1995, Phys. Rev. E **52**, 2753–2762.
Lerman, L. S., and H. L. Frisch, 1982, Biopolymers **21**, 995–997.
Lerman, L. S., and D. Sinha, 1990, in *Electrophoresis of Large Molecules*, edited by E. Lai and B. W. Birren (Cold Spring Harbor Laboratory Press, Cold Spring Harbor, NY), pp. 1–18.
Levene, S. D., and B. H. Zimm, 1989, Science **245**, 396–399.
Lim, H. A., G. W. Slater, and J. Noolandi, 1990, J. Chem. Phys. **92**, 709–721.
Long, D., 1996, Ph.D. thesis (Université de Paris XI).
Long, D., and A. Ajdari, 1996, Electrophoresis **17**, 1161–1166.
Long, D., A. V. Dobrynin, M. Rubinstein, and A. Ajdari, 1998, J. Chem. Phys. **108**, 1234–1242.
Long, D., J. Harden, and J. L. Viovy, 1995, C. R. Acad. Sci., Ser. IIb: Mec., Phys., Chim., Astron. **321**, 239–246.
Long, D., L. Neltner, and J. L. Viovy, 1995 (unpublished).
Long, D., and J. L. Viovy, 1996, Phys. Rev. E **53**, 803–811.
Long, D., and J. L. Viovy, 1997, Physica A **244**, 238–253.
Long, D., J. L. Viovy, and A. Ajdari, 1996a, Phys. Rev. Lett. **76**, 3858–3861.
Long, D., J. L. Viovy, and A. Ajdari, 1996b, J. Phys.: Condens. Matter **8**, 9471–9475.
Long, D., J. L. Viovy, and A. Ajdari, 1997, Biopolymers **39**, 755–759.
Loomans, D., I. M. Sokolov, and A. Blumen, 1995, Macromol. Theory Simul. **4**, 145–154.
Loring, R. F., 1988, J. Chem. Phys. **88**, 6631–6640.
Louie, D., and P. Serwer, 1989, Appl. Theor. Electrophor. **1**, 169–173.
Lumpkin, O. J., 1984, J. Chem. Phys. **81**, 5201–5205.
Lumpkin, O. J., 1989, Phys. Rev. A **40**, 2634–2642.
Lumpkin, O., 1990, J. Chem. Phys. **92**, 3848–3852.
Lumpkin, O. J., 1993, Phys. Rev. E **48**, 1910–1915.
Lumpkin, O. J., P. Dejardin, and B. H. Zimm, 1985, Biopolymers **24**, 1573–1593.
Lumpkin, O. J., S. D. Levene, and B. H. Zimm, 1989, Phys. Rev. A **39**, 6557–6566.
Lumpkin, O. J., and B. H. Zimm, 1982, Biopolymers **21**, 2315–2316.
Lunney, J., A. Chrambach, and D. Rodbard, 1971, Anal. Biochem. **40**, 158–173.
Maaloum, M., N. Pernodet, and B. Tinland, 1998, Electrophoresis **19**, 1606–1610.
Madabhushi, R. S., 1998, Electrophoresis **19**, 224–230.
Madden, T. L., and J. M. Deutsch, 1991, J. Chem. Phys. **94**, 1584–1591.
Magnusdottir, S., B. Akerman, and M. Jonsson, 1994, J. Phys. Chem. **98**, 2624–2633.
Magnusdottir, S., H. Isambert, C. Heller, and J.-L. Viovy, 1998, Biopolymers **49**, 385–401.
Magnusdottir, S., J.-L. Viovy, and J. François, 1998, Electrophoresis **19**, 1699–1703.
Manning, G. S., 1969, J. Chem. Phys. **51**, 924–939.
Marko, J. F., and E. D. Siggia, 1994, Science **265**, 506–508.
Marko, J. F., and E. D. Siggia, 1995, Phys. Rev. E **55**, 2912–2938.
Masabuchi, Y., H. Oana, M. Matsumoto, M. Doi, and K. Yoshikawa, 1996, Electrophoresis **17**, 1065–1074.
Masabuchi, Y., H. Oana, K. Ono, M. Matsumoto, M. Doi, K. Minagawa, K. Matsuzawa, and K. Yoshikawa, 1993, Macromolecules **26**, 5269–5270.
Mathew, M. K., C. L. Smith, and C. R. Cantor, 1988a, Biochemistry **27**, 9204–9210.
Mathew, M. K., C. L. Smith, and C. R. Cantor, 1988b, Biochemistry **27**, 9210–9216.
Mathew, M. K., C. F. Hui, C. L. Smith, and C. R. Cantor, 1988c, Biochemistry **27**, 9222–9226.
Matsumoto, M., T. Sakaguchi, H. Kimura, M. Doi, K. Minagawa, K. Matsuzawa, and K. Yoshikawa, 1992, J. Polym. Sci., Part B: Polym. Phys. **30**, 779–783.
Maxam, A. M., and W. Gilbert, 1977, Proc Natl. Acad. Sci. USA **74**, 560–564.
Mayer, P., J. Bibette, and J. L. Viovy, 1998, Mater. Res. Soc. Symp. Proc. **463**, 57–67.
Mayer, P., G. W. Slater, and G. Drouin, 1994a, Electrophoresis **15**, 120–127.
Mayer, P., G. W. Slater, and G. Drouin, 1994b, Anal. Chem. **66**, 1777–1780.
Mayer, P., J. Sturm, and G. Weill, 1991, C.R. Acad. Sci. III **312**, 587–592.
Mayer, P., J. Sturm, C. Heitz, and G. Weill, 1993, Electrophoresis **14**, 330–336.
McCord, B. R., 1998, Ed., *Capillary Electrophoresis in Forensic Science*, Electrophoresis **19**, 1–126.
McDonnel, M. W., M. N. Simon, and F. W. Studier, 1977, J. Mol. Biol. **110**, 119–146.
Meistermann, L., 1999, Ph.D. thesis (Université Louis Pasteur, Strasbourg).
Meistermann, L., and B. Tinland, 1998, Phys. Rev. E **58**, 4801–4806.
Menchen, S., S. Johnson, M. A. Winnik, and B. Xu, 1996, Electrophoresis **17**, 1451–1459.
Mercier, J.-F., and G. W. Slater, 1998, Electrophoresis **19**, 1560–1565.

Mickel, S., V. Arena, and W. Barier, 1977, Nucleic Acids Res. **4**, 1465–1482.
Minarik, M., B. Gas, and E. Kenndler, 1997, Electrophoresis **18**, 98–103.
Mitnik, L., C. Heller, J. Prost, and J. L. Viovy, 1995, Science **267**, 219–222.
Mitnik, L., L. Salomé, J. L. Viovy, and C. Heller, 1995, J. Chromatogr., A **710**, 309–321.
Morris, C. J. O. R., 1966, Prot. Biol. Fluids **14**, 543–551.
Muthukumar, M., 1996, Electrophoresis **17**, 1167–1172.
Muthukumar, M., and A. Baumgartner, 1989, Macromolecules **22**, 1937–1941.
Müller, O., M. Minarik, and F. Foret, 1998, Electrophoresis **19**, 1436–1444.
Nathakarnkitkool, S., P. J. Oefner, G. Bartsch, M. A. Chin, and G. K. Bonn, 1992, Electrophoresis **13**, 18–31.
Neitzey, L. M., G. Holtzwarth, T. Duke, and J. L. Viovy, 1995, Biopolymers **35**, 307–317.
Neitzey, L. M., M. S. Hutson, and G. Holzwarth, 1993, Electrophoresis **14**, 296–303.
Nixon, G. I., and G. W. Slater, 1994, Phys. Rev. E **50**, 5033–5038.
Nixon, G. I., and G. W. Slater, 1996, Phys. Rev. E **53**, 4969–4980.
Noolandi, J., 1993, Electrophoresis **14**, 680–681.
Noolandi, J., J. Rousseau, G. W. Slater, C. Turmel, and M. Lalande, 1987, Phys. Rev. Lett. **58**, 2428–2431.
Noolandi, J., G. W. Slater, H. A. Lim, and J. L. Viovy, 1989, Science **243**, 1456–1458.
Norden, B., C. Elvingson, M. Jonsson, and B. Akerman, 1991, Q. Rev. Biophys. **24**, 103–164.
Oana, H., M. Doi, M. Ueda, and K. Yoshokawa, 1997, Electrophoresis **18**, 1912–1915.
Oana, H., Y. Masabuchi, M. Matsumoto, M. Doi, K. Matsuzawa, and K. Yoshikawa, 1994, Macromolecules **27**, 6061–6067.
Obukhov, S. P., and M. Rubinstein, 1993, J. Phys. II **3**, 1455–1459.
Odijk, T., 1977, J. Polym. Sci. **15**, 477–483.
Ogston, A. G., 1958, Trans. Faraday Soc. **54**, 1754–1757.
Olivera, B. M., P. Baine, and N. Davidson, 1964, Biopolymers **2**, 245–257.
Olson, M. V., 1989a, in *Genetic Engineering*, edited by J. K. Setlow (Plenum, New York), pp. 183–227.
Olson, M. V., 1989b, J. Chromatogr. **470**, 377–383.
Olvera de la Cruz, M., J. M. Deutsch, and S. F. Edwards, 1986, Phys. Rev. A **33**, 2047–2055.
Perego, M., C. Gelfi, A. V. Stoyanov, and P. G. Righetti, 1997, Electrophoresis **18**, 2915–2920.
Pernodet, N., M. Maaloum, and B. Tinland, 1997, Electrophoresis **18**, 55–58.
Pernodet, N., and B. Tinland, 1997, Biopolymers **42**, 471–478.
Platt, K. J., and G. Holzwarth, 1989, Phys. Rev. A **40**, 7292–7300.
Pluen, A., 1996, Ph.D. thesis (Université Louis Pasteur, Strasbourg).
Pluen, A., B. Tinland, J. Sturm, and G. Weill, 1998, Electrophoresis **19**, 1548–1559.
Popelka, S., Z. Kabatek, J. L. Viovy, and B. Gas, 1999, J. Chromatogr. A **838**, 45–53.
Quesada, M. A., 1997, Curr. Opin. Biotechnol. **8**, 82–93.
Radko, S. P., and A. Chrambach, 1996, Electrophoresis **17**, 1094–1102.
Radko, S. P., and A. Chrambach, 1997, Biopolymers **42**, 183–189.
Rayleigh, Lord, 1916, Philos. Mag. **37**, 321.
Righetti, P. G., 1989, J. Biochem. Biophys. Methods **19**, 1–20.
Righetti, P. G., 1996, Ed., *Capillary Electrophoresis in Analytical Biotechnology*, CRC Series in Analytical Biotechnology (CRC, Boca Raton).
Righetti, P. G., and C. Gelfi, 1997, in *Analysis of Nucleic Acids by Capillary Electrophoresis*, edited by C. Heller, Chromatographia, CE Series No. 1 (Vieweg, Wiesbaden), pp. 255–271.
Rill, R., T. Liu, B. R. Locke, and D. H. Van Winkle, 1998, Proc. Natl. Acad.. Sci. USA **95**, 1534–1539.
Rodbard, D., and A. Chrambach, 1970, Proc. Natl. Acad. Sci. USA **4**, 970–977.
Rodbard, D., and A. Chrambach, 1971, Anal. Biochem. **40**, 95–134.
Rubinstein, M., 1987, Phys. Rev. Lett. **59**, 1946–1949.
Russel, W. B., D. A. Saville, and W. K. Schowalter, 1989, *Colloidal Dispersions* (Cambridge University, Cambridge, England).
Sanger, F., and A. R. Coulson, 1975, J. Mol. Biol. **94**, 441–448.
Sanger, F., S. Nicklen, and A. R. Coulson, 1977, Proc. Natl. Acad. Sci. USA **74**, 5453–5467.
Shaefer, D. W., J. F. Joanny, and P. Pincus, 1980, Macromolecules **13**, 1280–1289.
Schaffer, E. O., and M. Olvera de la Cruz, 1989, Macromolecules **22**, 1351–1355.
Schellman, J. A., and D. Stigter, 1977, Biopolymers **16**, 1415–1434.
Schwartz, D. C., and C. R. Cantor, 1984, Cell **37**, 67–75.
Schwartz, D. C., and M. Koval, 1989, Nature (London) **338**, 520–522.
Semenov, A. N., T. A. J. Duke, and J. L. Viovy, 1995, Phys. Rev. E **51**, 1520–1537.
Semenov, A. N., and J. F. Joanny, 1997, Phys. Rev. E **55**, 789–799.
Serwer, P., and S. Hayes, 1987, Electrophoresis **8**, 244–246.
Serwer, P., 1987, Electrophoresis **8**, 301–304.
Serwer, P., 1990, Biotechnol. Genet. Eng. Rev. **8**, 319–343.
Serwer, P., and G. A. Griess, 1998, Anal. Chim. Acta **372**, 299–306.
Serwer, P., and S. J. Hayes, 1989a, Appl. Theor. Electrophor. **1**, 95–98.
Serwer, P., and S. J. Hayes, 1989b, Biochemistry **28**, 5827–5832.
Serwer, P., S. J. Hayes, E. T. Moreno, and C. Y. Park, 1992, Biochemistry **31**, 8397–8405.
Sewick, E. M., and R. M. Williams, 1996, Phys. Rev. Lett. **76**, 2595–2598.
Shi, X., R. W. Hammond, and M. D. Morris, 1995a, Anal. Chem. **67**, 1132–1138.
Shi, X., R. W. Hammond, and M. D. Morris, 1995b, Anal. Chem. **67**, 3219–3222.
Skolnick, J., and M. Fixman, 1977, Macromolecules **10**, 944–948.
Slater, G. W., 1992, J. Phys. II **2**, 1149–1158.
Slater, G. W., 1993, Electrophoresis **14**, 1–7.
Slater, G. W., C. Desruisseaux, C. Villeneuve, H. L. Guo, and G. Drouin, 1995, Electrophoresis **16**, 704–712.
Slater, G. W., and G. Drouin, 1992, Electrophoresis **13**, 574–582.
Slater, G. W., and H. L. Guo, 1995, Electrophoresis **16**, 11–15.

Slater, G. W., and H. L. Guo, 1996a, Electrophoresis **17**, 977–988.
Slater, G. W., and H. L. Guo, 1996b, Electrophoresis **17**, 1407–1415.
Slater, G. W., H. L. Guo, and G. I. Nixon, 1997, Phys. Rev. Lett. **78**, 1170–1173.
Slater, G. W., T. B. L. Kist, H. Ren, and G. Drouin, 1998, Electrophoresis **19**, 1525–1541.
Slater, G. W., P. Mayer, and G. Drouin, 1993, Electrophoresis **14**, 961–966.
Slater, G. W., P. Mayer, and G. Drouin, 1993, Analusis **21**, M25.
Slater, G. W., P. Mayer, S. J. Hubert, and G. Drouin, 1994, Appl. Theor. Electrophor. **4**, 71–79.
Slater, G. W., and J. Noolandi, 1985, Phys. Rev. Lett. **55**, 1579–1582.
Slater, G. W., and J. Noolandi, 1986a, Biopolymers **25**, 431–454.
Slater, G. W., and J. Noolandi, 1986b, Europhys. Lett. **1**, 347–353.
Slater, G. W., and J. Noolandi, 1989, Electrophoresis **10**, 413–428.
Slater, G. W., and J. Noolandi. 1990, in *Proceedings of "International Symposium on New Trends in Physics and Physical Chemistry of Polymers Honoring Professor P. G. de Gennes*," 1989, Toronto (Plenum, New York), p. 547.
Slater, G. W., J. Noolandi, and A. Eisenberg, 1991, Macromolecules **24**, 6715–6720.
Slater, G. W., J. Rousseau, and J. Noolandi, 1987, Biopolymers **26**, 863–872.
Slater, G. W., J. Rousseau, J. Noolandi, C. Turmel, and M. Lalande, 1988, Biopolymers **27**, 509–524.
Slater, G. W., and C. Villeneuve, 1992, J. Polym. Sci., Part B: Polym. Phys. **30**, 1451–1457.
Slater, G. W., and S. Y. Wu, 1995, Phys. Rev. Lett. **75**, 164–167.
Smisek, D. L., and D. A. Hoagland, 1990, Science **248**, 1221–1223.
Smith, C. L., 1993, Ed., *Changing Directions in Electrophoresis*, Electrophoresis **14**, pp. 249–370.
Smith, C. L., and C. R. Cantor, 1986, Nature (London) **319**, 701–702.
Smith, C. L., and C. R. Cantor, 1987, Methods Enzymol. **155**, 449–467.
Smith, C. L., T. Matsumoto, O. Niwa, S. Klco, J.-B. Fan, M. Yanagida, and C. R. Cantor, 1987, Nucleic Acids Res. **15**, 4481–4489.
Smith, D. E., T. T. Perkins, and S. Chu, 1996, Macromolecules **29**, 1372–1373.
Smith, S. B., P. K. Alridge, and J. B. Callis, 1989, Science **243**, 203–206.
Smith, S. B., C. Heller, and C. Bustamante, 1991, Biochemistry **30**, 5264–5274.
Smoluchowski, M., von, 1903, Bull. International de l'Academie des Sciences de Cracovie **8**, 182–200.
Song, L., and M. F. Maestre, 1991, J. Biomol. Struct. Dyn. **9**, 525–535.
Sor, F., 1987, Nucleic Acids Res. **15**, 4853–4863.
Sor, F., 1992, Methods Mol. Cell. Biol. **3**, 65–70.
Southern, E., R. Anand, W. R. A. Brown, and D. S. Fletcher, 1987, Nucleic Acids Res. **15**, 5925–5943.
Starchev, K., J. Sturm, and G. Weill, 1996, Electrophoresis **17**, 465–470.
Stellwagen, N., 1985, J. Biomol. Struct. Dyn. **3**, 299–314.
Stellwagen, N. C., 1987, Adv. Electrophoresis **1**, 179–228.
Stellwagen, N. C., 1988, Biochemistry **27**, 6417–6424.
Stellwagen, N., 1998, Electrophoresis **19**, 1542–1547.
Stellwagen, N., C. Gelfi, and P. G. Righetti, 1997, Biopolymers **42**, 687–703.
Stellwagen, N. C., and J. Stellwagen, 1989, Electrophoresis **17**, 1537–1548.
Stigter, D., 1978a, J. Chem. Phys. **82**, 1417–1423.
Stigter, D., 1978b, J. Chem. Phys. **82**, 1424–1429.
Sturm, J., and G. Weill, 1989, Phys. Rev. Lett. **62**, 1484–1487.
Subbotin, A. V., and A. N. Semenov, 1996, Electrophoresis **17**, 1018–1026.
Sudor, J., and M. V. Novotny, 1994, Anal. Chem. **66**, 2446–2450.
Sudor, J., and M. V. Novotny, 1995, Anal. Chem. **67**, 4205–4209.
Tietz, D., 1988, Adv. Electrophoresis **2**, 109–169.
Tinland, B., 1996, Electrophoresis **17**, 1519–1523.
Tinland, B., N. Pernodet, and A. Pluen, 1998, Biopolymers **46**, 201–214.
Tinland, B., N. Pernodet, and G. Weill, 1996, Electrophoresis **17**, 1046–1051.
Tinland, B., A. Pluen, J. Sturm, and G. Weill, 1997, Macromolecules **30**, 5763–5765.
Tiselius, A., 1937, Trans. Faraday Soc. **33**, 524–531.
To, K. Y., and T. R. C. Boyde, 1993, Electrophoresis **14**, 597–600.
Turmel, C., E. Brassard, G. W. Slater, and J. Noolandi, 1990, Nucleic Acids Res. **18**, 569–575.
Turmel, C., and M. Lalande, 1988, Nucleic Acids Res. **16**, 4727.
Ueda, M., and Y. Baba, 1997, Anal. Sci. **13**, 10966112.
Ueda, M., H. Oana, Y. Baba, M. Doi, and K. Yoshikawa, 1998, Biophys. Chem. **71**, 113–123.
Ueda, M., K. Yoshikawa, and M. Doi, 1997, Polym. J. (Tokyo) **29**, 1040–1043.
Ulanovsky, L., G. Drouin, and W. Gilbert, 1990, Nature (London) **343**, 190–192.
van Leeuwen, J. M. F., 1991, J. Phys. I **11**, 1675–1680.
van Leeuwen, J. M. F., and A. Kooiman, 1992, Physica A **184**, 79–97.
Viovy, J. L., 1987a, C. R. Acad. Sci., Ser. II **305**, 181–184.
Viovy, J. L., 1987b, Biopolymers **26**, 1929–1940.
Viovy, J. L., 1988a, Europhys. Lett. **7**, 657–661.
Viovy, J. L., 1988b, Phys. Rev. Lett. **60**, 855–858.
Viovy, J. L., 1989, Electrophoresis **10**, 429–441.
Viovy, J. L., 1996, Mol. Biotechnol. **6**, 31–46.
Viovy, J. L., F. Caron, F. Miomandre, M. C. Miquel, and F. Sor, 1992, Electrophoresis **13**, 1–6.
Viovy, J. L., and T. A. J. Duke, 1993, Electrophoresis **14**, 322–329.
Viovy, J. L., and T. A. J. Duke, 1994, Science **264**, 112–113.
Viovy, J. L., and C. Heller, 1996, in *Capillary Electrophoresis: An Analytical Tool in Biotechnology*, Analytical Biotechnology Series, edited by P. G. Righetti (CRC Press, Boca Raton), pp. 477–508.
Viovy, J. L., B. Ladoux, H. Isambert, S. Magnusdottir, J. Sudor, M. Stefansson, and P. Doyle, 1998, in *Proceedings of IUPAP STATPHYS 20*, 1998, Paris (Imprimerie de l'Ecole Polytechnique, Palaiseau), p. P006/43.
Volkmuth, W., and R. H. Austin, 1992, Nature (London) **358**, 600–602.

Volkmuth, W. D., T. Duke, R. H. Austin, and E. C. Cox, 1995, Proc. Natl. Acad. Sci. USA **92**, 6887–6891.
Volkmuth, W. D., T. Duke, M. C. Wu, and R. H. Austin, 1994, Phys. Rev. Lett. **72**, 2117–2120.
Vollrath, D., and R. W. Davies, 1987, Nucleic Acids Res. **15**, 7865–7876.
Wang, Z., and B. Chu, 1989, Phys. Rev. Lett. **63**, 2528–2531.
Whitcomb, R., and G. Holzwarth, 1990, Nucleic Acids Res. **18**, 6331–6338.
Widom, B., J. L. Viovy, and A. D. Défontaines, 1991, J. Phys. I **12**, 1759–1784.
Widom, M., and I. Al-Lehyani, 1997, Physica A **244**, 510–521.
Wu, C., T. Liu, and B. Chu, 1998, Electrophoresis **19**, 231–241.
Wu, C., L. Tianbo, B. Chu, D. K. Schneider, and V. Graziano, 1997, Macromolecules **30**, 1534–1539.
Wu, C., Z. Wang, and B. Chu, 1990, Biopolymers **29**, 491–500.
Wu, S. Y., and G. W. Slater, 1993, Macromolecules **26**, 1905–1913.
Yan, J., N. Best, J. Z. Zhang, H. Ren, R. Jiang, J. Hou, and N. J. Dovichi, 1996, Electrophoresis **17**, 1037–1045.
Yanagida, M., Y. Hiraoka, and I. Katsura, 1983, in *Cold Spring Harbor Symposium on Quantum Biology*, Cold Spring Harbor Symposium Series No. 47 (Cold Spring Harbor Press, Cold Spring Harbor, NY), pp. 177–187.
Zhang, T. Y., C. L. Smith, and C. R. Cantor, 1991, Nucleic Acids Res. **19**, 1291–1296.
Zimm, B. H., 1988, Phys. Rev. Lett. **61**, 2965–2968.
Zimm, B. H., 1991, J. Chem. Phys. **94**, 2187–2206.
Zimm, B. H., 1993, Curr. Opin. Struct. Biol. **3**, 373–376.
Zimm, B. H., 1996, Electrophoresis **17**, 996–1002.
Zimm, B. H., and S. D. Levene, 1992, Q. Rev. Biophys. **25**, 171–204.
Zimm, B. H., and O. Lumpkin, 1993, Macromolecules **26**, 226–234.